Physics – Uspekhi **37** (11) 1043 – 1077 (1994)

REVIEWS OF TOPICAL PROBLEMS PACS numbers: 14.20.–c

Exotic baryons

L G Landsberg

Contents

Abstract. A review of the present status of the physics of exotic baryons is given. The models for these baryons are discussed as well as their production and decay processes, and methods of their identification. The results of recent experiments in this field are presented, in which some unusual states are observed. These states are candidates for cryptoexotic baryons with hidden strangeness. Prospects for further studies of these processes are discussed.

1. Introduction

The last decade has been marked by a significant increase in studies in the field of spectroscopy of hadrons, that is, the particles participating in strong interactions. It has been firmly established that hadrons are not truly elementary, but composite particles. Similar to atomic nuclei, which consist of nucleons, hadrons are bound systems composed of fundamental particles known as quarks. Quarks are those structural elements that define the variety of the hadronic matter. In addition to having a fractional electric charge, quarks have a 'strong-interaction charge' called colour.

The interaction between quarks occurs by exchange of colour virtual particles, gluons, in a similar way as the interaction between electric charges is effected by exchange of virtual photons. However, in contrast to neutral photons, which bear no charge and do not interact with each other, gluons are characterised by colour 'charges' and are capable of interacting not only with colour quarks but between themselves, thus forming even bound gluon states — glueballs. The interaction between colour quarks and gluons is described by quantum chromodynamics.

Apparently, colour quarks and gluons cannot exist in a free state. Such a hypothesis is experimentally based on the long-standing unsuccessful efforts to find free quarks. Therefore, the concept of confinment ('the quark imprisonment') arose, according to which only the particles without colour charge can freely exist, the so-called 'colourless' or

L G Landsberg Institute for High Energy Physics, Protvino
142284, Moscow Region
Fax (7-095) 230 2337
E-mail: lgl@mx.decnet.ihep.su

Received 2 August 1994
Uspekhi Fizicheskikh Nauk **164** (11) 1129 – 1164 (1994)
Translated by K A Postnov and L G Landsberg; edited by J R Briggs

'white' hadrons. All these hadrons are divided by their quark content and quantum numbers into two large groups: baryons and mesons. Baryons consist of three quarks, antibaryons of three antiquarks ($B = qqq$, $\overline{B} = \bar{q}\bar{q}\bar{q}$), and mesons of a quark and an antiquark ($M = q\bar{q}$).

Only so-called valence quarks are considered here, which determine the hadron nature and its main characteristics (quantum numbers). According to the current theoretical perceptions, well confirmed by numerous experiments, the valence quarks in a hadron are surrounded by a 'cloud' of virtual quark – antiquark pairs and gluons, which are constantly emitted and absorbed by the valence quarks. This 'cloud' or, as one says now, the 'sea' of quark – antiquark pairs and gluons, is a physical reality defining many properties of hadron (for example, space distribution of its electric charge and magnetic moment, intrinsic distribution of quark and gluon constituents by momenta, etc.).

The wave function of an 'ordinary' baryon can be represented, with the quark – gluon 'sea' taken into account, as

$$|B\rangle = (qqq)[\text{const} + \text{'sea' of virtual } q\bar{q}\text{-pairs and gluons}] .$$

Thus a baryon spends part of its lifetime in a 'pure' valence (qqq) state, and another part in states with additional 'sea' components. An analoguous situation exists for mesons.

A very important question is whether there exist 'colourless' hadrons with a more complex inner valence structure, such as multiquark mesons ($M = qq\bar{q}\bar{q}$) and baryons ($B = qqqq\bar{q}$), dibaryons ($D = qqqqqq$), hybrid states ($M = q\bar{q}g$ and $B = qqq\bar{g}$), and glueballs, which are mesons composed only of gluons ($M = gg$, ggg). Of course, in such new forms of hadronic matter, known as exotic hadrons, effects of the quark – gluon 'sea' must also appear in addition to the valence quark and gluon structure. For example, the wave function of an exotic multiquark baryon, unlike that of the 'ordinary' baryon, can be represented as

$$|B\rangle = (qqqq\bar{q})[\text{const} + \text{'sea' of virtual } q\bar{q}\text{-pairs and gluons}] .$$

The recent highlights in hadron spectroscopy which were mentioned above are strongly connected with the wide-scale searches for exotic hadrons, which take full advantage of modern experimental techniques. No theoretical prohibitions for the existence of exotic hadrons are known. However, these particles may prove to be extremely unstable, have a very large decay width, and thus be practically unobservable. The example of atomic nuclei shows that not all nucleon systems are stable enough to exist in reality. For instance, systems consisting of two or several bound protons are not observed in nature. Therefore, the question of the existence of exotic hadrons can be solved only experimentally.

How can one can distinguish exotic particles from ordinary ones, which, as was already noted, also spend a part of their lifetime in states with many quarks and gluons? Here are two possibilities.

1.1 Hadrons with open exotics (exotics of the first and second kinds)

Because of their complex valence structure, the exotic hadrons can be characterised by values of quantum numbers that are simply impossible for the ordinary hadrons. Electric charges and flavours of hadrons (strangeness, isospin etc.) can be taken as such clearly exotic quantum numbers: for mesons $|Q| = 2$, $I = 2$, $|S| = 2$; for baryons $|Q| = 3$, $I > 3/2$, $S = +1$. Of course, particles of this type can be easily distinguished from the ordinary hadrons. They are known as exotic states of the first kind.

There are other possibilities for which the difference between the exotic and ordinary hadrons can be less pronounced, although quite definite as well. For example, the charges and other flavours of hybrid exotic mesons $q\bar{q}g$ are determined by properties of the $q\bar{q}$-pair entering into the meson composition, and are the same as for the ordinary mesons. However, the hybrid mesons can be characterised by unusual (exotic) combinations of the spin J, parity P, and charge parity C, which cannot occur for $q\bar{q}$-mesons: $J^{PC} = 0^{+-}$, 0^{--}, 1^{-+}, 2^{+-}, 3^{-+}, etc. Such exotic combinations of J, P, and C also can occur for other exotic mesons (multiquark states or glueballs). The hadrons of this type are referred to as exotic states of the second kind.

1.2 Cryptoexotic hadrons (exotics of the third kind)

Apart from states with open exotics, the existence of exotic hadrons not differing from the ordinary qqq-baryons or $q\bar{q}$-mesons by their quantum numbers is also possible. These objects are known as particles with hidden exotics, or cryptoexotic hadrons. A complex internal colour structure of hadrons with hidden exotics can lead to significant peculiarities in their dynamical properties allowing one to establish their exotic nature. Such peculiarities can include anomalously small decay probabilities of such hadrons (small hadronic width), and unusual relationships among the branching ratios of their decay channels or special formation mechanisms of the considered states. Despite difficulties with unique identification of the cryptoexotic states, almost all principal exotic hadron candidates discovered so far belong to this category of particles. They are also called exotic states of the third kind.

The question about the possible existence of exotic hadrons is of great significance for the basic concepts about the nature of hadronic matter, for quantum chromodynamics and the concept of confinement, and for modern models of hadron structure (lattice, string, and bag models). Although the search for exotic hadrons has been carried out for a long time, the problem of their existence has remained unsolved for many years. The situation here has significantly changed in recent years. Several meson states have been discovered whose properties are very difficult to explain in the framework of the ordinary ideas of a naive quark model. These mesons are strong candidates for the exotic states. On the other hand, systematic searches for exotic baryons are still at the initial stage. The obtained results are contradictory in many respects and require further studies.

The development of the modern hadron spectroscopy and the search for exotic mesons are discussed in the proceedings of a number of international conferences, seminars, and workshops [1 – 10], as well as in reviews [11 – 19]. In the present review we analyse the possible properties of the exotic baryons and results of searching for these unusual states. We also consider prospects for further studies in this direction. The main content of the review relates to the spectroscopy of baryons consisting of light quarks (q = u, d, s; if strange quarks are specially marked,

then q = u, d). Exotic states with heavy (charmed) quarks are also briefly considered.

2. Systematics of qqq-baryons

Now we briefly remind the main ideas of the quark model that relates to description of the ordinary qqq-baryons (see [11, 20–25] and references therein). The overall wave function of a three-quark system has a form

$$\underbrace{|q_1q_2q_3\rangle}_{\text{antisymm.}} = \underbrace{|\text{colour. w. f.}\rangle|\text{spin. w. f.}\rangle|\text{flavour. w. f.}\rangle}_{\text{symm.}}\underbrace{|\text{colour. w. f.}\rangle}_{\text{antisymm.}} \quad (1)$$

Indeed, quarks obey Fermi–Dirac statistics, hence the full wave function $|q_1q_2q_3\rangle$ is antisymmetric in their permutations. The colour part of the wave function, being a singlet by $SU(3)_{\text{colour}}$, is antisymmetric, and the remaining part of the wave function is symmetric in the quark permutations:

$|q_1q_2q_3\rangle$ — antisymmetric function;

$|\text{coord. w. f.}\rangle$ — antisymmetric function;

$\{|\text{coord. w. f.}\rangle|\text{spin. w. f.}\rangle|\text{flavour. w. f.}\rangle\}$ — symmetric function.

The coordinate wave function of a three-quark system is described by two variables:

$$\boldsymbol{\rho} = \frac{1}{\sqrt{2}}(\boldsymbol{r}_1 - \boldsymbol{r}_2)\,, \quad \boldsymbol{\lambda} = \frac{1}{\sqrt{6}}(\boldsymbol{r}_1 + \boldsymbol{r}_2 - 2\boldsymbol{r}_3)\,. \quad (2)$$

Here $\boldsymbol{r}_1$, $\boldsymbol{r}_2$, $\boldsymbol{r}_3$ are position vectors of the quarks q_1, q_2, q_3, $\boldsymbol{\rho}$ describes the relative motion of q_1 and q_2, and $\boldsymbol{\lambda}$ describes the motion of q_3 with respect to the q_1, q_2 rest frame.

Orbital momenta of these motions are defined by the quantum numbers l_ρ and l_λ. The full orbital momentum for the $q_1q_2q_3$-system is

$$\boldsymbol{L} = \boldsymbol{l}_\rho + \boldsymbol{l}_\lambda\,. \quad (3)$$

The spatial parity for the coordinate wave function is defined by the relation

$$P = (-1)^{l_\rho + l_\lambda}\,. \quad (4)$$

The total angular momentum of the $q_1q_2q_3$-system is

$$\boldsymbol{J} = \boldsymbol{L} + \boldsymbol{S}\,. \quad (5)$$

where $\boldsymbol{S}$ is the intrinsic spin of the quark system ($S = 3/2$, $1/2$).

The spin and flavour parts of the wave function of the $q_1q_2q_3$-system correspond to SU(2) and SU(3) symmetry respectively, and their product to SU(6) symmetry.

Classification of baryonic states can be obtained by multiplying the corresponding representations with the use of the Young diagram technique (simple rules of such multiplications are formulated, for example, in [Refs 11, 24]).

In spin space [SU(2) representation] †

$$\underset{[2]}{\square} \otimes \underset{[2]}{\square} \otimes \underset{[2]}{\square} = \square \otimes \left[\square\square + \begin{smallmatrix}\square\\ \square\end{smallmatrix}\right] = \underbrace{\square\square\square}_{[4]} + \underset{[2]}{\begin{smallmatrix}\square\square\\ \square\end{smallmatrix}} + \underset{[2]}{\square}\,. \quad (6)$$

Therefore, by quark spin the baryons form one quartet of particles [4] with the spin $S = 3/2$ (that is, symmetric states by spin), and two doublets with a mixed symmetry [2], corresponding to the spin $S = 1/2$. This can be rewritten as

$$[2] \otimes [2] \otimes [2] = [4] + [2] + [2]\,.$$

In the space of flavour SU(3)-symmetry

$$\underset{[3]}{\square} \otimes \underset{[3]}{\square} \otimes \underset{[3]}{\square} = \square \otimes \left[\square\square + \begin{smallmatrix}\square\\ \square\end{smallmatrix}\right] = \underset{[10]}{\square\square\square} + \underset{[8]}{\begin{smallmatrix}\square\square\\ \square\end{smallmatrix}} + \underset{[8]}{\begin{smallmatrix}\square\square\\ \square\end{smallmatrix}} + \underset{[1]}{\begin{smallmatrix}\square\\ \square\\ \square\end{smallmatrix}}\,, \quad (8)$$

that is, the baryons form one symmetric SU(3)-decuplet, two mixed-symmetry SU(3)-octets and one antisymmetric SU(3)-singlet. This can also be written as

$$[3] \otimes [3] \otimes [3] = [10] + [8] + [8] + [1]\,. \quad (9)$$

Assuming SU(6) symmetry for the spin–flavour part of the baryon wave function $|\text{spin. w. f.}\rangle\,|\text{flavour. w. f.}\rangle$, we get

$$\underset{\{6\}}{\square} \otimes \underset{\{6\}}{\square} \otimes \underset{\{6\}}{\square} = \underset{\{56\}}{\square\square\square} + \underset{\{70\}}{\begin{smallmatrix}\square\square\\ \square\end{smallmatrix}} + \underset{\{70\}}{\begin{smallmatrix}\square\square\\ \square\end{smallmatrix}} + \underset{\{20\}}{\begin{smallmatrix}\square\\ \square\\ \square\end{smallmatrix}}\,, \quad (10)$$

that is, the baryons can belong to one symmetric SU(6)-56-plet, one antisymmetric SU(6)–20-plet, and to one of two

Table 1. Baryon classification in SU(6) symmetry.

Quark spin	SU(2)	SU(3)		
		[10] (*S*)	[8], [8] (*M*) (*M*)	[1] (*A*)
3/2	[4] (*S*)	^{4}[10] (*S*)	^{4}[8], ^{4}[8] (*M*) (*M*)	^{4}[1] (*A*)
1/2	[2], [2] (*M*) (*M*)	^{2}[10], ^{2}[10] (*M*) (*M*)	^{2}[8], ^{2}[8], ^{2}[8], ^{2}[8] (*S*) (*M*) (*M*) (*A*)	^{2}[1], ^{2}[1] (*M*) (*M*)

Note. $SU(6) = \underset{(S)}{56_{SU(6)}} + \underset{(M)}{70_{SU(6)}} + \underset{(M)}{70_{SU(6)}} + \underset{(A)}{20_{SU(6)}}$.

By muliplying SU(3) and SU(2) representations SU(6)-multiplets are formed with the following structure:

$\underset{(S)}{56_{SU(6)}} = \underset{(S)}{^4[10]} + \underset{(S)}{^2[8]}$ — symmetric representation;

$\underset{(M)}{70_{SU(6)}} = \underset{(M)}{^2[10]} + \underset{(M)}{^4[8]} + \underset{(M)}{^2[8]} + \underset{(M)}{^2[1]}$ — mixed representation;

$\underset{(A)}{20_{SU(6)}} = \underset{(A)}{^2[8]} + \underset{(A)}{^4[1]}$ — antisymmetric representation.

Notation: $56_{SU(6)}$ or {56} – SU(6)-plet of baryons; ^{4}[10] – SU(3)... decuplet of baryons with quark spin 3/2 (quartet by the quark spin) etc.; *S* – symmetric representation, *M* – mixed representation, *A* — antisymmetric representation.

† We use the following notation in the present review, unless otherwise indicated: {56} or $56_{SU(6)}$ — SU(6)-supermultiplet [SU(6)-plet, SU(6)-multiplet) and so on; [10] or $10_{SU(3)}$ — SU(3) supermultiplet (SU(3)-plet]; [2] — SU(2)-multiplet and so on. However, in some figures and tables taken from other papers, the original notations are preserved (see e.g. Fig. 1, Table 4).

SU(6)-70-plets with a mixed symmetry. This can also be written as

$$\{6\} \otimes \{6\} \otimes \{6\} = \{56\} + \{70\} + \{70\} + \{20\}\,. \qquad (11)$$

The structure of SU(6)-plets is known to be determined by multiplying the SU(2) and SU(3) representations (Table 1).

Now let us discuss the structure of the entire coordinate–spin–flavour part of the baryon wave function $|\text{coord. w. f.}\rangle\,|\text{spin. w. f.}\rangle|\text{flavour. w. f.}\rangle$, corresponding to the product of representations $\mathrm{SU}(6) \otimes \mathrm{O}(3)$. As is seen from Eqn (1), for $q_1q_2q_3$-baryons only symmetric states from $\mathrm{SU}(6) \otimes \mathrm{O}(3)$ occur.

Consider consecutively the lowest baryonic state classification.

N=0 — the ground baryonic states. They correspond to values $l_\rho = 0$, $l_\lambda = 0$ (we introduce the notation $|1s\rangle_\rho|1s\rangle_\lambda$). The total orbital momentum of the system is $L = 0$, parity $P = +1$, and the space part of the baryon wave function is symmetric. Therefore, the SU(6) component must be also symmetric. Thus, the states with $N = 0$ belong to a symmetric $\{56\}_{\mathrm{SU}(6)}$-representation.

We will denote the corresponding baryon families by $|\{\mathrm{SU}(6)\}; L^P\rangle_N$. The states with $N = 0$ form a supermultiplet of baryons with positive parity $|\{56\};\ 0^+\rangle_{N=0}$, to which belong the well-known SU(3)-octet of stable baryons with spin $J = 1/2$ ($^2[8]$) and SU(3)-decuplet of baryons with spin $J = 3/2$, including the Ω-hyperon ($^4[10]$):

$$|\{56\};\ 0^+\rangle_{N=0} = {}^2[8](J = 1/2) + {}^4[10](J = 3/2)\,. \qquad (12)$$

N=1 — the first excited level. This level corresponds to the orbital excitations of the $q_1q_2q_3$-system with $l_\rho = 0$, $l_\lambda = 1$ ($|1s\rangle_\rho|1p\rangle_\lambda$) and with $l_\rho = 1$, $l_\lambda = 0$ ($|1p\rangle_\rho|1s\rangle_\lambda$). For such states with mixed O(3)-symmetry $L^P = 1^-$, the corresponding SU(6)-supermultiplet must also have a mixed symmetry. Therefore baryons with $N = 1$ belong to the supermultiplet $|\{70\};\ 1^-\rangle_{N=1}$. The spins of these baryons are $J = 1/2,\ 3/2,\ 5/2$ according to the relation (5)

$$\begin{aligned}|\{70\}; 1^-\rangle_{N=1} = {}&{}^2[10](J = 1/2, 3/2)\\ &+ {}^4[8](J = 1/2, 3/2, 5/2)\\ &+ {}^2[8](J = 1/2, 3/2) + {}^2[1](J = 1/2, 3/2)\,, \qquad (13)\end{aligned}$$

that is, in total there are nine SU(3)-families with different baryon spins.

Excitation level N=2. The excited states with $N = 2$ have the form

$$|1s\rangle_\rho|1d\rangle_\lambda, |1s\rangle_\rho|2s\rangle_\lambda, |1p\rangle_\rho|1p\rangle_\lambda, |2s\rangle_\rho|1s\rangle_\lambda, |1d\rangle_\rho|1s\rangle_\lambda.$$

(All these levels with orbital and radial excitations turn out to be degenerated in the model with a harmonic oscillator potential, which is used in the description of the $q_1q_2q_3$-system). Hence the values $L^P = 0^+,\ 1^+,\ 2^+$ are possible. The states with $L = 0^+,\ 2^+$ correspond to symmetric and mixed O(3) representations, and the states with $L = 1^-$ to antisymmetric ones. Thus, the following structure of baryon supermultiplets with $N = 2$ is possible:

$|\{56\};\ 2^+\rangle_{N=2}$, $|\{56\};\ 0^+\rangle_{N=2}$ — symmetric SU(6)-representations;

$|\{70\};\ 2^+\rangle_{N=2}$, $|\{70\};\ 0^+\rangle_{N=2}$ — mixed SU(6)-representations;

$|\{20\};\ 1^+\rangle_{N=2}$ — antisymmetric SU(6)-representation.

A very complex system of the baryon SU(3)-multiplets with different baryon spins ($J = 1/2,\ 3/2,\ 5/2,\ 7/2$) arises.

The structure of the SU(6) supermultiplets corresponding to the excitations $N = 0,\ 1,\ 2,\ 3$ is shown in Fig. 1a. Fig. 1b shows the baryon families with $N = 0,\ 1,\ 2$ in the approximation excluding all the SU(6)-breaking interac-

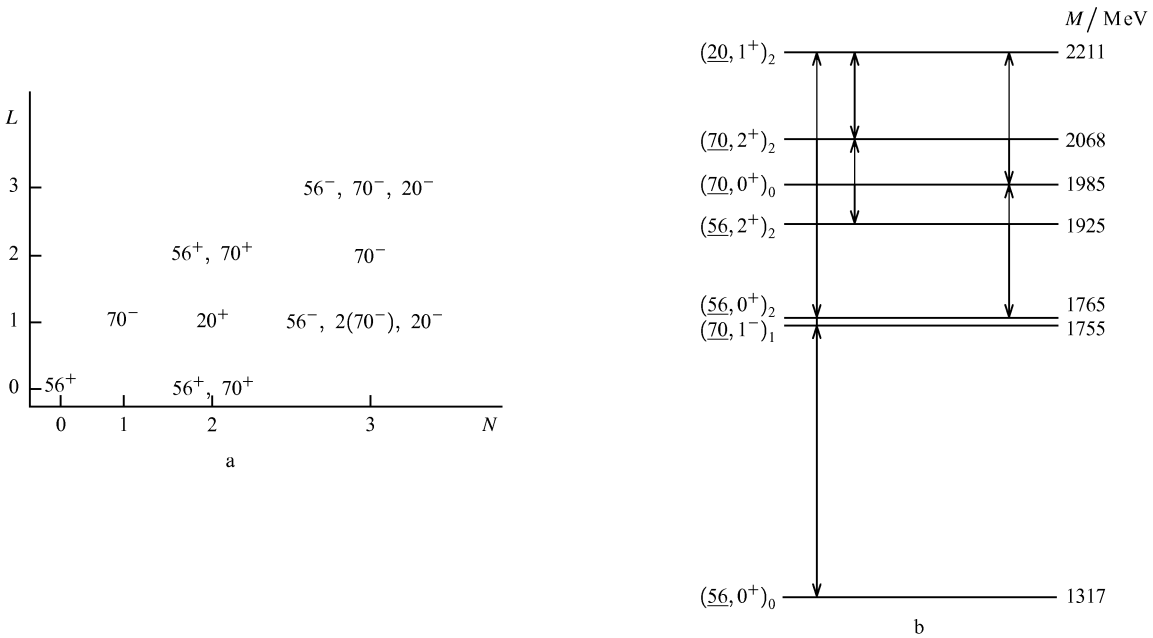

Figure 1. (a) Scheme of the baryonic SU(6)-supermultiplets depending on the orbital momentum L and the excitation number N. (b) Levels of the baryonic SU(6)-supermultiplets for $N = 0, 1, 2$ in the approximation of an unbroken SU(6)-symmetry [20]. The supermultiplet designation: $[\underline{\mathrm{SU}}(6),\ L^P]_N$.

tions. Splitting of the levels [SU(6) breaking] is determined by the spin–spin interactions $\boldsymbol{SS}$, by the unitary-spin interactions $\boldsymbol{FF}$ and by the spin–orbital interactions $\boldsymbol{SL}$. Mixing of the states with $S = 3/2$, $1/2$ from different SU(3)-multiplets with the same quantum numbers J^P also occurs. All that, together with account of radial excitations and upper excited states with $N = 3$, 4, leads to a very complicated systematics for the ordinary qqq-baryons.

The possibility of some simplification, however, was considered. If the quarks q_1 and q_2 form a 'nonexcited' diquark system ($l_\rho = 0$) and all excitations of new levels correpond to only one degree of freedom l_λ, the structure of the SU(6)-multiplets is somewhat simplified. In this case, symmetric O(3)- and SU(6)-representations for even N ($|\{56\};\ 0^+\rangle_{N=0}$, $|\{56\};\ 2^+\rangle_{N=2}$, $|\{56\};\ 4^+\rangle_{N=4}$ etc.) and mixed symmetry representations for odd N ($|\{70\};\ 1^-\rangle_{N=1}$, $|\{70\};\ 3\rangle_{N=3}$ etc.) correspond to the Nth orbital l_λ excitations.

Experimental data on the observed baryons and on the decay channels of nonstrange N^*- and Δ^*-isobars [11] are presented in Table 2 and 3. Table 4 shows attempts to classify the baryonic states corresponding to the excitations with $N \leqslant 2$, by $SU(6) \otimes O(3)$-representations [25].

Let us formulate some problems to be solved by further qqq-baryon investigations (see Refs [21, 24]).

1. Improvement of the data on baryon masses, decay widths, and branching ratios of different decay channels. All these parameters are so far known with large uncertainties and require new measurements. A number of baryonic resonances (especially with heavy masses) have a sufficiently uncertain status (for example, N^* and Δ^* isobars marked by one or two asterisks in Table 2 and 3). For their existence to be finally established, further independent studies are needed.

2. Search for new baryonic states predicted by the quark model, but not experimentally observed so far. In particular, possibilities of discovering the baryonic states that belong to the SU(6)-supermultiplets $|\{20\}; 1^-\rangle_{N=2}$, $|\{70\}; 0^+\rangle_{N=2}$, $|\{70\}; 2^+\rangle_{N=2}$ and those discussed above during consideration of the excited states for $N = 2$ level, are of great interest. Discovery of the majority of non-strange baryons (N^*- and Δ^*-isobar) resulted from the partial-wave analysis (PWA) of the elastic πN-scattering data. The corresponding experiments and the PWA-solutions are insensitive to the baryons that are weakly related to the elastic πN-channel. Precise investigations of the reactions $\pi N \to \pi\pi N$, ΛK, ΣK, ηN, as well as photoproduction processes for these states, which are still at the initial stages, open new possibilities of searching for both the ordinary baryonic resonances of qqq-type, and cryptoexotic states $|qqqq\bar{q}\rangle$ and $|qqqg\rangle$ as well (see Section 4.2).

3. Understanding the nature of baryonic resonance mass spectrum clusterisation. A clustering of nonstrange baryonic isobars is observed in some mass ranges. For example, in the range 1620 MeV $< M <$ 1720 MeV six N^*- and two Δ^*-isobars were registered, and eight Δ^*-

Table 2. The known baryonic resonance data (notation, $L_{2I,\,2J}$, status) [11].

p	P_{11}	****	$\Delta(1232)$	P_{33}	****	Λ	P_{01}	****	Σ^+	P_{11}	****	Ξ^0	P_{11}	****
n	P_{11}	****	$\Delta(1600)$	P_{33}	***	$\Lambda(1405)$	S_{01}	****	Σ^0	P_{11}	****	Ξ^-	P_{11}	****
N(1440)	P_{11}	****	$\Delta(1620)$	S_{31}	****	$\Lambda(1520)$	D_{03}	****	Σ^-	P_{11}	****	$\Xi(1530)$	P_{13}	****
N(1520)	D_{13}	****	$\Delta(1700)$	D_{33}	****	$\Lambda(1600)$	P_{01}	***	$\Sigma(1385)$	P_{13}	****	$\Xi(1620)$		*
N(1535)	S_{11}	****	$\Delta(1750)$	P_{31}	*	$\Lambda(1670)$	S_{01}	****	$\Sigma(1480)$		*	$\Xi(1690)$		***
N(1650)	S_{11}	****	$\Delta(1900)$	S_{31}	***	$\Lambda(1690)$	D_{03}	****	$\Sigma(1560)$		**	$\Xi(1820)$	D_{13}	***
N(1675)	D_{15}	****	$\Delta(1905)$	F_{35}	****	$\Lambda(1800)$	S_{01}	***	$\Sigma(1580)$	D_{13}	**	$\Xi(1950)$		***
N(1680)	F_{15}	****	$\Delta(1910)$	P_{31}	****	$\Lambda(1810)$	P_{01}	***	$\Sigma(1620)$	S_{11}	**	$\Xi(2030)$		***
N(1700)	D_{13}	***	$\Delta(1920)$	P_{33}	***	$\Lambda(1820)$	F_{05}	****	$\Sigma(1660)$	P_{11}	***	$\Xi(2120)$		*
N(1710)	P_{11}	***	$\Delta(1930)$	D_{35}	***	$\Lambda(1830)$	D_{05}	****	$\Sigma(1670)$	D_{13}	****	$\Xi(2250)$		**
N(1720)	P_{13}	****	$\Delta(1940)$	D_{33}	*	$\Lambda(1890)$	P_{03}	****	$\Sigma(1690)$		**	$\Xi(2370)$		**
N(1900)	P_{13}	*	$\Delta(1950)$	F_{37}	****	$\Lambda(2000)$		*	$\Sigma(1750)$	S_{11}	***	$\Xi(2500)$		*
N(1990)	F_{17}	**	$\Delta(2000)$	F_{35}	*	$\Lambda(2020)$	F_{07}	*	$\Sigma(1770)$	P_{11}	*			
N(2000)	F_{15}	**	$\Delta(2150)$	S_{31}	*	$\Lambda(2100)$	G_{07}	****	$\Sigma(1775)$	D_{15}	****	Ω^-		****
N(2080)	D_{13}	**	$\Delta(2200)$	G_{37}	*	$\Lambda(2110)$	F_{05}	***	$\Sigma(1840)$	P_{13}	*	$\Omega(2250)^-$		***
N(2090)	S_{11}	*	$\Delta(2300)$	H_{39}	**	$\Lambda(2325)$	D_{03}	*	$\Sigma(1880)$	P_{11}	**	$\Omega(2380)^-$		**
N(2100)	P_{11}	*	$\Delta(2350)$	D_{35}	*	$\Lambda(2350)$	H_{09}	***	$\Sigma(1915)$	F_{15}	****	$\Omega(2470)^-$		**
N(2190)	G_{17}	****	$\Delta(2390)$	F_{37}	*	$\Lambda(2585)$		**	$\Sigma(1940)$	D_{13}	***			
N(2200)	D_{15}	**	$\Delta(2400)$	G_{39}	**				$\Sigma(2000)$	S_{11}	*	Λ_c^+		****
N(2220)	H_{19}	****	$\Delta(2420)$	$H_{3,11}$	****				$\Sigma(2030)$	F_{17}	****	$\Lambda_c(2625)^+$		***
N(2250)	G_{19}	****	$\Delta(2750)$	$I_{3,13}$	**				$\Sigma(2070)$	F_{15}	*	$\Sigma_c(2455)$		****
N(2600)	$I_{1,11}$	***	$\Delta(2950)$	$K_{3,15}$	**				$\Sigma(2080)$	P_{13}	**	$\Sigma_c(2530)$		*
N(2700)	$K_{1,13}$	**							$\Sigma(2100)$	G_{17}	*	Ξ_c^+		***
									$\Sigma(2250)$		***	Ξ_c^0		***
									$\Sigma(2455)$		**	Ω_c^0		*
									$\Sigma(2620)$		**			
									$\Sigma(3000)$		*	Λ_b^0		***
									$\Sigma(3170)$		*			

Note. For stable and quasistable states, the mass and notation of the baryon are not shown. The baryon status is indicated as follows: **** — existence is certain, and properties are at least fairly well explored; *** — existence ranges from very likely to certain, but further confirmation is desirable and/or quantum numbers, branching fractions, etc, are not well determined; ** — evidence of existence is only fair; * — evidence of existence is poor.

Table 3. Status of N^*- and Δ^*-resonances (those having status *** or **** are included into the main baryon table in Ref. [11]).

Particle	$L_{2I,2J}$	General status	Status as seen in decay channels						
			$N\pi$	$N\eta$	ΛK	ΣK	$\Delta\pi$	$N\rho$	$N\gamma$
N(939)	P_{11}	****							
N(1440)	P_{11}	****	****	*			***	*	***
N(1520)	D_{13}	****	****	*			****	****	****
N(1535)	S_{11}	****	****	****			*	**	***
N(1650)	S_{11}	****	****	*	***	**	***	**	***
N(1675)	D_{15}	****	****	*	*		****	*	****
N(1680)	F_{15}	****	****				****	****	****
N(1700)	D_{13}	***	***	*	**	*	**	*	**
N(1710)	P_{11}	***	***	**	**	*	**	*	***
N(1720)	P_{13}	****	****	*	**	*	*	**	**
N(1900)	P_{13}	**	**					*	
N(1990)	F_{17}	**	**	*	*	*			*
N(2000)	F_{15}	**	**	*	*	*	*	**	
N(2080)	D_{13}	**	**	*	*				*
N(2090)	S_{11}	*	*						
N(2100)	P_{11}	*	*						
N(2190)	G_{17}	****	****	*	*	*		*	*
N(2200)	D_{15}	**	**	*	*				
N(2220)	H_{19}	****	****	*					
N(2250)	G_{19}	****	****	*					
N(2600)	$I_{1,11}$	***	***						
N(2700)	$K_{1,13}$	**	**						
Δ(1232)	P_{33}	****	****	Forbidden by isospin conservation					****
Δ(1600)	P_{33}	***	***				***	*	**
Δ(1620)	S_{31}	****	****				****	****	***
Δ(1700)	D_{33}	****	****			*	***	**	***
Δ(1750)	P_{31}	*	*						*
Δ(1900)	S_{31}	***	***			*	*	**	***
Δ(1905)	F_{35}	****	****			*	**	**	*
Δ(1910)	P_{31}	****	****			*	*	*	*
Δ(1920)	P_{33}	***	***			*	**		**
Δ(1930)	D_{35}	***	***			*			
Δ(1940)	D_{33}	*	*						***
Δ(1950)	F_{37}	****	****			*	****	*	
Δ(2000)	F_{35}	**						**	
Δ(2150)	S_{31}	*	*						
Δ(2200)	G_{37}	*	*						
Δ(2300)	H_{39}	**	**						
Δ(2350)	D_{35}	*	*						
Δ(2390)	F_{37}	*	*						
Δ(2400)	G_{39}	**	**						*
Δ(2420)	$H_{3,11}$	****	****						
Δ(2750)	$I_{3,13}$	**	**						
Δ(2950)	$K_{3,15}$	**	**						

and three N^*-isobars appear in the range 1900 MeV $< M <$ 2000 MeV (see Table 2). Is this clusterisation accidental or do certain regularities take place?

4. Studies of the inner structure of baryonic resonances in the processes of electro- and photoproduction. A wide programme of such experiments to be done on high-current electron accelerators (ELSY, CEBAF), promises to bring a lot of new important results for baryon physics.

3. Models for exotic baryons

Questions connected with possible manifestations of exotic hadron states have been discussed for a very long time. In particular, many dynamical models were elaborated, predicting existence of exotic baryons both with hidden and with open exotics (nonstrange baryons with $I \geqslant 5/2$, strange hyperons with $S > 0$, $S = -1$ and $I > 1$, $S = -2$ and $I > 1/2$, $S = -3$ and $I > 0$). These predictions were made on the grounds of bootstrap calculations, by the

Table 4. Systematics of the known states with light quarks (u, d, s) for SU(6) ⊗ O(3)-representation and N ⩽ 2 [25].

N	$SU(6)^P_L$	$^{2J+1}(F,\ 2S+1)$	Baryons				
0	56^+_0	$^2(8.2)$	N(939)	Λ(1116)	Σ(1193)	Ξ(1318)	
		$^4(10.4)$	Δ(1232)		Σ(1385)	Ξ(1530)	Ω(1672)
1	70^-_1	$^2(1.2)$		Λ(1405)			
		$^4(1.2)$		Λ(1520)			
		$^2(8.2)$	N(1535)	Λ(1670)	Σ(1620)	Ξ(1690)	
		$^4(8.2)$	N(1520)	Λ(1690)	Σ(1690)		
		$^2(8.4)$	N(1650)	Λ(1800)	Σ(1750)		
		$^4(8.4)$	N(1700)		Σ(1670)	Ξ(1820)	
		$^6(8.4)$	N(1675)		Σ(1775)		
		$^2(10.2)$	Δ(1620)				
		$^4(10.2)$	Δ(1700)				
2	56^+_2	$^4(8.2)$	N(1720)	Λ(1890)	Σ(1840)		
		$^6(8.2)$	N(1680)	Λ(1820)	Σ(1915)	Ξ(2030)	
		$^2(10.4)$	Δ(1910)				
		$^4(10.4)$	Δ(1920)		Σ(2080)		Ω(2250)
		$^6(10.4)$	Δ(1905)		Σ(2070)		Ω(2380)
		$^8(10.4)$	Δ(1950)		Σ(2030)		Ω(2470)
	70^-_2	$^4(1.2)$					
		$^6(1.2)$					
		$^4(8.2)$					
		$^6(8.2)$					
		$^2(8.4)$	N(2100)				
		$^4(8.4)$	N(1900)				
		$^6(8.4)$	N(2000)	Λ(2100)			
		$^8(8.4)$	N(1990)	Λ(2020)			
		$^4(10.2)$					
		$^6(10.2)$	Δ(2000)				
	20^+_1	$^2(8.2)$					
		$^4(8.2)$					
		$^2(1.4)$					
		$^4(1.4)$					
		$^6(1.4)$					
	56^+_0	$^2(8.2)$	N(1440)	Λ(1660)	Σ(1660)		
		$^4(10.4)$	Δ(1660)				
	70^+_0	$^2(1.2)$					
		$^2(8.2)$	N(1710)	Λ(1810)	Σ(1770)		
		$^4(8.4)$					
		$^2(10.2)$	Δ(1750)		Σ(1880)		

Note. Notation: F, SU(3)-representation; S, summary quark spin; J, baryon spin; P and L its parity and orbital quantum number. Classification of the states in the Table is not unique. One should bear in mind that the observed baryons with given J^P are, generally speaking, mixed states (from various multiplets by SU(3) and quark spins). The experimental data seem to be in favour of approximate conservation of the quantum numbers L and S.

method of superconvergent sum rules (SSR) for the amplitudes of reggeon scattering on baryons, in the soliton, bag, and chromodynamic string (with junctions) models and in some other approaches. A short review of these theoretical possibilities is given in Ref. [26], where one can find the corresponding references.

The exotic-hadron properties predicted by different models are characterised by a wide diversity. The idea was put forward that the exotic particles may consist of 'quasireal white hadrons' and decay into colourless components without creating additional $q\bar{q}$-pairs from vacuum (these are the so-called super-allowed transitions) [27]. If

Table 5. Classification of exotic baryons in the model of colour clusters with octet and sextet bonds [35, 36].

$(qqq)_{8c}$	$(q\bar{q})_{8c}$	$\lvert(qqq)_{8c} \otimes (q\bar{q})_{8c}\rangle$	Properties of $\lvert(qqq)_{8c} \otimes (q\bar{q})_{8c}\rangle$-baryons		
			Multiplicity by flavours	Summary quark spin	'Mass defect' caused by H'
$\theta^1(8;2)$	$D^9(8;3)$	$\theta^1(8;2) \cdot D^9(8;3)$	$\{9\}$	3/2, 1/2	$-(44/3)\bar{C}$
$\theta^1(8;2)$	$D^9(8;1)$	$\theta^1(8;2) \cdot D^9(8;1)$	$\{9\}$	1/2	$-12\bar{C}$
$\theta^{10}(8;2)$	$D^9(8;3)$	$\theta^{10}(8;2) \cdot D^9(8;3)$	$\{90\}$	3/2, 1/2	$-(28/3)\bar{C}$
$\theta^{10}(8;2)$	$D^9(8;1)$	$\theta^{10}(8;2) \cdot D^9(8;1)$	$\{90\}$	1/2	$12\bar{C}$
$\theta^8(8;4)$	$D^9(8;3)$	$\theta^8(8;4) \cdot D^9(8;3)$	$\{72\}$	5/2, 3/2, 1/2	$-(4/3)\bar{C}$
$\theta^8(8;4)$	$D^9(8;1)$	$\theta^8(8;4) \cdot D^9(8;1)$	$\{72\}$	3/2	$4\bar{C}$
$\theta^8(8;2)$	$D^9(8;3)$	$\theta^8(8;2) \cdot D^9(8;3)$	$\{72\}$	3/2, 1/2	$-(8/3)\bar{C}$
$\theta^8(8;2)$	$D^9(8;1)$	$\theta^8(8;2) \cdot D^9(8;1)$	$\{72\}$	1/2	0

Note. Notation: $\theta^F(c;2s+1)$, wave function $(qqq)_c$; $D^F(c;2s+1)$, wave function $(q\bar{q})_c$; here c is representation by colour, F multiplicity of the multiplet by flavours, s the summary quark spin. $\bar{C} \approx 15$ MeV.

$(qq\bar{q})_{\bar{6}c}$	$(qq)_{6c}$	$\lvert(qq\bar{q})_{\bar{6}c} \otimes (qq)_{6c}\rangle$	Properties of $\lvert(qq\bar{q})_{\bar{6}c} \otimes (qq)_{6c}\rangle$-baryons		
			Multiplicity by flavours	Summary quark spin	'Mass defect' caused by H'
$A(\bar{6};2)$	$D^{\bar{3}}(6;3)$	$A(\bar{6};2) \cdot D^{\bar{3}}(6;3)$	$\{27\}$	3/2, 1/2	$-(28/3)\bar{C}$
$S(\bar{6};4)$	$D^{\bar{3}}(6;3)$	$A(\bar{6};4) \cdot D^{\bar{3}}(6;3)$	$\{54\}$	5/2, 3/2, 1/2	0
$S(\bar{6};2)$	$D^{\bar{3}}(6;3)$	$S(\bar{6};2) \cdot D^{\bar{3}}(6;3)$	$\{54\}$	3/2, 1/2	$4\bar{C}$
$A(\bar{6};2)$	$D^6(6;1)$	$A(\bar{6};2) \cdot D^6(6;1)$	$\{54\}$	1/2	$-4\bar{C}$
$S(\bar{6};4)$	$D^6(6;1)$	$S(\bar{6};4) \cdot D^6(6;1)$	$\{108\}$	3/2	$(16/3)\bar{C}$
$S(\bar{6};2)$	$D^6(6;1)$	$S(\bar{6};2) \cdot D^6(6;1)$	$\{108\}$	1/2	$(28/3)\bar{C}$

Note. Notation: $A(c;2s+1)$ is antisymmetric function (by qq) for $(qq\bar{q})_{\bar{6}c}$-clusters, $S(c;2s+1)$ is symmetric function (by qq) for $(qq\bar{q})_{\bar{6}c}$-cluster; $D^F(c;2s+1)$ is wave function for $(qq)_{6c}$-cluster. Multiplicity structure of the states $A(\bar{6};2)$ and $(\bar{6};4$ and $2)$ by flavours is $(3+\bar{6})$ and $(3+15)$, respectfuly. $\bar{C} \approx 15$ MeV.

there is no kinematic suppressions such hadrons can have very large decay widths and are, therefore, practically unobservable. According to Ref. [28], they can only appear as singularities in the P-matrix.

In Refs [29, 30] predictions were made about the possible existence of a whole series of exotic baryons with increasing spin J and isospin I, for which the relationship $I = J$ is valid. These predictions rely on the SSR-formalism-based analysis of scattering of reggeons α_i with isospins $I_i = 1$ on nucleons and isobars. Introduction of the corresponding exotic baryons saturating the sum rules was shown to be necessary in order to obtain self-consistent results. Cascade decays like $|I, J\rangle \to |I-1, J-1\rangle + \pi$ etc. must dominate for the exotic baryons considered in this model. The lightest exotic baryon has the quantum numbers $J = I = 5/2$ and is denoted E_{55}.

The SSR model predicts possible masses for this baryon to be $1.4\ \text{GeV} < M(E_{55}) < 1.7\ \text{GeV}$. For the E_{55}-baryons with $M < 1.5$ GeV, a narrow enough decay width $\Gamma(E_{55} \to \Delta + \pi) < 100$ MeV is predicted. However, the decay widths of such baryons rapidly increase with mass [29–31]. Strange exotic hyperons must also exist in this model [26], for example Σ_E^* with $S = -1$, $I = 2$, Ξ_E with $S = -2$ and $I = 3/2$, Ω_E with $S = -3$ and $I = 1$. The large decay width makes states of this type practically unobservable if their masses exceed the decay threshold by 250– 300 MeV.

However, it was also suggested that there are relatively narrow exotic states whose existence is due to the complex internal colour structure of these objects and the peculiarities of colour dynamics [32–35]. If an exotic hadron consists of two coloured parts that are separated in space (for example, because of the presence of a centrifugal barrier), then its decay to colour singlet final states will be suppressed. Such exotic particles can be characterised by normal or even anomalously narrow decay widths depending on the degree of suppression that, in turn, is associated with the mechanism of the quark rearrangement of the decaying states.

Let us consider a model with colour clusters applied to five-quark baryons [34, 35]. These baryons with the valence quark content $|qqqq\bar{q}\rangle$ are colour singlets, like all the observed hadrons. We assume that their inner structure consists of two colour clusters separated by a centrifugal barrier. For the lightest exotic baryons, the colour clusters are in the states with zero intrinsic angular momenta, and the orbital momentum L is between the clusters.

The following colour representations of clusters are possible (in $SU(3)_{\text{colour}}$, or $SU(3)_c$ group):

$$|qqqq\bar{q}\rangle_{1c} = |(qqq)_{8c} \otimes (q\bar{q})_{8c}\rangle \tag{14}$$

(system with colour octet bonds),

$$|qqqq\bar{q}\rangle_{1c} = |(qq\bar{q})_{\bar{6}c} \otimes (qq)_{6c}\rangle \tag{15}$$

(system with colour sextet bonds),

$$|qqqq\bar{q}\rangle_{1c} = |(qq\bar{q})_{3c} \otimes (qq)_{\bar{3}c}\rangle \tag{16}$$

(system with colour triplet bonds).

Indeed, by using the Young diagram multiplication technique, one can easily show that the corresponding quark clusters are characterised by the following representations of the $SU(3)_c$ group:

$$qqq\}[3]_c \otimes [3]_c \otimes [3]_c = [10]_c + [8]_c + [8]_c + [1]_c\,,$$

$$q\bar{q}\}[3]_c \otimes [\bar{3}]_c = [8]_c + [1]_c\,,$$

$$qq\bar{q}\}[3]_c \otimes [3]_c \otimes [\bar{3}]_c = [15]_c + [\bar{6}]_c + [3]_c + [3]_c\,,$$

$$qq\}[3]_c \times [3]_c = [6]_c + [\bar{3}]_c\,.$$

Therefore, the colour singlet exotic five-quark baryons can indeed have a structure presented by expressions (14)–(16).

Of course, the baryon state $(qqq)_{1c} \otimes (q\bar{q})_{1c}$ is also possible, but for this state a super-allowed decay into a baryon and a meson will take place. Such an exotic baryon is expected to have a very large decay width and is practically unobservable†. The $|(qq\bar{q})_{3c} \otimes (qq)_{\bar{3}c}\rangle$ system is also sufficiently unstable and can be easily dissociated into baryons and mesons:

$$|(qq\bar{q})_{3c} \otimes (qq)_{\bar{3}c}\rangle \to |q\bar{q}\rangle_{1c} + |q_{3c} \otimes (qq)_{\bar{3}c}\rangle$$
$$\to |q\bar{q}\rangle_{1c} + |qqq\rangle_{1c}\,. \tag{17}$$

Here again, a super-allowed decay with a large width will occur.

On the other hand, the decays of baryons with colour octet or sextet bonds may be greatly suppressed by the decolourising mechanism of the quark rearrangement for colour clusters in the decay processes. Therefore, there are reasons to expect a possible existence of comparatively narrow or even anomalously narrow exotic baryonic states of the $|(qqq)_{8c} \otimes (q\bar{q})_{8c}\rangle$ and $|(qq\bar{q})_{\bar{6}c} \otimes (qq)_{6c}\rangle$ types.

We can now consider a model of baryons with colour octet and sextet bonds in more detail. We will designate the colour clusters as

$$(qqq)_{8c} = \theta^F(c; 2s+1), \qquad (q\bar{q})_{8c} = D^F(c; 2s+1)\,,$$

$$(qq\bar{q})_{\bar{6}c} = \begin{cases} A(c;2s+1), \text{ if two quarks qq are in an antisymmetric by flavour state,} \\ S(c;2s+1), \text{ if qq are in a symmetric by flavour state,} \end{cases}$$

$$(qq)_{6c} = D^F(c;\, 2s+1)\,,$$

(see Refs [34, 35]). Here c is $SU(3)_c$, representation, s the combined quark spin of the cluster, and F specifies its flavour multiplicity. By using the Pauli exclusion principle, one can obtain characteristics of the quark clusters and octet-bounded and sextet-bounded baryon states shown in Table 5.

At the present time, estimates for the masses of exotic baryons in the model of colour clusters cannot be reliably obtained from theoretical considerations. As was discussed in Refs [34, 35], multiquark baryons fall on Regge trajectories $L = \alpha_0 + \alpha'_c M^2$ (L is the orbital momentum between the coloured clusters, M is the baryon mass). The slopes of the trajectories α'_c depend on the colour of the clusters. They are estimated in the bag model as $\alpha'_8 = (2/3)\alpha'_3$, $\alpha'_6 = (2/5)\alpha'_3$ with the quadratic Casimir operators for colour. The slope of the trajectory α'_3 is known to be $\alpha'_3 \approx 0.9\ \mathrm{GeV}^{-2}$ from the hadron spectroscopy data. This gives $\alpha'_8 \approx 0.6\ \mathrm{GeV}^{-2}$ and $\alpha'_6 \approx 0.57\ \mathrm{GeV}^{-2}$. In order to fix the parameter α_0 it should be possible to use the experimental data on the first multiquark baryons which would be observed, and their quantum numbers‡.

After that, masses of all these exotic baryons can be estimated to a first approximation with the use of a phenomenological relation $M_L = [(L - \alpha_0)/\alpha'_c]^{1/2}$ that accounts for the orbital excitation.

Furthemore, one needs to take into account the corrections connected with quark–quark interactions in clusters that induce mass splitting. These corrections can be rather reliably determined by accounting for the short-range colour–magnetic spin–spin interactions inside the clusters (in the one-gluon approximation), described by the Hamiltonian

$$H' = -\sum_{i>j} C_{ij}\lambda_i^\alpha \sigma_i \lambda_j^\alpha \sigma_j\,. \tag{18}$$

Here σ_i are the Pauli spin matrices, λ_i^α are the Gell-Mann SU(3)-matrices, and the summation is performed over all quarks entering the cluster. For the coefficients C_{ij}, the averaged value $C_{ij} = \bar{C} = 15$ MeV is used. Values of H' for different states are listed in Table 5.

In addition to the L-excitation and mass splitting due to the colour–magnetic interactions (18), one needs to take into account the strange quark mass excess relative to the constituent mass of the u- and d-quarks, which is $\Delta m \approx 175$ MeV for each strange quark in the baryon.

Consider now some consequences of the colour octet and colour sextet models discussed in Refs [32–35]. As is seen from Table 5, the simplest five-quark baryon family consists of flavour nonets with the combined quark spins $S = s_1 + s_2 = 3/2,\ 1/2$, which are denoted as [9; 3/2] and [9; 1/2]. They correspond to the octet-bounded cluster structures with $\theta^1(8;\,2) \cdot D^9(8;\,3)$ and $\theta^1(8;\,2) \cdot D^9(8;\,1)$. The five-quark baryons belong to the families with spin $J = L + 3/2$ and $J = L + 1/2$. As $\theta^1(8;\,2)$ is a flavour singlet, it has the uds quark content. Therefore, all five-quark baryons belonging to these flavour nonets contain strange quarks (states with open and hidden strangeness). Baryons with open exotics ($S > 0$, $I > 3/2$, $Q > 2$) do not belong to such nonets.

The model with colour octet bonds predicts the existence of baryon pairs with a mass splitting around 40–50 MeV because of a difference in 'mass defects' H' for the clusters $D^9(8;3)$ and $D^9(8;1)$ (see Table 5). An interesting feature of the model is a 'mass inversion' for the colour octets: $M[D^9(8;3)] < M[D^9(8;1)]$. As is well known, for colourless mesons the situation is reversed: the masses of vector mesons exceed the pseudoscalar ones (in the notations in use $M[D^9(1;3)] > M[D^9(1;1)]$)).

Flavour 90- and 72-plets of five-quark baryons in the model with colour octet bonds (see Table 5) have a much more complicated structure and include both states with strange quarks and those containing only u- and d-quarks. Baryons with open exotic quantum numbers belong to these families as well. It should be stressed that not all the five-quark baryons can be narrow enough (owing to decolourising quark rearrangement mechanism for colour clusters

† Unless this decay is very strongly suppressed because of kinematics (i.e. decay close to the threshold or even a bound state).

‡ The data used in Refs [34, 35] for α_0 estimation were not confirmed by later works.

during decays), because of cascade decays of more heavy exotic baryons into lighter ones with emission of additional pions.

The possibility of the five-quark baryon decays into hybrid hadrons due to disruption of a colour 'string' between the θ- and D-clusters with creation of a gluon pair at the 'place of disruption' $|\theta D\rangle \to |qqqG\rangle + |q\bar{q}G\rangle$ was also considered. Analysis made in Ref. [35] showed that the most narrow five-quark baryons with colour octet bonds probably must belong to the [9; 3/2] and [72; 5/2] families.

Baryon families with colour sextet bonds (see Table 5) also have a rather complex structure. Some properties of these baryons are discussed in Refs [34–36]. In particular, for the exotic sextet-bounded state without strange quarks, one predicted the decays with a very pronounced signature — into a baryon and an M-baryonium, which in turn decays into a baryon-antibaryon pair, for example

$$|(qq\bar{q})_{\bar{6}c} \otimes (qq)_{6c}\rangle \to |qq\bar{q}\bar{q}\rangle + |qqq\rangle \to p\bar{p}p\,.$$

To conclude this section, one should stress that, although the model of hadrons with colour clusters allows one qualitatively to explain existence of narrow and even anomalously narrow baryons and mesons, it nevertheless gives no precise a priori predictions in this field (see, for example, Ref. [37]). The problem of the possible existence of such unusual particles can be solved only experimentally, so the search for exotic baryons in the mass range 1.5–4 GeV seems to be very interesting.

4. Methods for selecting exotic hadrons

The search for exotic states plays a particular role in recent experiments on nanobarn hadron spectroscopy. One of the most complicated problems is the identification of cryptoexotic hadrons, because only indirect dynamical properties, such as unusual decay channels, anomalously narrow decay width, anomalous production processes, and so on, can give one information on the exotic valence structure of these particles. The experimental facilities assigned to the study of exotic hadrons should have large acceptance and high sensitivity because the cross sections for their production are, as a rule, not very large.

For the reliable selection of the signal against the background, the studied process should have as distinct signature a as possible.

The success of experiments aimed at the search for exotic hadrons is, to a great extent, determined by the appropriate choice of exclusive and quasi-exclusive processes with hadronic systems for which some qualitative consideration can predict more distinct manifestations of the exotic states. We provide some examples of such an approach in sections 4.1–4.3. Noticeable progress has been made in searching for the exotic particles, in spite of all the difficulties discussed above, and several serious exotic meson candidates have been established here in the last few years.

In contrast to the large advances made in searching for exotic mesons, the situation with exotic baryons looks less hopeful. The searches for baryons with open exotics (with an anomalous isospin, strangeness, etc.) have so far brought no definite results, although there were several experiments in which some evidences for these objects was obtained. However, all of them have poor statistical significance. Theoretical considerations connected with the search for such exotic baryons can be found in Refs [29–30], and some experimental results will be discussed below (see section 7).

The search for cryptoexotic baryons also encounters some difficulties, which can be illustrated below by example of baryons with hidden strangeness $B_\phi = |qqqs\bar{s}\rangle$. The notation B_ϕ is introduced in analogy with mesons (ϕ-meson is a state with hidden strangeness $s\bar{s}$).

The possibilities of detecting cryptoexotic baryons are to a large extent connected with the use of peculiarities of their decay properties:

(a) unusual branchings of some decay channels;

(b) existence of massive baryons with anomalously narrow widths.

Initially we consider the characteristic decay channels for cryptoexotic baryons.

4.1 Decay channels for baryons with hidden strangeness

One would expect that the main decay channels for multiquark exotic baryons with isotopic spins $I = 1/2$ or 3/2 and with hidden strangeness $B_\phi = |qqqs\bar{s}\rangle$ must be as follows:

$$B_\phi \to \begin{cases} KY & (19)\\ K^+K^-N;\ K^+K^-\Delta & (20)\\ \phi N;\ \phi\Delta & (21)\\ \eta N;\ \eta\Delta & (22)\\ \eta' N;\ \eta'\Delta & (23)\end{cases}$$

(Of course, the emission of additional pions is possible in all these decays.) Here $Y = \Lambda;\ \Sigma;\ \Sigma^*(1385)$ and other hyperon states.

Processes (19)–(23) seems to be quite natural decay channels of exotic baryons with hidden strangeness B_ϕ for the emission of their strange valence quark constituents (the ϕ-meson is an almost pure $s\bar{s}$ state, and wave functions of η- and η'-mesons contain large admixtures of the $s\bar{s}$-component due to a strong mixing in the pseudoscalar meson nonet). Decays of B_ϕ, in which strange quarks do not appear in particles formed at the final states, are suppressed by a continuous quark line rule (OZI selection rule), and must be less probable.

Decay processes of type (19)–(23) can also occur with a significant probability for hybrid exotic baryons $B_G = |qqqg\rangle$. Data on radiative decays $J/\psi \to \gamma\eta;\ \gamma\eta'$ show that, η- and η'-mesons prove to be strongly coupled with two-gluon intermediate states (see, for example, review [17]). Hence a conclusion was drawn about the comparatively high probability of processes with the η- and η'-meson emission for glueballs and hadrons with enriched valence gluon component (for information on this mechanism of gluon decolourisation see Ref. [38]).

On the other hand, since gluons are characterised by flavour independent coupling with quark–antiquark pairs, decays of the hybrids with emission of strange particles or particles enriched by the $s\bar{s}$-component would be expected to have a higher probability in comparison with the same decays of the ordinary nonstange qqq-baryons. Note that the strong breaking of the ideal mixing in a pseudoscalar meson nonet means that the η- and η'-mesons are just the hadrons with enriched valence $s\bar{s}$-component.

Let us consider the experimental data on decays of the known N^*- and Δ^*-isobars, presented in [11] (see also Table 3). These data show that the majority of the non-

strange baryons have a very low probability to decay by ηN; ΛK; ΣK channels. Such decays are reliably registered only for a few baryon states. The probability of these decays does not exceed a few per cents, as a rule. However, there are two states (see [11]) with an anomalously large decay branching $BR(N^* \to N\eta)$:

$$N(1535) = S_{11}(1535),\ J^P = 1/2^-,$$
$$BR[N(1535) \to \eta N] \approx 30\% - 50\% \ ; \tag{24}$$
$$N(1710) = P_{11}(1710),\ J^P = 1/2^+,$$
$$BR[N(1710) \to \eta N] = 20\% - 40\% \tag{25}$$

(see Ref. [14] for further details).

Note that the state N(1710) is also characterised by the relatively high probability of decaying with emission of strange particles:

$$BR[N(1710) \to K\Lambda] \approx 15\% \ ,$$
$$BR[N(1710) \to \Sigma K] \approx 2 - 10\% \ .$$

What is the nature of this anomaly and is it possible to assume that the isobars N(1535) and N(1710) are actually hybrid baryons? In order to answer these questions, we should consider the systematics of the lightest hybrid baryons and their quantum numbers [15, 39, 40]†.

As was shown in Section 2, the ground states for the ordinary colourless baryons $(qqq)_{1c}$ belong to the SU(6)-representation

$$|\{56\};\ 0^+\rangle = {}^2[8]\,(J^P = 1/2) + {}^4[10]\,(J^P = 3/2^+)\,,$$

and the following orbitally-excited isobars belong to a 70-plet

$$|\{70\};\ 1^-\rangle = {}^2[1]\,(J^P = 1/2^-) + {}^2[8]\,(J^P = 1/2) + {}^4[8]\,(J^P = 3/2^-) + {}^2[10]\,(J^P = 1/2^-).$$

But for hybrid baryons $[(qqq)_{8c} \cdot g_{8c}\rangle$ the colour quark parts of the wave functions of the ground states belong to the $\{70\}^+$ super-multiplet because of the Pauli principle. The lightest hybrid baryons with orbital momentum between $(qqq)_{8c}$ and g_{8c} is $L_g = 0$ have then the following structure:

$$\begin{aligned} &|\{70\}^+ \otimes g_{TE}(1^+)\rangle \\ &= ([1],\ 1/2^+ \text{ or } 3/2^+) + ([8],\ 1/2^+ \text{ or } 3/2^+) \\ &\quad + ([8],\ 1/2^+ \text{ or } 3/2^+,\ \text{ or } 5/2^+) \\ &\quad + ([10],\ 1/2^+ \text{ or } 3/2^+)\,. \end{aligned} \tag{26}$$

The N(1535) baryon is the $J^P = 1/2^-$ state and thus does not belong to this family. It may be interpreted as an $N\eta$-molecule (its mass is close to the threshold for $N^* \to N\eta$ decay). On the other hand, N(1710) is a $1/2^+$-baryon that can be a member of the $|\{70\}^+ \otimes g_{TE}\rangle$ supermultiplet.

There were also discussions on the possible hybrid interpretation of other isobars, for example $[N(1470);\ 1/2^+]$ (Roper resonance), $[N(1600);\ 3/2^+]$, $[N(1720);\ 3/2^+]$ (see Refs [15, 39]). We will consider these possibilities below (see Section 4.3.5).

To summarise the results of this section, it should be noted that although some not very reliable hybrid baryon candidates can be among the known N^*- and Δ^*-isobars (see Table 3), there are no readily serious candidates for five-quark baryons with hidden strangeness among them (especially for narrow baryonic states). Does this mean that we already know all baryonic resonances and that such exotic pentaquark states do not exist at all? Certainly this is not the case! In order to make sure of this, one should consider processes in which all the known N^*- and Δ^*-isobars were detected. As is known, all such processes can be divided into two classes:

(a) formation reactions with direct registration of resonance in the s-channel for the corresponding process;

(b) production reactions for hadrons at high energies.

4.2 Formation reactions (resonances in the s-channel)

Practically all of the known isobars were observed as s-channel resonances (Fig. 2a) in the formation processes by a detailed partial-wave analysis of pion elastic πN-scattering and charge-exchange reaction data. This partial-wave analysis was performed by a number of independent groups. Some limited data on the reactions $\pi N \to \eta N$, $\pi N \to \Lambda K$, $\pi N \to \Sigma K$, $\pi N \to \pi\pi N$ and on pion photoproduction were also used in this study. However, the key results were obtained by studying elastic processes $\pi N \to \pi N$.

A distinctive feature of all known N^*- and Δ^*-isobars is their strong elastic channels $[BR(N^*, \Delta^* \to N\pi) \gtrsim 5\% - 10\%]$, resulting in large resonance cross sections. Indeed, the Breit–Wigner resonance cross section in the s-channel has the form

$$\sigma_{res} = \frac{2J+1}{(2S_1+1)(2S_2+1)}\,\frac{4\pi}{K^2}\,BR_{in}BR_{out}\,. \tag{27}$$

Here J is the resonance spin, S_1 and S_2 are the spins of the colliding particles, K is their momentum, and BR_{in} and BR_{out} are the branching ratios for the input and output decay channels. The resonance cross-sections for all known baryons that appear in the elastic scattering are estimated as follows:

$$\sigma_{res} = \frac{2J+1}{2}\,\frac{4\pi}{K^2}\,[BR(B \to \pi N)]^2 > 10^{-27} - 10^{-28}\ \text{sm}^2\,. \tag{28}$$

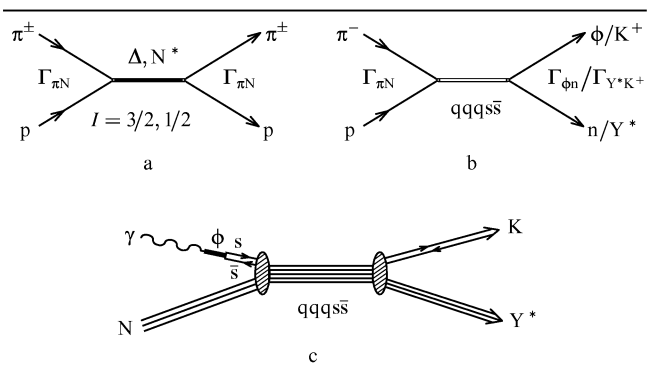

Figure 2. Diagrams for baryonic resonance formation processes in the s-channel: (a) baryons $|qqq\rangle$ in the elastic πN-scattering; (b) exotic baryons with hidden strangeness $B_\phi = |qqqs\bar{s}\rangle$ in the reactions $\pi^- + p \to B_\phi \to \phi n$, Y^*K; (c) exotic baryons B_ϕ in the photoproduction reaction $\gamma + N \to B_\phi \to Y^*K$ (vector meson dominance approach).

† As is known from the bag model, the gluon excitation energy is approximately 550 – 700 MeV, and the expected masses of the lightest hybrid baryons can be as low as 1500 MeV. In some other models these masses exceed 2000 – 2200 MeV.

If there are states that are weakly coupled with the elastic channel, they cannot be seen in the analysis of elastic processes because of the large nonresonance background. For example, for cryptoexotic baryons with hidden strangeness $B_\phi = qqqs\bar{s}$, the decay mode $B_\phi \to \pi N$ is suppressed by the OZI selection rule and is estimated as $BR(B_\phi \to \pi N) \sim 10^{-3}$. For these baryons, produced in elastic πp scattering, $\sigma_{res} \sim 10^{-31} - 10^{-32}$ cm^2, and they cannot be seen in this process.

On the other hand, high-precision scanning of the cross sections over the energy may offer certain prospects for the search for the resonance production of the cryptoexotic baryons with hidden strangeness (Fig. 2b) in a number of exclusive processes [41]

$$\pi^- + p \to B_\phi\,(I = 1/2) \to \phi + n\,, \qquad (29)$$
$$\hookrightarrow K^+K^-$$

$$\pi^- + p \to B_\phi\,(I = 3/2) \to \phi \qquad + \Delta(1232)^0, \qquad (30)$$
$$\hookrightarrow K^+K^- \quad \hookrightarrow p\pi^-$$

$$\pi^- + p \to B_\phi\,(I = 3/2) \to \phi \qquad + \Delta(1232)^{++}, \qquad (31)$$
$$\hookrightarrow K^+K^- \quad \hookrightarrow p\pi^-$$

$$\pi^- + p \to B_\phi\,(I = 1/2) \to \Lambda \qquad + K^0, \qquad (32)$$
$$\hookrightarrow p\pi^- \quad \hookrightarrow \pi^+\pi^-$$

$$\pi^- + p \to B_\phi\,(I = 3/2,\ 1/2) \to \Sigma^0 \qquad + K^0, \qquad (33)$$
$$\hookrightarrow \Lambda\gamma \quad \hookrightarrow \pi^+\pi^-$$
$$\hookrightarrow p\pi^-$$

$$\pi^- + p \to B_\phi\,(I = 3/2,\ 1/2) \to \Sigma^- + K^+, \qquad (34)$$
$$\hookrightarrow n\pi^-$$

$$\pi^+ + p \to B_\phi\,(I = 3/2) \to \Sigma^+ + K^+, \qquad (35)$$
$$\hookrightarrow p\pi^0$$

$$\pi^- + p \to B_\phi\,(I = 3/2,\ 1/2) \to \Sigma(1385)^- + K^+, \qquad (36)$$
$$\hookrightarrow \Lambda\pi^-$$

$$\pi^+ + p \to B_\phi\,(I = 3/2) \to \Sigma(1385)^+ + K^+, \qquad (37)$$
$$\hookrightarrow \Lambda\pi^+$$

$$\pi^- + p \to B_\phi\,(I = 1/2) \to \Lambda(1520) + K^0\,. \qquad (38)$$
$$\hookrightarrow pK^-$$

Reactions (29)–(31), forbidden by the OZI rule, can be especially useful for this purpose. In fact, nonresonance processes of that kind may be more strongly suppressed by the OZI rule than processes of formation of multiquark hadrons with a complex internal colour structure. Therefore the background conditions for distinguishing exotic resonance B_ϕ in the direct channels (29)–(31) may be much more favorable than for ordinary reactions with large cross sections. For baryons with hidden strangeness the expected branching ratio for this process is $BR(B_\phi \to \phi N) > 0.05 - 0.1$. It follows from this inequality and from Eqn (27) that the resonance cross section in Eqn (29) must be $\sigma_{res}(B_\phi) \gtrsim 10^{-29}$–$10^{-30}$ cm^2.

The existing data on reactions (29)–(38) (see, for example, Ref. [42]) are rather poor (they are obtained in different experiments, that is with additional normalisation and other systematic uncertainties). The accuracy reached even for the comparatively well-studied processes (32)–(35) are completely insufficient. These data are not very useful for the systematic search for the B_ϕ resonances in the direct channel (especially for narrow resonances).

Thus, it is clear that new precise and high-luminosity experiments with global energy scan of total cross sections and angular distributions for reactions (29)–(38) in the intermediate energy range ($P_\pi = 1.25 - 6.0$ GeV, i.e. 1.8 GeV $\leqslant \sqrt{s} \leqslant 3.5$ GeV) with steps of the order of $\Delta(\sqrt{s}) \approx 25 - 30$ MeV are required in order to reduce statistical and systematic uncertainties down to 2% – 3% and to perform a detailed partial-wave analysis of these processes.

Note that in such an analysis the study of angular correlations in cascade decays of the secondary particles (for example, $\phi \to K^+K^-$ or $\Sigma(1385) \to \Lambda\pi$, $\Lambda \to p\pi^-$) may play a major role. In order to reduce additional systematic errors, it is desirable to perform simultaneous measurements for different reactions on the same setup.

In addition to processes (29)–(38), it would also be interesting to scan the cross sections of the reactions

$$\pi^- + p \to \begin{cases} \omega + n, & (39) \\ \hookrightarrow \pi^+\pi^-\pi^0;\ \pi^0\gamma & \\ \eta' + n\,, & (40) \\ \hookrightarrow \pi^+\pi^-\gamma;\ \pi^+\pi^-\eta & \end{cases}$$

as well as for the corresponding processes with $\Delta(1232)$-isobar and for a number of other reactions. The study of process (39) in conjunction with process (29) is important for the interpretation of results of measuring cross-sections of this process from the point of view of the OZI selection rules. The data given by process (40) could be used in searching for the hybrid baryons $B_G = qqqg$, decaying by the channel $B_G \to \eta' n$ which can have an anomalously large branching in this case.

In connection with the initial work of the CEBAF strong current electron accelerator of continuous action with the energy $E_e = 4$ GeV (and some other accelerators of lower energy and intensity), one should bear in mind that it becomes possible to study baryon resonances within the energy range $\sqrt{s} \lesssim 2.75$ GeV in the direct channels, with a detailed energetic scanning of the cross sections for photoproduction reactions $\gamma p \to \phi p$; $\phi\Delta^+$; ΛK^+; $\Sigma(1385)^0 K^+$ and so on. These reactions are analoguous to (29)–(38).

The formation processes in the photon beam (Fig. 2c) can be more favourable to the search for cryptoexotic baryons with hidden strangeness as resonances in the direct channel, than the πN-reactions, since a factor caused by the 'elastic' decay width $\Gamma(B_\phi \to \pi N)$ for the input channel, is present in the resonance cross-sections for the last processes. Small 'elastic' widths for exotic states complicate their observation against the background, formed by non-resonance hadron processes and the ordinary isobar contribution. On the other hand, as is seen from Fig. 2c, the vector dominance model, in which the photon is characterised by a significant coupling with the ϕ-meson, can be a natural mechanism for effective s-channel formation of the cryptoexotic baryons with hidden strangeness in the photoproduction reactions.

4.3 Production reactions

As we have seen above, the study of formation reactions and baryon resonances in the s-channel have not yet allowed one to undertake effective search for cryptoexotic baryons.

Another method of isolating exotic states is connected with the detailed study of the effective-mass spectra of ϕp, $\Lambda(1520)K^+$, $\Sigma(1385)^0K^+$ and other baryon systems enriched by $s\bar{s}$-quarks, in a number of production reactions (for example, in the diffractive production or in exclusive and semi-exclusive processes). During the last decade a number of experiments of this type were performed. Some of their results will be discussed below (see Section 5).

The first data obtained in the new, very sensitive SPHINX experiment for the diffractive production of baryon states by means of a proton beam with an energy of $E_p = 70$ GeV will also be presented in this review (see Section 6). However, before discussing the results of the study of baryon production reactions, we outline briefly some general properties of the most promising processes of this type.

4.3.1 Diffractive and coherent production processes. As noted in a number of papers (see Refs [33, 34, 12–14, 43–46]), the diffractive production processes with pomeron exchange offer new possibilities to the search for exotic hadrons. Such considerations were put forward rather a long time ago and were first discussed in connection with the possible exotic component of pomeron. One even estimated on these grounds the crosssections of the exotic hadron production in diffractive reactions, predicted to be at the microbarn level [34]. According to modern theoretical ideas, pomeron is a multigluon system, which leads to special mechanisms of exotic states production in diffractive processes (see the diagrams in Fig. 3).

It is apparent that only the states with the same charge and flavour as those of the primary hadrons can be produced in diffractive processes. Moreover, there are additional restrictions on the spin and parity of the formed hadrons which are stipulated by the Gribov–Morrison selection rule. According to this rule, the change in parity ΔP occurring as a result of the transition from the primary hadron to the diffractively produced hadronic system, is connected with the corresponding change in the spin ΔJ through the relation $\Delta P = (-1)^{\Delta J}$. For example, because of this rule, in the proton diffraction (for proton $J^P = 1/2^+$), only baryonic states with natural sets of quantum numbers $1/2^+$, $3/2^-$, $5/2^+$, $7/2^-$, etc. can be excited. The Gribov–Morrison selection rule is not a rigorous law and has an approximate character.

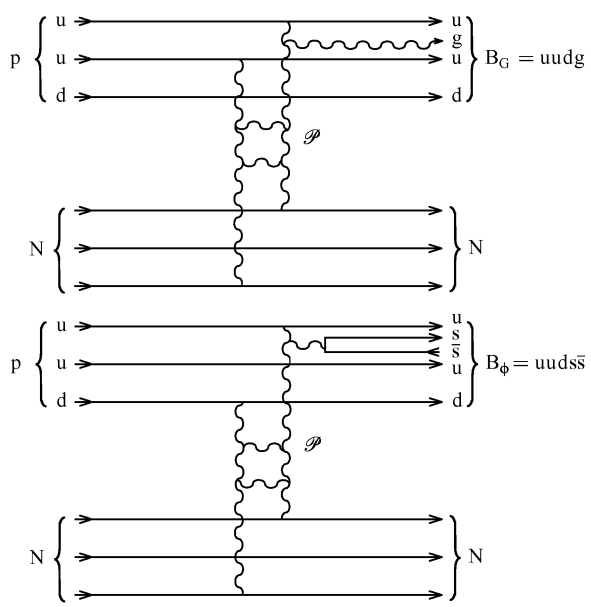

Figure 3. Diagrams for exotic baryon production in the diffraction processes with pomeron exchange. The pomeron $\mathscr{P}$ is a multigluon system.

In reactions of diffractive particle production, the mechanism of pomeron exchange can induce coherent processes on the target nucleus; in such processes the nucleus acts as a discrete unit. These processes are easily identified from the event distribution in the transverse momentum of the final-state particle systems. They manifest themselves as diffractive peaks with large values of the cone slope parameter, determined by the size of the nucleus: $dN/dP_T^2 \approx \text{const} \times \exp(-bP_T^2)$, $b \sim (8-10)A^{2/3}$ GeV^{-2}.

Owing to the different absorption mechanisms of single-particle and multiparticle objects in nuclei, coherent processes could serve as an effective tool for isolating resonances against the multiparticle nonresonant background (see, for example, Ref. [47]).

To search for states A with flavours different from those of the primary particles it is possible to use the diffractive associated pair production processes for the hadron systems under study: $h + N \to [AB] + N$ [48, 49]. Note that the cross section of the diffractive reaction with the inclusive on bottom vertex is only by 10% larger than the 'elastic' part of this cross section because the ratio of these cross sections is equal to

$$\frac{\sigma[h + N \to [AB] + X_{\text{bottom vertex}}]}{\sigma[h + N \to [AB] + N]} \approx \frac{\sigma_D + \sigma_{DD}}{\sigma_D} \approx 1.1. \quad (41)$$

Here σ_D and σ_{DD} are single and double diffractive dissociation cross sections ($\sigma_{DD}/\sigma_D \approx 0.1$, [50]). Therefore, in what follows only 'elastic' processes for the bottom vertex will be considered for the diffractive production processes (see Ref. [49] for further details).

Processes with the pomeron exchange are of a special interest in high-energy experiments, as the cross sections of such exclusive reactions do not decrease with energy.

4.3.2 Nonperipheral reactions and the effects of rescattering with multipomeron exchange. The use of conherent diffractive production reactions on nuclei (i.e. processes with very small P_T^2) is a very perspective, but not very unique method in the search for heavy resonance states in the high-energy domain. For some states (and especially for those formed at small distances) the background from peripheral processes can be so large that it makes their observation difficult.

In order to reduce the background caused by peripheral processes, one can use an intermediate transverse momenta domain. For example, anomalously narrow meson states $X(1740) \to \eta\eta$ and $X(1910) \to \eta\eta'$, which are candidates for cryptoexotic mesons, were observed after the events with $P_T^2 > 0.2-0.3$ GeV^2 in charge-exchange reactions $\pi^- + p \to (\eta\eta) + \Delta^0$ and $\pi^- + p \to (\eta\eta') + n$ have been selected. The exotic meson states can be formed by a rescattering mechanism with multipomeron exchange [53]

(i.e. again their production is caused by gluon-enriched processes).

In the very high primary energy region which, for example, corresponds to the search for exotic states with heavy quarks, diffractive production reactions with rescattering can be used, instead of the charge-exchange processes with rescattering (see the diagram in Fig. 4). Cross sections of these diffractive processes also do not die out with energy rise.

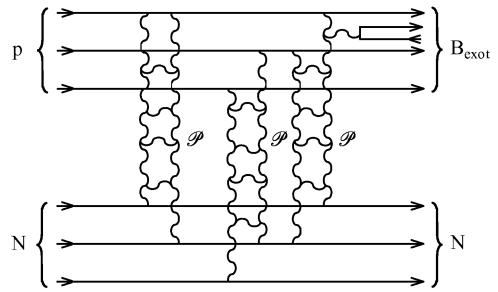

Figure 4. Diagram for exotic hadron production in processes of rescattering with multipomeron exchange in proton reaction of diffractive type ($P_T^2 > 0.2-0.3$ GeV^2).

4.3.3 Inclusive processes in the fragmentation region. It is well known that the combinatorial background in the inclusive processes, which strongly complicate the search for resonance states, is significantly decreased in the fragmentation region ($x_F > 0.5-0.6$). This is illustrated by the EGS data on the $\pi^+\pi^-$ production in the reaction $\pi^- + p \to \pi^+\pi^- + X$ at $P_\pi = 360$ GeV [54]. For this reaction, even the well-known ρ-meson is very difficult to observe (owing to a high background level). At the same time, the combinatorial background is sharply reduced in the fragmentation region ($x_F > 0.6$) and the $\rho \to \pi^+\pi^-$ induced peak is very clearly distinguished. Therefore, one can expect comparatively favorable conditions for the identification of new resonance states, including exotic hadrons, to be achieved in the fragmentation region.

It seems that the best possibilities for resonance searches occur in the region of a deep fragmentation ($x_F > 0.85-0.9$), for example in the quasi-exclusive reactions, that is in processes with the inclusive in the bottom vertex (Fig. 5):

$$a + N \to b + X_{\text{bottom vertex}} \,. \tag{42}$$

Here all admissible states in the bottom vertex are summed over. The cross sections of such reactions with reggeon exchange increase in comparison with processes like

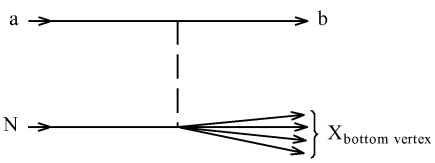

Figure 5. Diagram for reaction in the deep-fragmentation region ($x_F > 0.85-0.9$) with inclusive in the bottom vertex $a + N \to b + X_{\text{bottom vertex}}$.

$a + N \to b + N$ and may very weakly depend on initial energy E_a. At sufficiently high E_a secondary particles from the bottom and top vertices in the diagram in Fig. 5 will be well separated by their rapidities.

Therefore, in studying resonances produced in the top vertex the inclusive character of the reaction in the bottom vertex does not create an undesirable combinatorial background.

4.3.4 'Backward scattering' reactions with baryon exchange. There has been much discussion on the possibilities of more effective excitation of inner colour degrees of freedom, at which the exotic quark or quark–gluon system can be formed in processes with large momentum transfers and, in particular, in reactions of backward scattering caused by baryon exchange (see, for example, Refs [12–14, 55–58], in which the search for exotic mesons is discussed, and Refs [29, 30], where processes with exotic baryons are considered).

The production of exotic states in such processes is expected to be characterised by cross sections comparable with those of ordinary particles. As an example, one can consider some reactions with baryon exchange:

$$p + N \to [M_{exot}]_f + pN \,, \tag{43}$$

$$\pi^+ + p \to [B_{exot}^{+++}]_f + \pi^- , \tag{44}$$

$$K^- + p \to [Y_{exot}^{+}]_f + \pi^- \,. \tag{45}$$

The exotic hadron produced in such reactions will go forward in the lab system (this is denoted as h_f). These processes are convenient for studies in experiments with magnetic spectrometers, in which decay products of M_{exot} or B_{exot} can be relatively easily recorded (see Ref. [58] for more detail).

The exclusive cross sections with baryon exchange decrease rather rapidly with the growth of the primary energy. Thus, the experiments for studying reactions (43)–(45) should be performed at not too high an energy. The range 10–15 GeV seems to be optimal (as a result of a compormise between the rapid fall of cross sections and growth of the registration efficiency for the decays M_{exot} and B_{exot} with increasing primary energy).

Nevertheless the search for exotic hadrons in baryon exchange processes may be performed at higher initial energies as well (which in a number of cases is of a considerable interest, since it allows one to increase detection efficiency and to identify more precisely secondary particles). For this purpose the quasi-exclusive processes like (42) of an inclusive type in the bottom vertex should be used. A study of such possibilities for the reactions with baryon exchange like

$$p + N \to M_f + X_{\text{bottom vertex}} \tag{46}$$

is presented in Refs. [58, 59].

Use of the backward scattering mechanism for exciting exotic baryons with $J = I \geqslant 5/2$ in πN-reactions was proposed, in particular in Refs [29–31], where the existence of exotic baryons with $J = I \geqslant 5/2$ was predicted by means of the SSR (see Section 3). Experimental searches for such processes with baryon exchange will be considered in Section 7. However, as was already said above, the results obtained in these experiments are not very reliable and have an insufficient statistical confidence level.

4.3.5 Photoproduction and electroproduction reactions. Processes of photo- and electroproduction of baryon resonances open new possibilities in studying the baryon structure and, in particular, in searching for and identificating hybrid baryons. Owing to differences in the inner structure of hybrid baryons, ordinary baryons and their radial-excited states (in the coordinate space, in the space of flavour and spin, in colour structure), the study of isobar production, and especially their electroproduction, can provide information about the nature of these states. For example, data on Q^2-dependence for isobar transition form-factors can be used to distinguish between the excited isobar being the ordinary or hybrid hadron [60, 61].

In processes of electroproduction of baryonic resonances, the $\gamma_N N^*$-vertex is well known as being described by three spiral transition form-factors: $A_{|\lambda|=3/2}(Q^2)$, $A_{|\lambda|=1/2}(Q^2)$, and $S_{|\lambda|=1/2}(Q^2)$. Here A are transversal form-factors and S is a longitudal form-factor. There are only two form-factors with a helicity $|\lambda|= 1/2$ for the states with $J= 1/2$. The calculations made in the framework of the quark model shows that if, for example, the N(1440) and N(1710) isobars are hybrids, their transversal transition form-factors $A(Q^2)_{3/2}$ and $A(Q^2)_{1/2}$ must decrease like Q^2, faster than for ordinary baryons. The longitudal form-factor $S(Q^2)_{1/2}$ for hybrid baryons must vanish complety in contrast to the case of ordinary baryons for which it is sufficiently large at small Q^2. Thus, the transfer momentum dependence of the transition form-factors in the electroproduction processes for baryon resonances can be used as a filter to distinguish between exotic hybrid states and ordinary isobars.

For electroproduction processes, the Barnes–Close selection rule was formulated (see [62]), according to which $A^{(p)}_{|\lambda|=1/2}(Q^2) = 0$ for hybrid baryon production on a proton target (for neutrons $A^{(n)}_{|\lambda|=1/2}(Q)^2 \neq 0$).

On the other hand, baryonic states photoproduction data can also be used for hybrid baryon selection. The photoproduction amplitudes for ordinary qqq-type baryons are expected to be in a good agreement with the Konjuk–Isgur quark model [63]. At the same time, in case of wrong identification of a hybrid baryon as an ordinary isobar, one can expect a significant disagreement between the experimental data and predictions of the model [63] made for the ordinary baryons.

The experimental data analysis showed that such serious disagreement with theoretical predictions exists for the photoproduction amplitudes of four baryons: N(1535), N(1440), N(1710), N(1720) [39]. The last three states have masses close to the predicted values for the hybrid baryons. Of course, the data presented above are only some indications of possible hybrid interpretation of several known nonstrange baryons. The experimental and theoretical situation in this field must be substantially improved in order to take this disagreement seriously.

The wide programme on the precise study of isobar photoproduction and electroproduction processes in new experiments on CEBAF and other high-current electron machines has been discussed in detail many times (see, for example, Refs 64–67]). One would hope that in the framework of this programme it will be possible to clarify the nature of many baryon resonances in the near future.

5. The search for anomalously narrow baryons with hidden strangeness

The searches for heavy baryons with anomalously narrow decay widths, if they are successful, make it possible to obtain the best evidence for the existence of cryptoexotic baryon states. So far these searches have been mostly aimed at the observation of multiquark baryons with hidden strangeness, such as $B_\phi = |qqqs\bar{s}\rangle$ (here q are u or d quarks). Theoretical possibilities for the existence of such states are rather uncertain. If, for example, the mass of the baryon with hidden strangeness is smaller that $M(\Lambda) + M(K) < 1.6$ GeV, this state can decay only through the OZI-suppressed processes and must be very narrow.

Its possible decay modes are

$$B^+_\phi \to p\pi^0; \quad p\pi^+\pi^-.$$

The observation of such states is hindered due to background from numerous baryonic isobar decay. Moreover, because of the rather large constituent mass of the s quark it seems unlikely that the mass value of B_ϕ is smaller than 1.6–1.7 GeV.

For heavier baryons, decays of $B_\phi \to YK^+$; $p\phi$ types are possible. If such a cryptoexotic baryon with a complicated internal structure consists of two coloured parts separated in space (e.g. because of a centrifugal barrier), then its decay into colour singlet final states may be suppressed. This issue is discussed in more detail in Section 3.

Depending on the mechanism of quark rearrangement of colour clusters in an exotic hadron, its decay probability can be quite small. Therefore, such heavy states can have, in principle, anomalously narrow decay widths (of the order of several tens of MeV). Theoretical predictions here are very arbitrary, and the problem of existence of very narrow massive exotic resonances can be solved only by experiment. Some candidates for exotic meson states with anomalously narrow width have been previously observed: X(1740) [51], X(1910) [52], U(3100) [67–69], M_ϕ(3250) [68, 69]. Thus, a thorough study of the poorly known heavy baryons mass region (M ≈1.5–4 GeV) would seem to be quite interesting.

In this section we present the data on several experiments in which were obtained possible indications of the existence of anomalously narrow heavy baryons, the candidates for cryptoexotic states.

5.1 Σ(3170)-baryon

In the high-statistics experiments in K^--meson beams with momenta 8.25 and 6.5 GeV with liquid hydrogen bubble chambers CERN (2 m) and Argonne (15 ft) a systematic search for quasi-two-body processes of the type

$$K^- + p \to Y^{*+} + \pi^-$$

was performed. In this Δ^{++}-exchange reaction [see Eqn (45)], the strange baryon system Y^{*+} is produced in the forward direction, while the π^--meson is flying out into the backward hemisphere. Processes of this type were discussed in Section 4.3.4. The total statistics for the two exposures in the bubble chambers are about 145 events μb^{-1} [70]. The events (45), which correspond to the decays of Y^{*+} into more than one strange particle in the final state, were singled out:

$$Y^{*+} \to \begin{cases} \Sigma K\bar{K} + \geqslant 2\pi, \\ \Lambda K\bar{K} + \geqslant 2\pi, \\ \Xi K + \geqslant 3\pi. \end{cases} \quad (47)$$

The missing mass spectra (MM) of this Y^{*+} system for the events (47), were determined from the data on the recoil π^--meson. The combined spectrum from two independent bubble chamber experiments is shown in Fig. 6. A narrow peak with mass $M = 3170 \pm 5$ MeV and a small width $\Gamma < 20$ MeV, corresponding to the formation of the $\Sigma(3170)^+$ state, was observed in this combined spectrum with a statistical significance of more than 6.5 standard deviations. The $\Sigma(3170)$ production cross sections [with decays by the channels (47)] for two momenta P_{K^-} are

$$\sigma[\Sigma(3170)^+;\ 6.5\ \text{GeV}]\text{BR}(47) = 1.0 \pm 0.3\ \mu\text{b},$$

$$\sigma[\Sigma(3170)^+;\ 8.25\ \text{GeV}]\text{BR}(47) = (0.7 \pm 0.2)\ \mu\text{b},$$

respectively [70].

The decay rate of $\Sigma(3170)^+$ into the three strange particle final states should be compared with that of the final states containing only one strange particle. For ordinary Σ^*-hyperons, the latter channels dominate. However, in these experiments [70] no structure at 3170 MeV is seen in the mass spectra of the states with one strange particles. Upper limits for such 'ordinary' decay modes of the $\Sigma(3170)$-baryon do not exceed the probabilities for multistrange modes (47). These characteristics (together with an anomalously narrow width for the massive structure $\Sigma(3170)^+$) make it a possible candidate for the exotic five-quark baryon of the $|uuss\bar{s}\rangle$ type. If such a state actually exists, then it is possible to predict the same type of a non-strange exotic baryon $B_\phi = |qqqs\bar{s}\rangle$ with a mass of approximately 3 GeV.

The search for the $\Sigma(3170)$-baryon was also performed in the experiment on the LASS spectrometer [71] at the K^--beam with the momentum $P_{K^-} = 11$ GeV in the reaction

$$K^- + p \to [\Xi^- K + m\pi] + \pi^- . \quad (48)$$

Analysis of the missing-mass spectra with respect to the π^--meson in reaction (48) yielded an upper limit for the cross section of the $\Sigma(3170)^+$-production in this process at a level of 0.07 μb (95% confidence level). With the aid of extrapolation of the preceding experimental data [70] [for the decay channel $\Sigma(3170)^+ \to \Xi^- K + m\pi$) to the kaon momentum $P_{K^-} = 11$ GeV, the predicted value of this cross section to be about 0.05 – 0.10 μb, in agreement with the LASS upper limit.

Therefore, the results of the LASS experiment neither confirm, nor rule out the existence of the narrow heavy $\Sigma(3170)$-baryon which was observed in [70].

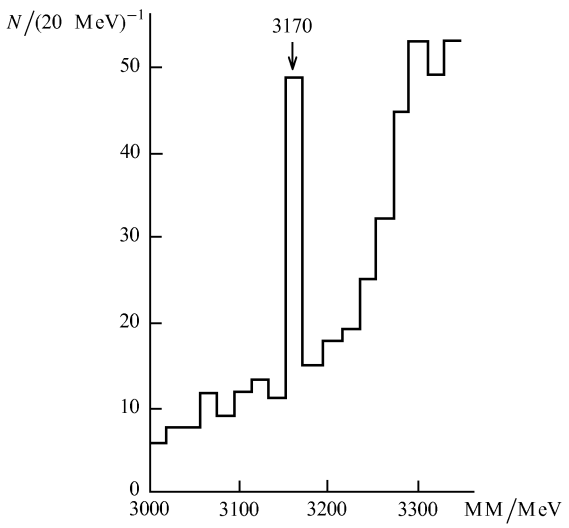

Figure 6. Missing-mass (MM) spectrum for the Y^{*+}-system in the reaction $K^- + p \to Y^{*+} + \pi^-$ [for events like (47)]. The spectrum contains the combined data obtained by CERN and Argonne liquid hydrogen bubble chambers at $P_{K^-} = 8.25$ GeV and $P_{K^-} = 6.5$ GeV, respectively.

5.2 $N_\phi(1960)$-baryon

In the experiment on the BIS-2 setup (JINR) using the neutron beam of the IHEP 70 GeV proton synchrotron with the mean energy $\langle E_n \rangle = 40$ GeV, the following reactions with Λ-hyperons and two additional charged particles in the final state (recorded in the magnetic spectrometer of the setup) were studied [44]:

$$n + N \to (\Lambda h^+ h^-) + \ldots$$
$$\hookrightarrow p\pi^-$$

In the BIS-2 measurements the charged hadrons h^+ and h^- were not directly identified. Kinematic methods were used for their identification. Under the assumption that $h^- \equiv \pi^-$, the effective mass spectrum of the $\Lambda\pi^-$-system was studied (Fig. 7). A peak was observed in this spectrum which corresponds to the formation of a $\Sigma(1385)$-hyperon, i. e. to the reaction

$$n + N \to \Sigma(1385)^- h^+ + \ldots \quad (49)$$
$$\hookrightarrow \Lambda\pi^-$$

in the neutron fragmentation region selected by the setup. However, the background conditions for this reaction were quite poor: the number of background events under the peak in Fig. 7 is twice as large as the number of real $\Sigma(1385)^-$-hyperons.

Furthermore, by the assumption $h^+ \equiv K^+$, the data on the reaction

$$n + N \to \Sigma(1385)^- K^+ + \ldots \quad (50)$$

were obtained. A narrow peak was shown to appear in the $\Sigma(1385)^- K^+$ mass spectrum, which is more clearly seen in the region of small transverse momenta: $P_T^2 < 0.24$ GeV^2 (Fig. 8). The parameters of the observed structure are as follows: $M = (1956^{+8}_{-6})$ and $\Gamma = 27 \pm 15$ MeV (here a correction to the experimental mass resolution is introduced). This state was interpreted in Ref. [44] as a candidate exotic baryon with hidden strangeness $|qqqs\bar{s}\rangle$ and denoted as $N_\phi(1960)$.

The cross section for the $N_\phi(1960)$ production is

$$\sigma[n + (C) \to N_\phi(1960)^0 + \ldots] \times \text{BR}[N_\phi(1960)^0 \to \Sigma(1385)^- K^+] = 1150 \pm 190\ \text{nb/C nucleus} \quad (51)$$

(or $\sigma \times \text{BR} \approx 220 \pm 40$ nb/nucleon for $\sigma \propto A^{2/3}$)†. From

† Symbol (C) means that this reaction is not the coherent production process on carbon nucleus as a whole. The reaction (51) with a limited charge multiplicity is not a truly inclusive process. However, formation of additional neutral particles in the final state together with the $N_\phi(1960)$ is possible in this reaction. We call (51) the process with limited inclusiveness. The cross sections (51), (52) seem to be determined in Ref. [44] not quite correctly and must be increased by a factor of 1.7 – 2.

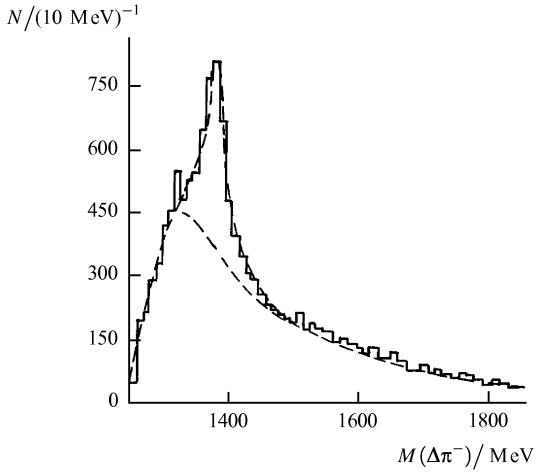

Figure 7. Effective mass spectrum of the $\Lambda\pi^-$-system produced in the reaction $n + N \to (\Lambda\pi^- h^+) + \ldots$ in the BIS-2 experiment. The $\Sigma(1385)$-hyperon production is clearly seen in this spectrum; however, the background under the $\Sigma(1385)$-peak is approximately twice as large as the value of the resonance signal.

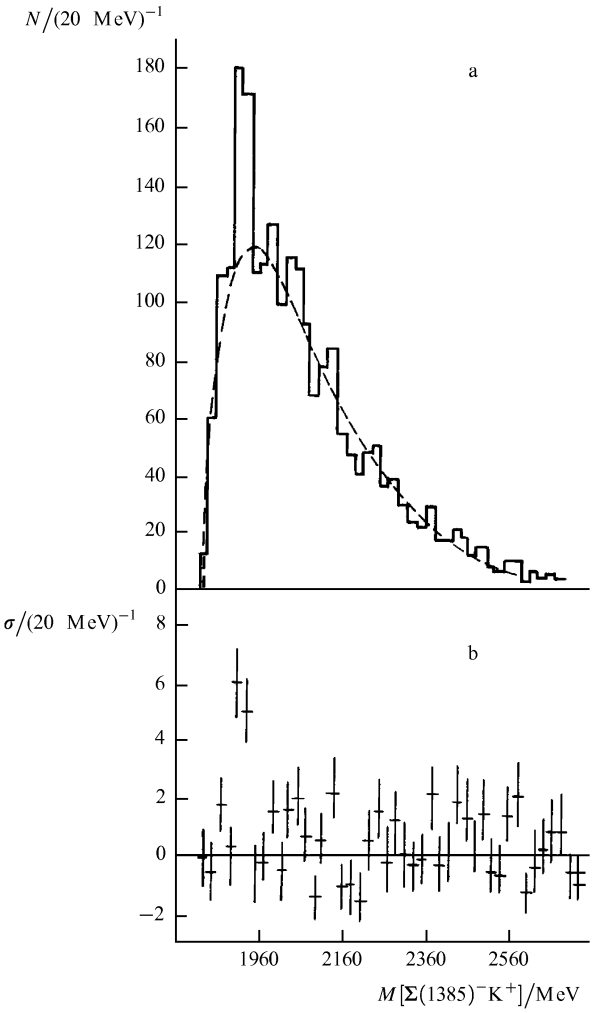

Figure 8. (a) Effective mass spectrum of the $\Sigma(1385)^-K^+$-system in the reaction $n + N \to \Sigma(1385)^-K^+ \ldots$ in the primary beam fragmentation region after cut-off $P_T^2 < 0.24\ \mathrm{GeV}^2$ (the histogram) and results of fitting this spectrum by a smooth background curve. (b) Number of standard deviations in the experimental spectrum from the background curve.

these data and isotopic relations it is possible also to find the cross section

$$\sigma[n + (C) \to N_\phi(1960)^0 + \ldots] \times BR[N_\phi(1960)^0 \to \Sigma(1385)K] = 1725 \pm 285\ \mathrm{nb/C\ nucleus} \tag{52}$$

(if the $N_\phi(1960)$ isospin is $I = 1/2$).

The P_T^2-distribution for the $N_\phi(1960)$ production reaction has the form $\exp(-bP_T^2)$ with a slope $b = 9.9 \pm 3.0\ \mathrm{GeV}^{-2}$. The study of angular distributions in the cascade decays

$$N_\phi(1960)^0 \to \Sigma(1385)^-K^+,\ \Sigma(1385)^- \to \Lambda\pi^-$$

leads to the following possible values of quantum numbers of $N_\phi(1960)$-baryon: $J^P = 5/2^+,\ 7/2^-, \ldots$

It was stated in Ref. [44] that the $N_\phi(1960)$ is produced by neutron diffractive dissociation. This conclusion, however, seems to be doubtful. It cannot be supported by energy considerations because the primary neutron energy is unknown. If a diffractive production process for the $N_\phi(1960)$-baryons does in fact dominate, it should manifest itself in the coherent reaction on C nuclei with the slope in the P_T^2-distribution $b \gtrsim 30 - 40\ \mathrm{GeV}^{-2}$, which is much larger than the observed value $b = 9.9 \pm 3.0\ \mathrm{GeV}^{-2}$.

5.3 R(3520)-baryon

During the analysis of the experimental data on neutral strange particle production in π^-p-interactions in the 2 m CERN liquid-hydrogen bubble chamber exposed to the $P_\pi = 16$ GeV pion beam the reaction of the production of the well-identified K_S^0-meson and the four change particles in the final state was singled out

$$\pi^- p \to (K_S^0 h^+ h^+ h^- h^-) + X^0 \tag{53}$$

and 1684 events of this type were identified [72]. The masses of known particles (π, K, p) were assigning to the charge tracks and the effective masses of all admitted final states were calculated. Thus, the effective mass spectra for the combinations $pK^-K^0\pi^+\pi^-$ and $pK^+K^0\pi^-\pi^-$ were determined.

In order to reduce the combinatorial background from false combinations the results of the kinematical fits and particle identification via ionisation measurements were taken into account. This procedure permitted the reduction of the numbers of weighted combinations to 2183 for the $pK^-K_S^0\pi^+\pi^-$ assignment and to 1057 for the $pK^+K_S^0\pi^-\pi^-$ assignment. Mass spectra for these systems have the same shape, with the exception of the region around 3.5 GeV, where the $pK^+K_S^0\pi^-\pi^-$ system acquires a sharp peak of more than 5 standard deviations over the background, while the $pK^-K_S^0\pi^+\pi^-$ spectrum does not show such a structure.

Further analysis shows that this peak is manifested more clearly in the central rapidity region $0.18 < y < 0.38$ and for the events with one of the $K_S^0\pi^-$ combinations lying in the $K^*(890)$-meson mass range. It should be noted that the introduction of this and other addtional kinematical selection criteria virtually leaves unchanged the number of events at the peak, but significantly suppress the background level.

Thus, in the resulting mass spectrum (Fig. 9) a narrow structure with mass $M = 3520 \pm 3$ MeV and width $\Gamma = 20 \pm 16$ MeV is clearly seen (with account of the

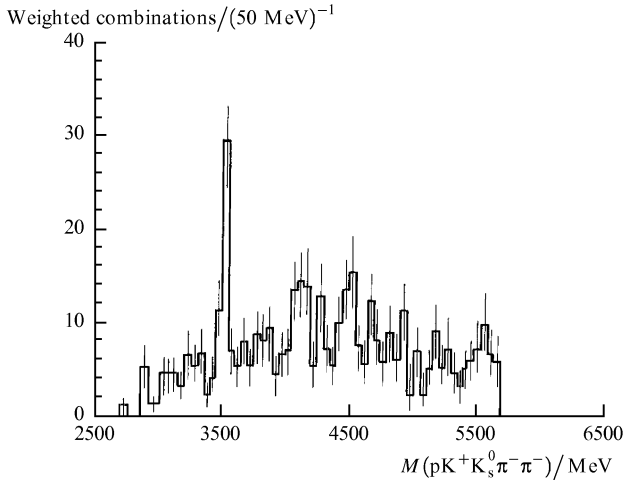

Figure 9. Effective mass spectrum of the $pK^+K^0_s\pi^-\pi^-$-system for the events with $0.7\ \mathrm{GeV} < M(K^0_s\pi^-) < 1.05\ \mathrm{GeV}$ and rapidities $0.18 < y < 0.38$ (that is, for the central production events with a $K^*(890)$-meson at the final state) and with additional kinematic selections for further suppression of the combinatory background (see Ref. [72] for more details).

experimental mass resolution the width is $\Gamma = 7^{+20}_{-7}$ MeV). The statistical significance of the observed peak is 8.9 standard deviations. This structure is denoted as R(3520). It is characterised by zero strangeness. The cross section for the production of the R(3520) state is found to be $\sigma \times \mathrm{BR} = 14 \pm 3\ \mu\mathrm{b}$.

The analysis of the missing mass spectrum for the X^0 system in reaction (53) for the state $pK^+K^0_S\pi^-\pi^-$ shows that, for the R(3520) events, the $M(X^0)$ mass values are grouped in the relatively narrow region 1.4–2.1 GeV. Therefore, it is conceivable that the quasi-two-body reaction

$$\pi^- + p \to R(3520) + \text{meson}\ (1.4\ \mathrm{GeV} < M < 2.1\ \mathrm{GeV}). \quad (54)$$

takes place.

The cross secton for the R(3520) production in π^-p-collisions at a momentum of 16 GeV is sufficiently large and leaves no room for the possibility of identifying this new baryon as a pentaquark state with hidden charm ($uddc\bar{c}$). Such an interpretation was proposed in Ref. [72], but fails as soon as we recall that the cross section for inclusive production of meson with hidden charm at the π^- meson momentum of 27 GeV is $\sigma(\pi^-N \to J/\psi + X) \approx 6$ nb [73], that is lower than the R(3520)-baryon production cross section by three orders of magnitude. Even the total cross section of charmed particles pair production in π^-p-reactions at $P_\pi = 16$ GeV is much less than 1 μb (that is, the cross-section of a process permitted by the OZI rule) . It seems that the state R(3520), if it really exists, can be considered as a candidate for an exotic baryon $|uds\bar{s}\rangle$ with hidden strangeness.

6. The search for exotic baryons in diffractive reactions at the SPHINX facility

A broad research programme devoted to the study of diffractive hadron production by $E_p = 70$ GeV protons and to the search for exotic baryons in such processes is underway in the experiments of the SPHINX collaboration (IHEP–ITEP). This programme was discussed in detail in Refs [14, 46].

Experimental data of a number of the diffractive reactions

$$p + N \to \begin{cases} (K^+K^-p) + N, & (55)\\ (\phi p) + N, & (56)\\ \quad \hookrightarrow K^+K^- & \\ [\Lambda(1520)K^+] + N, & (57)\\ \quad \hookrightarrow K^-p & \\ (\Lambda K^+) + N, & (58)\\ \quad \hookrightarrow p\pi^- & \end{cases}$$

$$p + N \to \begin{cases} (\Sigma^0K^+) + N, & (59)\\ \quad \hookrightarrow \Lambda + \gamma & \\ [\Sigma(1385)^0K^+] + N, & (60)\\ \quad \hookrightarrow \Lambda\pi^0 & \\ [\Sigma(1385)^+K^0] + N, & (61)\\ \quad \hookrightarrow \Lambda\pi^+ \quad \hookrightarrow \pi^+\pi^- & \\ [\Lambda(1405)K^+] + N, & (62)\\ \quad \hookrightarrow \Sigma^+\pi^-;\ \Sigma^0\pi^0 & \\ (\pi^+\pi^-p + m\gamma) + N \quad (m = 0-4), & (63)\\ (\omega p) + N, & (64)\\ \quad \hookrightarrow \pi^+\pi^-\pi^0 & \\ (\eta p) + N, & (65)\\ \quad \hookrightarrow \pi^+\pi^-\pi^0 & \end{cases}$$

$$p + N \to \begin{cases} (\eta' p) + N, & (66)\\ \quad \hookrightarrow \pi^+\pi^-\eta & \\ (p\bar{p}p) + N, & (67)\\ (\Delta^{++}\pi^-) + N & (68) \end{cases}$$

as well as of some other processes, are obtained at the present time. Here N denotes a nucleon or a light nucleus (C, Be)

At the same time, some partially inclusive inelastic processes with additional neutral particles, such as the reactions

$$p + N \to \begin{cases} [\Sigma(1385)^0K^+] + N + \text{neutral particles}, & (69)\\ \quad \hookrightarrow \Lambda\pi^0 & \\ (pK^+K^-) + N + \text{neutral particles}, & (70) \end{cases}$$

and the process

$$p + N \to (\Sigma^+K^+) + \pi^- + N\,. \quad (71)$$
$$\hookrightarrow p\pi^0$$

were also studied. It must be stressed that the study of these reactions with additional pion production (the associative diffractive pair production processes) makes it possible to look for resonance structures in the mass spectra $\Sigma(1385)^0K^+$, pK^+K^-, Σ^+K^+ corresponding to possible states with isospin $I = 3/2$. Such structures cannot be generated in diffractive reactions with pomeron exchange like (55)–(68), where the isospin of baryon systems in the final state must be equal to the proton isospin $I = 1/2$.

The SPHINX facility [46] used for the measurements in the proton beam consists of a wide-aperture magnetic spectrometer equipped with scintillation hodoscopes, proportional chambers and drift chambers, as well as a multichannel γ-spectrometer with total-absorption Cherenkov lead-glass counters. The differential detector of the RICH type, which provides for the simultaneous registration of several rings of Cherenkov radiation, and two multichannel gas threshold Cherenkov counters were used for the identification of secondary charged particles. The details of the setup, measurements on the accelerator, and experimental data processing are contained in Refs [46, 74].

At the present time, a significant body of statistics has been collected on the SPHINX experiment, which is now undergoing processing. Practically all reactions (55)–(71) and some other processes are well selected. The first results of these studies connected with the search for the massive baryons with hidden strangeness in reactions (55)–(57), (59), (60) and (67)–(69), are presented below (see [46, 74–79]).

6.1 Search for heavy exotic baryons with hidden strangeness in reactions of type $\mathbf{p + N \to (K^+K^-p) + N}$

Reactions (55)–(57) may be very effective in searches for exotic baryons with hidden strangeness of the $|qqqs\bar{s}\rangle$ type. For this purpose reaction (56), forbidden by the OZI rule, is especially interesting. As was stated above, nonresonance processes of this kind may be more strongly suppressed by the OZI rule than processes leading to the production of multiquark $B_\phi = |qqqs\bar{s}\rangle$ baryons with complex internal colour structure. Therefore, the background conditions for the observation of the B_ϕ-baryons could be more favorable in reaction (56) than in other processes without such suppression.

The study of reactions (55)–(57) was performed earlier in only one experiment of the ANL group at the proton momentum of 11.75 GeV [80]. In this experiment the setup had a limited acceptance, which was practically zero for masses greater than 2.6–2.8 GeV, and there was no statistically significant evidence of a specific structure in the effective-mass spectra of ϕp- and $\Lambda(1520)K^+$- states. The upper bounds for the corresponding cross sections from Ref. [80] are presented in Table 6.

In the experiment of the SPHINX collaboration the reaction $p + N \to (K^+K^-p) + N$ was studied at the energy $E_p = 70$ GeV. In the course of the experiment the integral proton flux $N_p = 1.12 \times 10^{11} p$ was passed through the SPHINX setup target (0.48×10^{24} CH_2/cm^2). The detector was triggered by signals corresponding to the registration of three charged particles in the magnetic spectrometer. At least two (one) of these particles were required to produce no signal in the first (second) threshold Cherenkov counter, that is they were candidates for protons with $P_p < 40$ GeV or kaons with $P_K < 21$ GeV. The final identification of the particles were made by off-line analysis with the help of the RICH detector (see Ref. [46]).

Very distinct peaks corresponding to ϕ meson and $\Lambda(1520)$ baryon formation are observed in the invariant mass spectra of the K^+K^-- and K^-p-systems (Fig. 10), which permit one to select reaction (56) and (57) [46]. Analysis of the distribution of the events (55)–(57) over the square of the transverse momentum dN/dP_T^2 (Fig. 11) shows that coherent diffractive production processes of the K^+K^- p-, ϕp- and $\Lambda(1520)K^+$-systems on carbon nuclei significantly contribute to these reactions. The coherent processes are characterised by large values of the diffractive slope parameters, $b \approx 30-40$ GeV^{-2}. This is

Table 6. The upper limits for the cross sections of resonance state production in the reactions $p + p \to (\phi p) + p$, $p + p \to [\Lambda(1520)K^+] + p$ and $p + p \to (K^+K^-p) + p$ for the proton momentum of 11.75 GeV [80] (for resonance width $\Gamma = 10$ MeV).

Mass/GeV	Cross-section limits for the production of baryonic resonances/nb		
	ϕp	$\Lambda(1520)K^+$	K^+K^-p
2.0	14	–	10
2.2	19	41	50
2.4	18	50	75
2.6	19	47	78
2.8	–	50	89

Note. The limits correspond to five standard deviations and increase with the resonance width as $\sqrt{\Gamma}$.

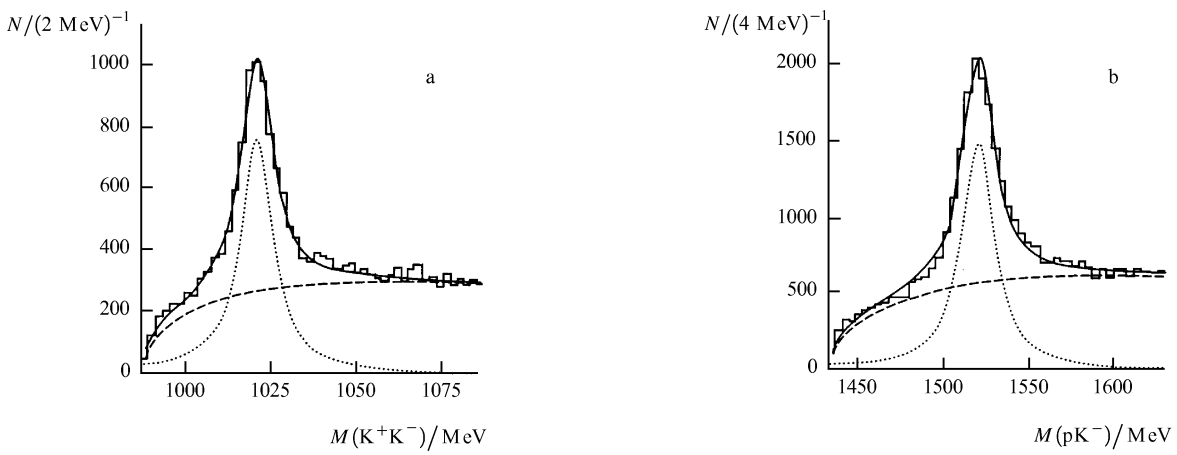

Figure 10. Effective mass spectra of the secondary particles in the reaction $p + N \to (K^+K^-p) + N$ at $E_p = 70$ GeV: (a) K^+K^--system; a ϕ-meson peak with $M = 1020.0 \pm 0.2$ MeV is clearly apparent in the spectrum; (b) K^-p-system; a $\Lambda(1520)$-peak with the parameters $M = 1520.0 \pm 0.3$ MeV and $\Gamma = 22.0 \pm 0.8$ MeV is observed in this spectrum (the errors are only statistical). The parameters of ϕ and $\Lambda(1520)$ are consistent with their tabular values (with account taken of the apparatus resolution).

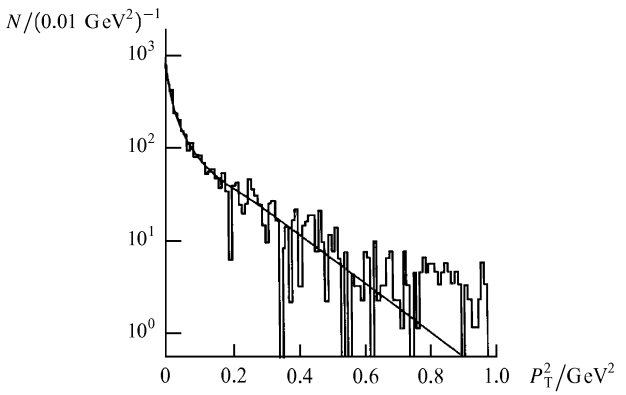

Figure 11. Distribution of the events for the process of diffractive production $p + N \to (\phi p) + N$ in the square of the transverse momentum of the ϕp-system. This distribution is fitted by the form $dN/dP_T^2 = C_1 \exp(-b_1 P_T^2) + C_2 \exp(-b_2 P_T^2)$ with slope parameters $b_1 = 48.0 \pm 0.6\ \mathrm{GeV}^{-2}$ and $b_2 = 6.2 \pm 0.2\ \mathrm{GeV}^{-2}$. Large value of b_1 corresponds to the coherent process (56) on the carbon nucleus.

illustrated by the dN/dP_T^2-distribution for reaction (56) shown in Fig. 11. The dN/dP_T^2-distributions for reactions (55), (57), (59), (60), and a number of other diffractive processes have a similar shape.

A structure with a mass $M \approx 2170$ MeV and a width $\Gamma \approx 110$ MeV is observed in the effective mass spectra of the ϕp-system in reaction (56) and the $\Lambda(1520)K^+$-system in reaction (57) (Figs 12a, b) in the coherent region ($P_T^2 < 0.075\ \mathrm{GeV}^2$). Because the shapes of the two spectra are quite similar, the sum of the spectra can be used in a more detailed study of this structure. The combined mass spectrum $M[\phi p + \Lambda(1520)K^+]$ is shown in Fig. 12c. It should be noted that the origin of the 'X(2170)' state is not yet clear and requires further investigation. This circumstance is underlined by the use of the quotation marks.

The considerably high acceptance of the SPHINX setup in the region of large masses of baryon states made it possible to search for heavy baryons with $M < 4.5$ GeV and, above all, for baryon resonances with anomalously narrow width. The latter might be the exotic pentaquark baryons with hidden strangeness.

Fig. 13 shows the results of searches for the K^+K^-p-, ϕp- and $\Lambda(1520)K^+$-systems produced in reactions (55)–(57) for $M > 2.75$ GeV. No statistically significant resonant structures are observed in the investigated spectra. Upper limits for the cross sections for the production of heavy baryons were obtained in these experiments and are shown in Fig. 14. As follows from this figure, the measurements on the SPHINX setup do not confirm the existence of the narrow resonance R(3520) which was observed earlier at $P_{\pi^-} = 16$ GeV in the reaction

$$\pi^- + p \to [pK^+K^*(890)^-\pi^-] + X^0 \qquad (72)$$

with the production cross section of $\sigma \times \mathrm{BR} = 14$ μb [72] (see Section 5.3).

The following upper limits for the R(3520) production cross-sections in reactions (55)–(57) were obtained in the SPHINX measurements:

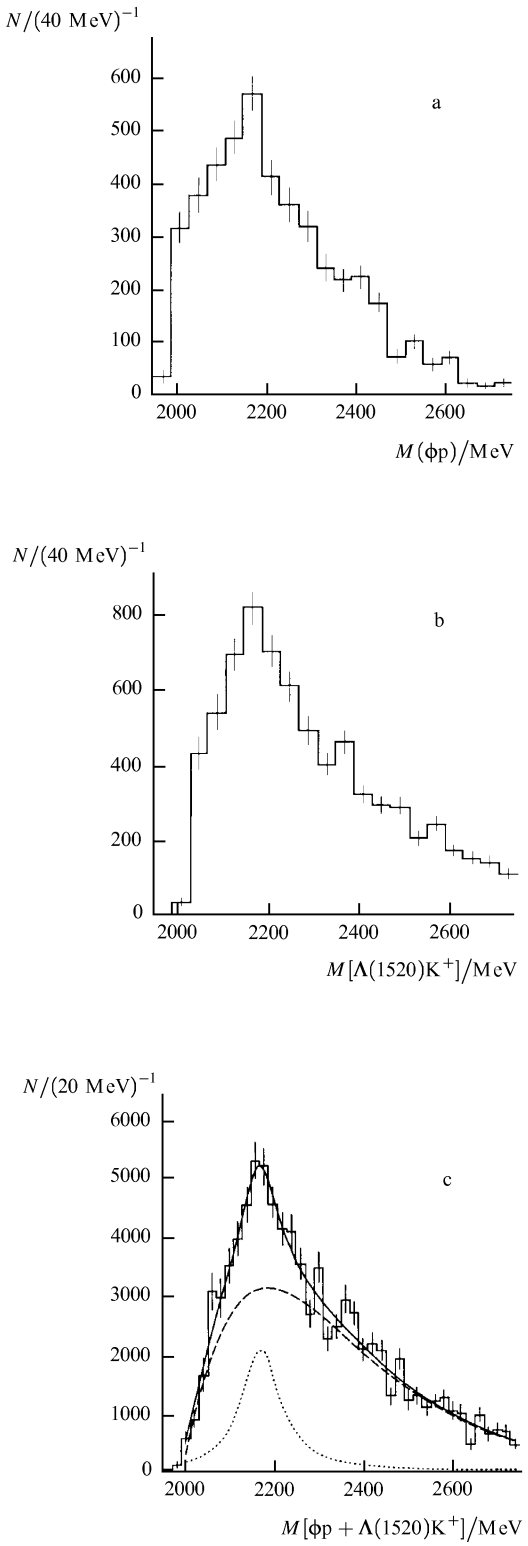

Figure 12. Effective mass spectra of ϕp- and $\Lambda(1520)K^+$-systems for the coherent diffractive processes (56) and (57) ($P_T^2 < 0.075\ \mathrm{GeV}^2$): (a) mass spectrum $M(\phi)$p in the reaction (56); (b) mass spectrum $M[\Lambda(1520)K^+]$ in the reaction (57); (c) the combined effective mass spectrum $M[\phi p + \Lambda(1520)K^+]$ in the reactions (56) and (57). The mass spectra for the ϕp and $\Lambda(1520)K^+$ are weighted with the setup efficiency and decay branching ratios $\mathrm{BR}(\phi \to K^+K^-) = 0.49$ and $\mathrm{BR}[\Lambda(1520) \to K^-p] = 0.225$. The combined spectrum is fitted by the Breit–Wigner peak with $M \approx 2170$ MeV and $\Gamma \approx 110$ MeV (the dotted curve) and by a smooth polynomial background (the dashed line).

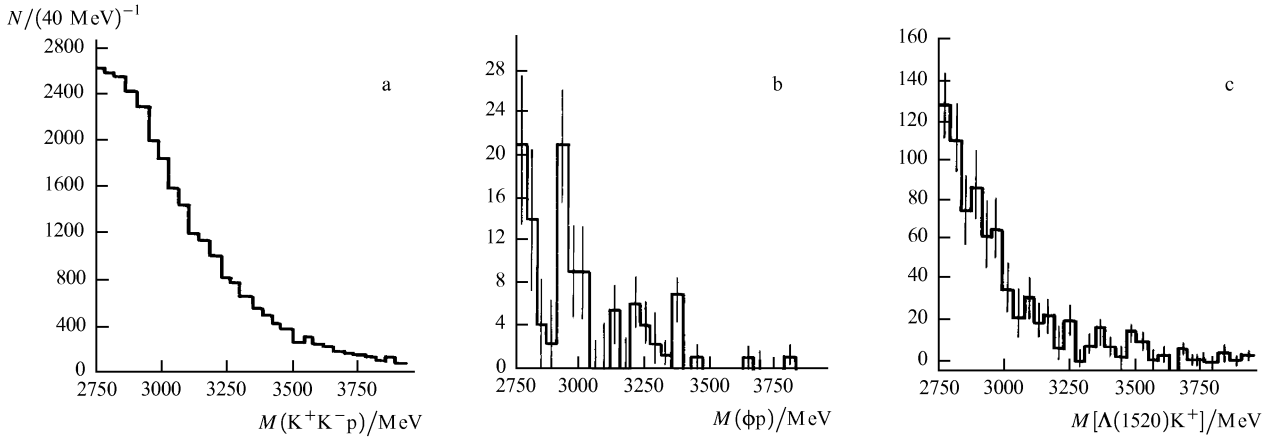

Figure 13. Results of the search for narrow exotic baryons with hidden strangeness $B_\phi = |qqqs\bar{s}\rangle$ (for $M > 2.75$ GeV), that can be produced in the diffractive process $p + N \to B_\phi + N$ (for the entire P_T^2 range) and decaying through the channels: (a) $B_\phi \to K^+K^-p$; (b) $B_\phi \to \phi p$; (c) $B_\phi \to \Lambda(1520)K^+$.

$$\sigma[R(3520)^+]_{\text{nucleon}} BR[R^+ \to K^+K^-p] < 2.6\,\text{nb/nucleon}, \quad (73)$$

$$\sigma[R(3520)^+]_{\text{nucleon}} BR[R^+ \to \phi p] < 0.27\,\text{nb/nucleon}, \quad (74)$$

$$\sigma[R(3520)^+]_{\text{nucleon}} BR[R^+ \to \Lambda(1520)K^+] < 3.4\,\text{nb/nucleon} \quad (75)$$

(the confidence level is 95%). These values are 4–5 orders of magnitude lower than the $R(3520)^0$ production cross section in reaction (72) presented in Ref. [72].

The existing sensitivity is insufficient for obtaining statistically significant evidence for the existence of a nonstrange analogue to the $\Sigma(3170)$ baryon with a mass near 3 GeV (Figs 13 and 14)

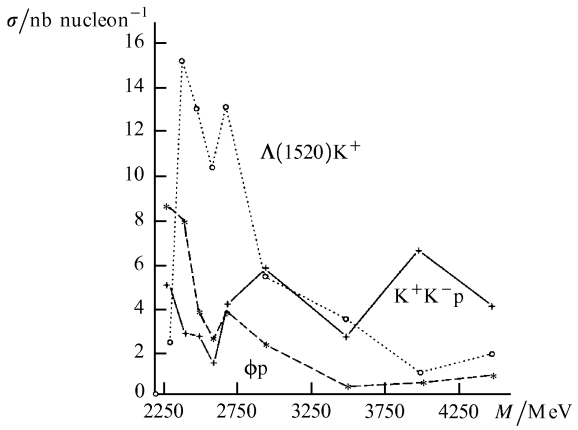

Figure 14. The upper limits (at the 95% confidence level) on the resonances with widths $\Gamma \leqslant 50$ MeV, that decay through the channels $B_\phi \to K^+K^-p$, $B_\phi \to \phi p$, and $B_\phi \to \Lambda(1520)K^+$ (with account taken of branching ratios $BR[\phi \to K^+K^-]$ and $BR[\Lambda(1520) \to K^-p]$).

Table 7. Estimates of cross sections for N_ϕ-baryon production.

BIS-2 data	SPHINX data (upper limits on cross sections at 95 % confidence level)	
Reaction with limited inclusiveness $n + N \to N_\phi(1960)^+$...	'Elastic' reaction $p + N \to N_\phi(1960) + N$	Partially-inclusive reaction $p + N \to N_\phi(1960) + N +$ neutral particles
$\sigma[N_\phi(1960)]_C BR = 1725 \pm 285$ nb/C nucleus or with account of factor 1.7 3×10^3 nb/C nucleus	Coherent process ($P_T^2 < 0.075$ GeV^2): $\sigma[N_\phi(1960)]_C BR < 660$ nb/C nucleus	Coherent process ($P_T^2 < 0.075$ GeV^2): $\sigma[N_\phi(1960)]_C BR < 820$ nb/C nucleus
$\sigma[N_\phi(1960)]_{\text{nucleon}} BR = 330 \pm 60$ nb/nucleon or with account of factor 1.7 550 nb/nucleon ($\sigma \propto A^{2/3}$)	$\sigma[N_\phi(1960)]_{\text{nucleon}} BR < \begin{cases} 55\ \text{nb/nucleon}\ (\sigma \propto A), \\ 125\ \text{nb/nucleon}\ (\sigma \propto A^{2/3}) \end{cases}$	$\sigma[N_\phi(1960)]_{\text{nucleon}} BR < \begin{cases} 70\ \text{nb/nucleon}\ (\sigma \propto A), \\ 150\ \text{nb/nucleon}\ (\sigma \propto A^{2/3}) \end{cases}$
	For all P_T^2 $\sigma[N_\phi(1960)]_{\text{nucleon}} BR < 120$ nb/nucleon ($\sigma \propto A^{2/3}$)	For all P_T^2 $\sigma[N_\phi(1960)]_{\text{nucleon}} BR < 230$ nb/nucleon ($\sigma \propto A^{2/3}$)

Note. Notation: $\sigma[N_\phi(1960)]_C$ are cross sections of the corresponding reactions related to the carbon nucleus C; $\sigma[N_\phi(1960)]_{\text{nucleon}}$ the same cross sections related to a nucleon; $BR = BR[N_\phi(1960) \to \Sigma(1385)K]$ for all isotopic states (if $I = 1/2$). For the coherent reaction on a nucleus with atomic number A, a dependence of the cross-section on A like $\sigma \propto A$, or even stronger, is possible, although 'naive expectations' of $\sigma \propto A^2$ seem to be invalid due to effects of pomeron screening during interaction with the nucleus. It should be borne in mind that the determination of reaction cross-sections in the BIS-2 experiment was somewhat incorrect. Applying the fitting procedure used in the analysis of the SPHINX data to the BIS-2 data, one find that the numbers of events in the N_ϕ peak and the corresponding cross section values should be multiplied by a factor of 1.7–2 (compared to the published BIS-2 results).

6.2 Further searches for the $N_\phi(1960)$-baryon

As was descibed in Section 5.2, the reaction

$$\mathrm{n} + \mathrm{N} \to (1385)^- \mathrm{K}^+ + \ldots \qquad (76)$$
$$\hookrightarrow \Lambda\pi^-$$

was investigated in the experiments on the BIS-2 setup in a neutron beam with mean energy $\langle E_\mathrm{n}\rangle \approx 40$ GeV [44]. A narrow structure with mass $M = 1956^{+8}_{-6}$ MeV and anomalously small width $\Gamma = 27 \pm 15$ MeV was observed in the effective mass spectrum of the $\Sigma(1385)^-\mathrm{K}^+$ system and interpreted as a candidate for the cryptoexotic baryon $\mathrm{N}_\phi = |\mathrm{udds}\bar{\mathrm{s}}\rangle$ with hidden strangeness. The BIS-2 results on the cross section of $\mathrm{N}_\phi(1960)$ production in reaction (76) are presented in Section 5.2 and Table 7.

The importance of the the problem of possible existence of the cryptoexotic $\mathrm{N}_\phi(1960)$ baryon leads to a new search for this state in reactions (60) and (69) in the SPHINX experiments [74, 75]. For the analysis of these reactions the same trigger sample of events with 3 charged secondaries considered in Section 6.1 was used. The obtained statistics corresponded to a proton flux $N_\mathrm{p} = 0.9 \times 10^{11}$ p passed through the setup target.

To select reaction (60), the events with three secondary charged particles that had been identified by the Cherenkov counters of the SPHINX setup as $\mathrm{p}\pi^-\mathrm{K}^+$, and with 2γ-clusters detected in the photon spectrometer satisfying the conditions for π^0-meson isolation — $0.10\ \mathrm{MeV} < M(\gamma_1\gamma_2) > 0.17$ GeV were preliminary selected (see Refs [74, 75] for more details).

In the events involving the production of $\mathrm{p}\pi^-\pi^0\mathrm{K}^+$ systems, the π^0 meson mass was fixed to its table value, and the energies and coordinates of the photons were redefined by taking into account the resolution of the γ-spectrometer (constraint on the m_{π^0} mass). Such an analysis finally led to the isolation of the process

$$\mathrm{p} + \mathrm{N} \to (\mathrm{p}\pi^-\pi^0\mathrm{K}^+) + \mathrm{N}\,, \qquad (77)$$

that satisfies the 'elasticity' requirement for energy

$$65\ \mathrm{GeV} < E_\mathrm{p} + E_{\pi^-} + E_{\pi^0} + E_{\mathrm{K}^+} < 75\ \mathrm{GeV} \qquad (78)$$

[in all, some 6000 'elastic' events (77)]. Analysis of the two-dimensional plot of the effective masses $M(\mathrm{p}\pi^-)$ and $M(\mathrm{p}\pi^0)$ showed [74] that this process is dominated by events with $\Lambda \to \mathrm{p}\pi^-$ and $\Sigma^+ \to \mathrm{p}\pi^0$ decays. The decay path of Λ hyperons in the SPHINX setup was restricted by triggering conditions to about 30 cm. The detection of the $\Sigma^+ \to \mathrm{p}\pi^0$ decays is possible over the whole decay path for Σ^+ hyperons.

In this way, in the analysis of reaction (77) the processes with Λ and Σ^+ hyperons

$$\mathrm{p} + \mathrm{N} \to (\Lambda\pi^0\mathrm{K}^+) + \mathrm{N}, \quad \Lambda \to \mathrm{p}\pi^-, \qquad (79)$$

$$\mathrm{p} + \mathrm{N} \to (\Sigma^+\pi^-\mathrm{K}^+) + \mathrm{N}, \quad \Sigma^+ \to \mathrm{p}\pi^0, \qquad (80)$$

were singled out.

Apart from the 'elastic' process (79) the inelastic partially inclusive reaction with additional neutral particles

$$\mathrm{p} + \mathrm{N} \to (\Lambda\pi^0\mathrm{K}^+) + \mathrm{N} + \text{neutral particles}\,, \qquad (81)$$

was also separated in the analysis of the SPHINX data. For this purpose, events with $\Lambda\mathrm{K}^+$ and two or more photon clusters detected in the photon spectrometer were analysed. The events, for which the effective mass of at least one photon pair was in the region of the π^0 mass, namely $0.10\ \mathrm{GeV} < M(\gamma_i\gamma_j) < 0.17$ GeV, were selected. If more than one $\gamma_i\gamma_j$-pair satisfied such a requirement for $M(\gamma_i\gamma_j)$, all the combinations $\Lambda\pi^0_{(1)}K^+$, $\Lambda\pi^0_{(2)}\mathrm{K}^+$ etc. with the corresponding weights were taken. Of course, the 'elasticity' condition (78) was not imposed in this case.

The number of detected events of the reaction (81) amounted to 2855 and exceeds the statistics of the 'elastic' events (79) by more than four times. The effective mass spectra of the $\Lambda\pi^0$ system in reactions (79) and (81) are shown in Fig. 15. The corresponding spectrum of 'elastic'

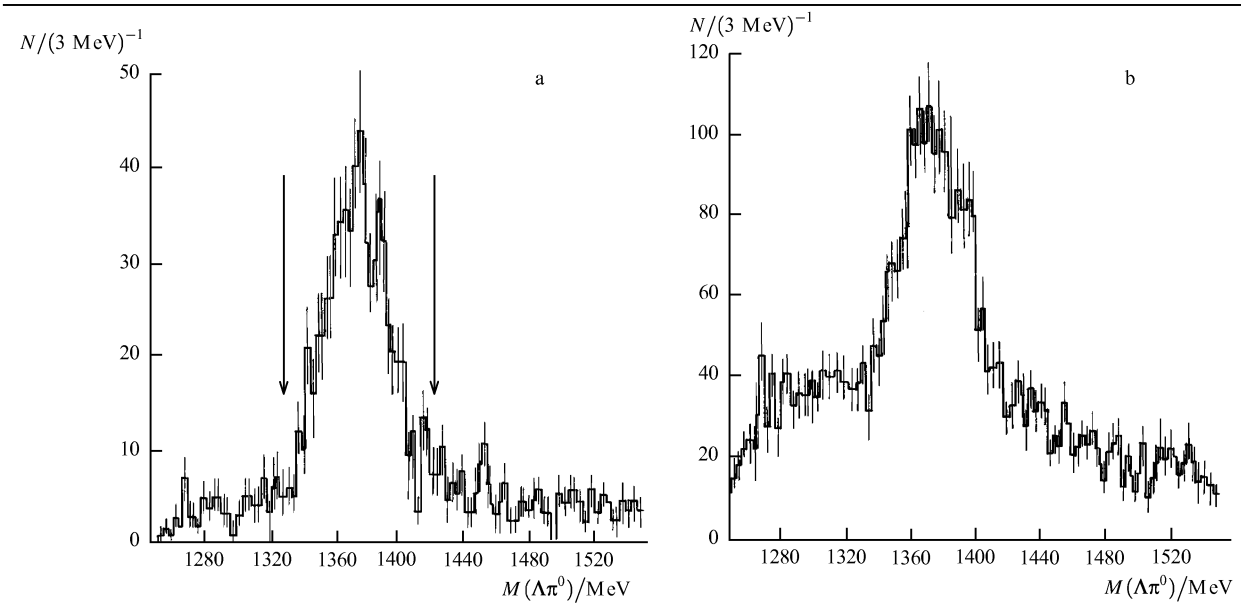

Figure 15. Invariant mass spectra of the $\Lambda\pi^0$-system: (a) in the 'elastic' diffractive production reaction (79); (b) in the partially inclusive inelastic reaction (81). The parameters of the $\Sigma(1385)^0$-peak are in agreement with the tabular data (with the apparatus mass resolution $\sigma = \pm 9$ MeV and systematic errors taken into account). The arrows mark the region of the $\Sigma(1385)^0$ band ($1330\ \mathrm{MeV} \leqslant M(\Lambda\pi^0) \leqslant 1424$ MeV).

reaction (79) is dominated by a peak of $\Sigma(1385)^0 \to \Lambda\pi^0$ decay process with a very low background under the peak.

The $\Sigma(1385)^0$-peak is also well seen for the partially inclusive reaction (81). Although the background under the resonance peak is significantly higher in this case than in the 'elastic' process, it is still much lower than that observed for the reaction (5) in the BIS-2 measurements, where the background was more than twice as high as the numbers of events in the $\Sigma(1385)^-$ peak (see Fig. 7). Thus, the reactions (60) and (69) were well identified in the experiments with the SPHINX setup.

The study of dN/dP_T^2-distributions for the reactions (60) and (69) shows that the processes of the coherent diffractive production on the carbon nucleus (with a slope parameter of diffractive cone $b \gtrsim 30$ GeV^{-2}) are also well exhibited in these reactions.

Analysis of the $M[\Sigma(1385)^0K^+]$ mass spectra in reactions (60) and (69) in various transverse-momentum intervals did not reveal any structures corresponding to $N_\phi(1960)$ baryon production neither in summary mass spectra (for all values of P_T^2), nor in mass spectra for the coherent processes, that is for $P_T^2 < 0.075$ GeV^2 (see, for example, Fig. 16).

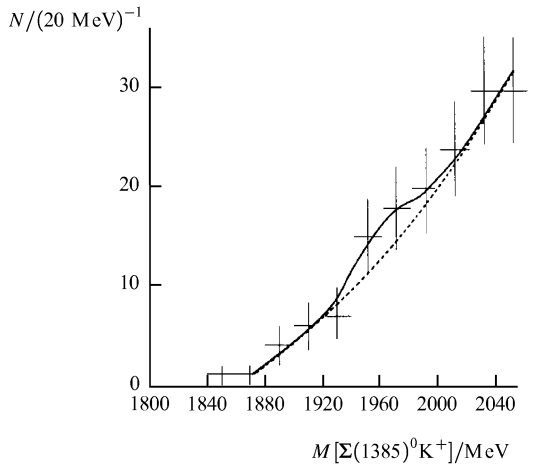

Figure 16. Results of the search for $N_\phi(1960)$-baryon in the mass spectra $M[\Sigma(1385)^0K^+]$ in the SPHINX experiments for the 'elastic' reaction (60) (for $P_T^2 < 0.075$ GeV^2). The spectrum was fitted by a sum (the solid line) of a polynomial background (the dashed line) and the $N_\phi(1960)$-peak with the parameters obtained from the BIS-2 data [44].

Table 7 contains the upper limits on cross sections of the reactions

$$p + N \to N_\phi(1960)^+ + N\,, \qquad (82)$$
$$\hookrightarrow \Sigma(1385)K$$

and

$$p + N \to N_\phi(1960)^+ + N + \text{neutral particles}\,, \qquad (83)$$
$$\hookrightarrow \Sigma(1385)K$$

obtained in the SPHINX experiments. These limits are significantly lower than the values of the cross sections for the $N_\phi(1960)$ production in the reaction with limited inclusiveness

$$n + N \to N_\phi(1960)^0 + ..., \qquad (84)$$
$$\hookrightarrow \Sigma(1385)^-K^+$$

that were obtained in the BIS-2 experiments (see Section 5.2 and Table 7).

Strictly speaking, there is no direct contradiction between the BIS-2 and SPHINX results, as they are related to somewhat different processes†. However, the large divergence between the cross-section estimations, as well as very hard background conditions for the $N_\phi(1960)$ selection in the BIS-2 experiment, cast some doubts on the real existence of the anomalously narrow $N_\phi(1960)$-baryons (for a more detailed discussion see [74, 75]).

6.3 Further analysis of the effective mass spectrum for the $[\Sigma(1385)^0K^+]$ system and observation of the baryon structure X(2050)

We next undertook to analyse further the effective mass spectrum $M[\Sigma(1385)^0K^+]$ in reaction (60). This spectrum is shown in Fig. 17a for the coherent events (with $P_T^2 < 0.075$ GeV^2), and a structure with a mass $M \approx 2060$ MeV and a width $\Gamma \approx 120$ MeV is observed in it. The physical origin of this 'X(2060)' structure is not clear at the moment. It might be partly connected with some resonance state, but an alternative interpretation in terms of a diffractive nonresonance threshold mechanism of the Deck type cannot be ruled out. Therefore, it is necessary to determine the quantum numbers of the 'X(2060)' state and to investigate the dynamics of reaction (60). As a first step in this direction the influence of P_T^2 cut on the isolation of the coherent diffractive process of particle production on carbon nuclei was studied.

Based on analysis of the dN/dP_T^2 distribution, the event selection criterion $P_T^2 < 0.075$ GeV^2 has been used up to this point to isolate coherent reactions and to suppress the noncoherent background. This is a very soft selection criterion which leaves over 30% of the noncoherent background events in the mass spectrum shown in Fig. 17a. Moreover, the measured value of the slope parameter of the diffractive cone for the carbon nuclei ($b \approx 30$ GeV^{-2}) is probably underestimated because of the setup resolution. If the slope parameter b is in fact close to the value expected for the carbon nucleus ($b \approx 50$ GeV^{-2}), an additional increase in the noncoherent background in the mass spectrum in Fig. 17a is possible.

To suppress the noncoherent background and to obtain the mass spectrum of the $\Sigma(1385)^0K^+$ system in the 'pure' process of coherent production on nuclei, the stringent event selection criterion $P_T^2 < 0.02$ GeV^2 was used (Fig. 17b). As one can see from comparison of effective mass spectra in Fig. 17a and 17b, this stringent selection criterion led to a clear observation in the spectrum for the 'pure' coherent process of a narrow X(2050) peak with a mass near 2050 MeV.

Further investigation of this narrow structure was performed by thorough study of the shape of the mass spectrum $M[\Sigma(1385)^0K^+]$ in the purely coherent reaction on a carbon nucleus

$$p + C \to [\Sigma(1385)^0K^+] + C \qquad (85)$$

(with $P_T^2 < 0.02$ GeV^2). This study was based on somewhat increased statistics with different subdivision into the mass bins. As is seen from Fig. 18, the narrow structure X(2050)

†One must uniquely conclude that the statement concerning the diffractive character of the N_ϕ (1960) production in the BIS-2-experiments [44] is incorrect (as we already mentioned in Section 5.3).

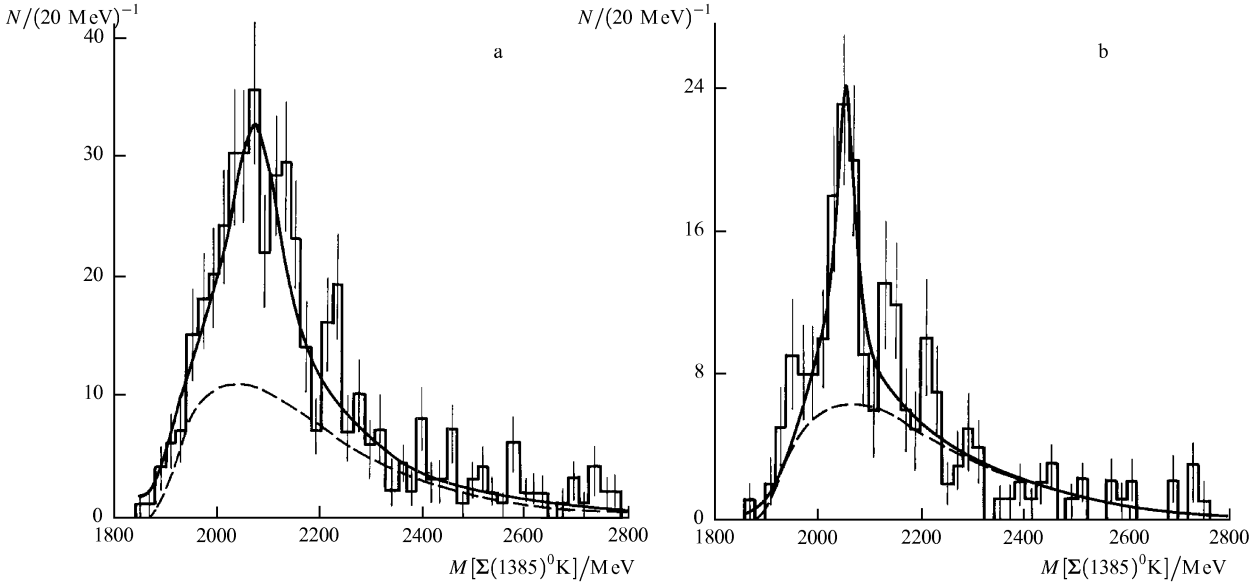

Figure 17. (a) Effective mass spectrum of the $\Sigma(1385)^0K^+$ in the SPHINX experiment for the coherent diffractive production reaction on the carbon nucleus (i.e. for $P_T^2 < 0.075$ GeV^2). The spectrum was fitted by the sum of a Breit–Wigner peak with $M = 2065 \pm 11$ MeV and $\Gamma = 118 \pm 19$ MeV and a polynomial background. With such a soft selection by P_T^2, the spectrum contains a significant background of noncoherent events (exceeding 30%, see the text). (b) The same spectrum, but under stringent transverse momentum cut-off $P_T^2 < 0.02$ GeV^2 for a more reliable selection of coherent events. The spectrum was fitted by the sum of a Breit–Wigner peak with $M = 2050 \pm 6$ MeV and $\Gamma = 50 \pm 20$ MeV and a polynomial background.

Table 8. Study of the X(2050) structure in the mass spectrum $M[\Sigma(1385)^0K^+]$ in reaction (85).

Bin ΔM / MeV	Parameters of the X(2050)-peak			
Number of of the standard		M/MeV	Γ/ MeV	Number of events in the peak
10	2053± 4	40± 15	74± 23	$> 8\sigma$
20	2049± 6	49± 20	75± 29	$> 6\sigma$
30	2053± 5	35± 16	59± 19	$> 7\sigma$
40	2052± 7	50± 24	75± 42	$> 6.5\sigma$

Note. The instrumental width of the peak is Γ_{app}= 25 MeV.

is very clearly observed in all these spectra. The results of the fitting of the data and the estimates of statistical significance of X(2050) structure are summarised in Table 8 (for this evaluation the maximal possible background under the peak was approximated by the sideband method, with the help of information in several adjacent channels around the observed structure position.

Thus in the study of coherent reaction (85) a new narrow peak X(2050) is observed with parameters

$$M = 2052 \pm 6\ \mathrm{MeV}, \qquad \Gamma = 35^{+22}_{-35}\ \mathrm{MeV} \tag{86}$$

(with experimental mass resolution taken into account). Its statistical significance exceeds six standard deviations. The anomalously narrow structure cannot be interpreted in terms of a diffractive nonresonance mechanism of the. Deck type and is probably a candidate for a new cryptoexotic baryon with hidden strangeness. However, this conclusion is considered as preliminary and must be confirmed in a new measurement with increased statistics.

The $M[\Sigma(1385)^0K^+]$ mass spectrum of reaction (60) in the region $M > 2750$ MeV was also investigated in the SPHINX experiments. No statistically significant resonant structures are observed in this spectrum. The upper limits of the corresponding cross sections lie within the range 15–25 nb/nucleon. In particular, the following upper limit for the $R(3520)$-baryon is found to be

$$\sigma[\mathrm{R}(3520)^+]_{\mathrm{nucleon}}\mathrm{BR}[\mathrm{R}^+ \to \Sigma(1385)^0\mathrm{K}^+] \leqslant 16\ \mathrm{nb/nucleon} \tag{87}$$

(the confidence level is 95%).

6.4 Study of the reaction p+ N → (Σ^0K^+)+ N and observation of the X(2000) baryon state

During the study of reactions with Λ hyperons and K^+ mesons the events that satisfied the standard selection criteria for the process with one and only one additional photon cluster

$$\mathrm{p} + \mathrm{N} \to (\Lambda\gamma\mathrm{K}^+) + \mathrm{N}\,, \tag{88}$$

were singled out. Analysis of these event showed that the main source of background in reaction (88) is an imitation of single photons by remaining hadronic showers in the γ-spectrometer of the SPHINX setup. The rather high level of this background suggests that the standard photon selection criteria used previously for $\pi^0 \to \gamma\gamma$ decay detection (where there is an additional π^0 mass requirement) are inadequate for the single-photon identification. Therefore, more stringent criteria were used for the last case which made it possible to suppress the hadron background to a considerable extent (the threshold energy for the detection of single photons was increased from $E_\gamma > 0.65$ GeV to $E_\gamma > 1.2$ GeV, the minimum distance between the photon shower and the closest hadron track in the detector was increased, and transverse size selection was introduced for the shower).

Fig. 19 shows the final mass spectrum of the $\Lambda\gamma$-system in reaction (88) obtained after these stringent criteria have

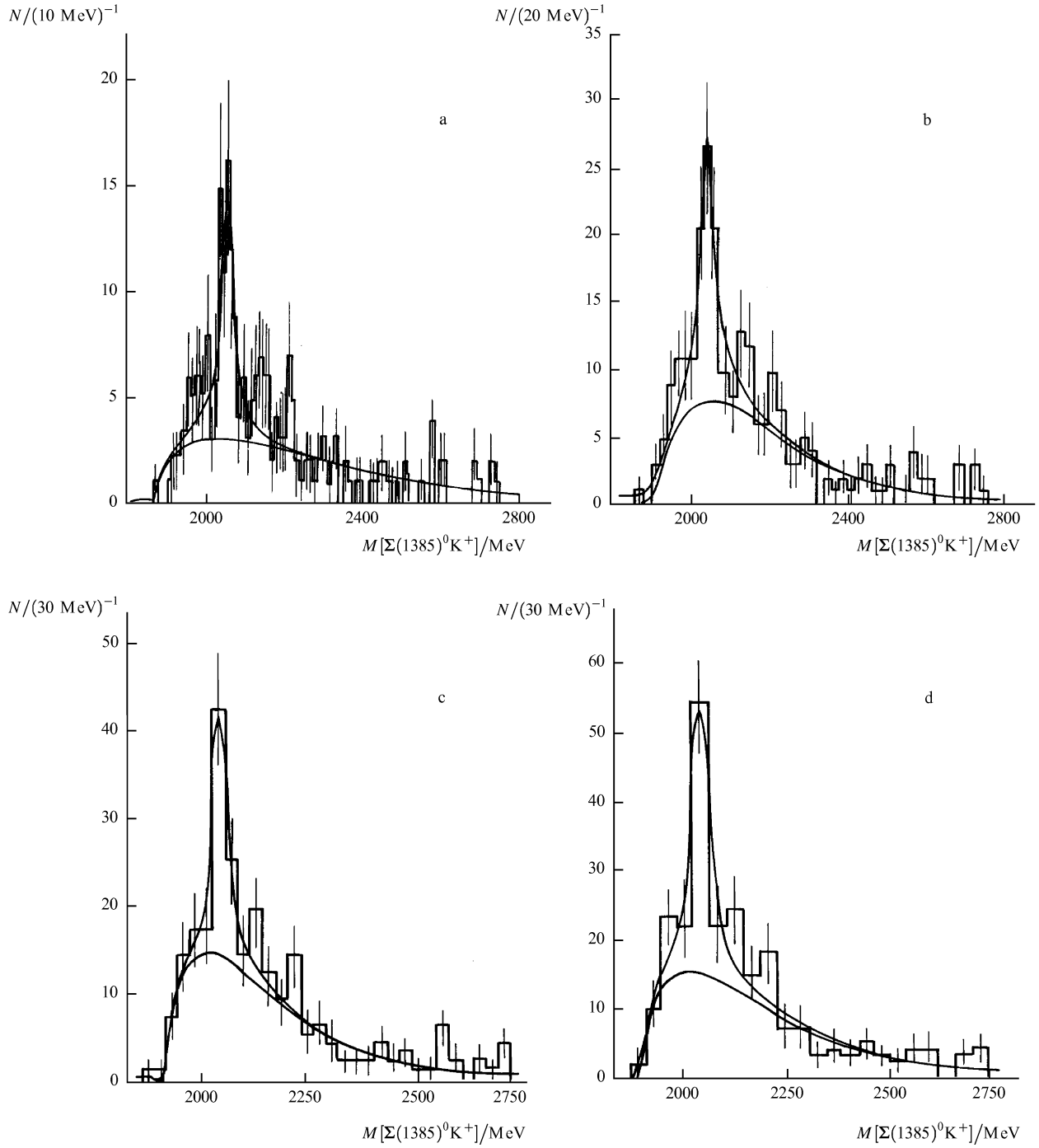

Figure 18. Detailed study of the effective mass spectrum $M[\Sigma(1385)^0K^+]$ in the coherent reaction $p + C \to [\Sigma(1385)^0K^+] + C$ at the stringent cut-off $P_T^2 < 0.02$ GeV^2 with different effective mass bins ΔM : (a) $\Delta M = 10$ MeV; (b) $\Delta M = 20$ MeV; (c) $\Delta M = 30$ MeV; (d) $\Delta M = 40$ MeV. Statistical coinfidence levels of the peaks are estimated on the assumption of maximal possible background (approximated by the sideband method, i.e. with the number of events in the adjacent mass intervals near the main peak in each spectrum).

been introduced. As is seen from the figure, a signal corresponding to $\Sigma^0 \to \Lambda\gamma$-decay in the reaction $p + N \to (\Sigma^0K^+) + N$ is very clearly distinguished in the mass spectrum. The favourable background conditions made it possible to study the effective mass spectrum $M(\Sigma^0K^+)$ in process (59).

Fig. 20 shows this spectrum for the coherent process of Σ^0K^+ diffractive production on the carbon nucleus (in the transverse momentum range $P_T^2 < 0.1$ GeV^2). In addition to a small structure in the near-threshold region with $M \simeq 1800$ MeV, a peak X(2000) with parameters

$$M = 1999 \pm 7\,\text{GeV}, \quad \Gamma = 91 \pm 17\ \text{GeV}$$

is distinctly observed (with a statistical significance of more that seven standard deviations).

Such a shape of effective mass spectrum (with additional structure in the near-threshold region) shows that the X(2000) peak cannot be explained by a nonresonant Deck-type diffractive singularity. It seems that this peak has a resonance origin.

The influence of more stringent transverse momentum cuts on the mass spectrum of $M(\Sigma^0 K^+)$ systems in the coherent reaction $p + C \to (\Sigma^0 K^+) + C$ was also studied (for $P_T^2 < 0.075$; 0.050; 0.040; 0.020 GeV^2). These cuts may reduce noncoherent background and more clearly single out the coherent production of the X(2000) state (as took place for the $X(2050) \to \Sigma(1385)^0 K^+$ state; see Section 6.3). However, as was shown by this analysis, such cuts do not change the shape of the mass spectrum, but only reduce the event statistics.

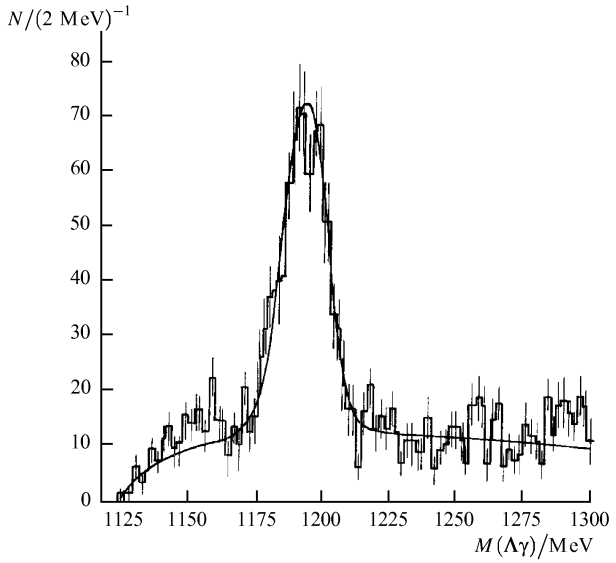

Figure 19. Effective mass spectrum of the $\Lambda\gamma$-system in the reaction $p + N \to (\Lambda\gamma K^+) + N$ (with elastic requirement for energies) after introduction of special criteria for the selection of single photons.

6.5 Decay channels for the X(2050)- and X(2000)-states

First data on the decay channels of the X(2050) and X(2000) states were obtained by simultaneously studying the coherent reactions $p + C \to \Sigma^0 K + C$ or $p + C \to \Sigma(1385)^0 K^+ + C$ together with $p + C \to p\pi^+\pi^- + C$ and $p + C \to \to \Delta^{++}\pi^- + C$ under the same kinematic conditions. From the mass spectra $M(p\pi^+\pi^-)$ and $M(\Delta^{++}\pi^-)$ analysis the upper limits for the branching ratios of the X(2050) and X(2000) decays on these channels were obtained.

As the X(2000) and X(2050) baryons are produced in the diffractive coherent processes, their isotopic spins must be the same as for initial protons, that is $I = 1/2$. Thus, taking into account the isotopic relations for the decay channels, the lower boundaries for the decay probability ratios can be obtained (with 95% confidence level):

$$R_1 = \frac{\mathrm{BR}[X(2050)^+ \to (\Sigma(1385)K)^+]}{\mathrm{BR}[X(2050)^+ \to (\Delta\pi)^+]} > 1.7 \qquad (90)$$

$$R_2 = \frac{\mathrm{BR}[X(2050)^+ \to (\Sigma(1385)K)^+]}{\mathrm{BR}[X(2050)^+ \to p\pi^+\pi^-]} > 2.6\,, \qquad (91)$$

$$R_3 = \frac{\mathrm{BR}[X(2000)^+ \to (\Sigma K)^+]}{\mathrm{BR}[X(2000)^+ \to (\Delta\pi)^+]} > 0.73\,, \qquad (92)$$

$$R_4 = \frac{\mathrm{BR}[X(2000)^+ \to (\Sigma K)^+]}{\mathrm{BR}[X(2000)^+ \to p\pi^+\pi^-]} > 7.8\,. \qquad (93)$$

A comparison of the limits for $R_1 - R_4$ with the corresponding data for isobars $N^* = |qqq\rangle$ with close mass values (see the data in Ref. [11] and Table 9) shows these ratios to be significantly higher than those for the ordinary isobars. As we saw above, the large probabilities for the decay channels with strange particles in the final states are specific properties of cryptoexotic baryons with hidden strangeness.

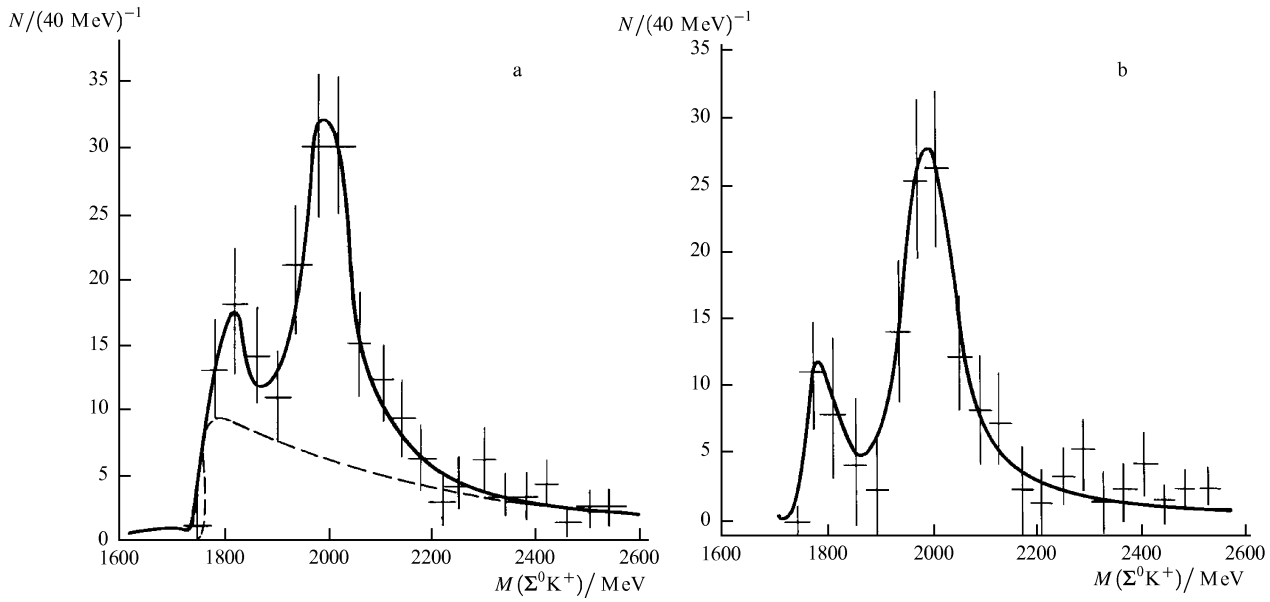

Figure 20. Effective mass spectra $M(\Sigma^0 K^+)$ for the coherent diffractive reaction $p + C \to \Sigma^0 K^+ + C$ ($P_T^2 < 0.1$ GeV^2): (a) for all events from the 'Σ^0 band' in Fig. 19; (b) after subtraction of the background under the Σ^0 peak (by the adjacent bands in the spectrum $M(\Lambda\gamma)$ in Fig. 19). Structures near the threshold region with $M = 1802 \pm 3$ MeV and a sharp peak with $M = 1999 \pm 7$ MeV and $\Gamma = 91 \pm 17$ MeV are observed in the mass spectra. The dashed line corresponds to a smooth polynomial background.

Table 9. Properties of massive isobars $N^* = |qqq\rangle$ (q = u, d-quarks).

N^* J^P (status)	Γ/MeV	Probability ratio for different decay channels					
		$\frac{N^* \to N\pi}{N^* \to tot}$	$\frac{N^* \to \Delta\pi}{N^* \to tot}$	$\frac{N^* \to N\pi\pi}{N^* \to tot}$	$\frac{N^* \to \Sigma K}{N^* \to tot}$	$\frac{N^* \to \Sigma K}{N^* \to \Delta\pi}$	$\frac{N^* \to \Sigma K}{N^* \to \Delta\pi}$
N(1900) $3/2^+(*)$	498 ± 78	0.26	0.4		—	—	—
N(1990) $7/2^+(*)$	200 – 500	0.06	0.3 – 0.9		$(2-60) \times 10^{-3}$		< 0.1
N(2000)	490 ± 310	0.06	0.15 – 0.20	0.6 – 0.7	$(1-4) \times 10^{-2}$	$(6-25) \times 10^{-2}$	$(1-3) \times 10^{-2}$
	...						
	170(ΣK)						
$5/2^+(**)$	95 ± 20						
N(2080) $3/2^-(**)$	200 – 600	0.13 – 0.16	0.25 – 0.30	0.5 – 0.6	$(1.5-40)\times10^{-3}$	$(6-40)\times10^{-3}$	$(3-20)\times10^{-3}$
N(2090) $1/2^-(*)$	414 ± 185	0.10 – 0.15	—	—	—		
	350 ± 100						
	95 ± 30						
N(2100) $1/2^+(*)$	113 ± 40	0.10 – 0.15	0.4	—	—		
	260 ± 10						
	200 ± 30						
N(2190) $7/2^-(****)$	450 ± 100	0.1 – 0.2	$\gtrsim 0.4$		$(1.5-3)\times10^{-3}$	$(3-6)\times10^{-3}$	

Note. For well-determined massive isobars N^* and Δ^* (with the status $****$ and $***$ — see Tables 2, 3 and Ref. [11]) with $M > 1900$ MeV, the decay widths $\Gamma > 200-300$ MeV. For not very reliable states (with the status $**$ and $*$), the widths and other properties are rather poorly determined. Therefore, several widths defined by different studies are often shown. For example, for N(2000) the $\Gamma \approx 170$ MeV is found by phase analysis of the reaction $\pi^- + p \to \Sigma + K$, and $\Gamma = 95 \pm 20$ MeV by analysis of the reaction $\pi N \to \pi N$ ($M = 1882 \pm 10$ MeV in this experiment).

Thus, comparatively small decay widths of X(2050) and X(2000) baryon states as well as the anomalously large branching ratios for their decay channels with strange particles (large values of $R_1 - R_4$) are serious grounds for the interpretation of these states as strong candidates for cryptoexotic baryons with hidden strangeness. The investigation of a possible connection between these two states and their further detailed study must be done in future experiments with significantly increased statistics.

The study of nonperipheral processes in reaction (59) and (60) in the region of intermediate transverse momenta $P_T^2 > 0.3$ GeV^2 was also performed in the SPHINX measurements. Although some interesting effects in this region might be observed, the presently existing statistics are insufficient to obtain any definite conclusion on this subject, and these measurements should be continued.

6.6 Study of $p + N \to pp\bar{p} + N$ reaction

As was stated in Section 3, the model of quark clusters with colour sextet bonds predicts a decay of pentaquark baryons into an M-baryonium and a proton. The massive M-baryonium, having a quark structure $|(qq)_{6c} \otimes (\bar{q}\bar{q})_{\bar{6}c}\rangle$, can decay, in turn, into a baryon – antibaryon pair. In this case, the decay of a massive exotic baryon which does not contain valence strange quark – antiquark pair, can occur by a channel with the very clear signature

$$|(qq\bar{q})_{\bar{6}c} \otimes (qq)_{6c}\rangle \to |(\bar{q}\bar{q})_{\bar{6}c} \otimes (qq)_{6c}\rangle + |qqq\rangle \to p\bar{p} + p\,. \qquad (94)$$

A search for such baryons were made by the SPHINX collaboration in studying reaction (67) (see [79]):

$$p + N \to pp\bar{p} + N\,.$$

This reaction was selected by analysing the same sample of trigger events with three charged particles in the final state, which were processed earlier during studies of the reactions

$$p + N \to (K^+K^-p) + N\,,$$
$$p + N \to [\Sigma(1385)^0K^+] + N,$$
$$p + N \to (\Sigma^0K^+) + N\,,$$

(see Sections 6.1 – 6.5).

To select events (67), the following criteria were used:

1. Events with three charged secondaries must satisfy the elasticity condition at energies

$$65 \text{ GeV} < E_p + E_{\bar{p}} + E_p < 75 \text{ GeV}\,.$$

2. For the identification of secondaries in the RICH detector according to the maximum likelihood method, the unambiguous identification of the proton and antiproton was required. The third particle was assumed to be a proton (as required by baryon number conservation) if the probability of the $pp\bar{p}$ hypothesis was not much less than of the best fit.

Some 7100 events of reaction (67) were selected by means of these criteria. To verify that these events had been correctly identified, the effective mass spectra were plotted under the assumption that the pK^+K^- and $p\pi^+\pi^-$ systems were formed in the final state. The $\Lambda(1520)$, $\phi(1020)$, and $\Delta(1232)$ peaks, which are typical for the production of these systems, were not observed in the corresponding mass spectra.

Study of P_T^2 distribution for events (67) shows that the main contribution into the $pp\bar{p}$-system formation for small transverse momenta ($P_T^2 < 0.075$ GeV^2)) is made by processes of coherent diffractive production on the carbon nuclei corresponding to the slope parameter of the diffractive cone $b \gtrsim 30$ GeV^{-2}. In connection with the search for exotic baryon decays by the channel with baryonium emission with its subsequent decay to the $p\bar{p}$-channel [see reaction (94)], it should be noted that the data on possible existence of such baryonia are, in general, quite controversal (see, for example, reviews [81, 82]). Experiments [82–88] were claimed to observe narrow baryonium resonances with masses 1.93, 2.02, and 2.20 GeV. At the same time, no statistically significant enhancements in the effective mass spectra of the $p\bar{p}$-system were found in papers [89–92]. The data on reaction (67) were used for further investigation of the problem of the possible existence of baryonia and other exotic hadrons. The invariant mass spectra for the systems $p\bar{p}$, pp, and $pp\bar{p}$ in the coherent region and for all events were studied. The distributions were fitted by smooth functions and did not contain clearly distinguished structures at a level exceeding two standard deviations.

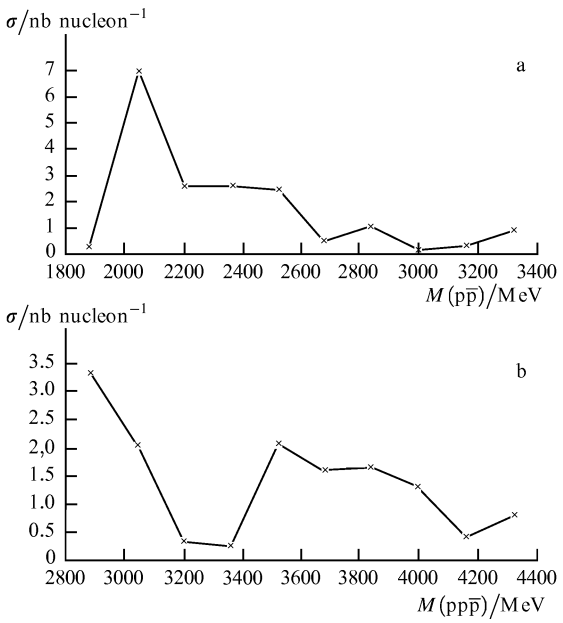

Figure 21. (a) The upper limits for diffractive production cross-sections of heavy narrow meson resonances (with $\Gamma \leqslant 50$ MeV), decaying by the channel $M \to p\bar{p}$ ('baryonia') in the reaction $p + N \to Mp + N$. (b) The upper limits for diffractive production cross sections of heavy narrow baryonic resonances B (with $B \to pp\bar{p}$) in the reaction $p + N \to B + N$.

Table 10. Cross-sections for production of $p\bar{p}$-states (nb nucleon^{-1}).

Reaction	Refs	Mass $M_{p\bar{p}}$/ GeV		
		1.93	2.02	2.20
$ep \to epp\bar{p}$	[87]	—	6.6± 2.2	5.0± 2.5
$\gamma p \to pp\bar{p}$	[92]	< 0.5	< 0.77	< 0.72
$\pi^- p \to ppp\bar{p}\pi$	[86]	16± 7	48± 13	17± 5
$\pi^+ p \to pp\bar{p}\pi$	[88]	—	23± 4	< 12
$pp \to pp\bar{p}p$	[90]	< 10	< 15	< 19
$pN \to pp\bar{p}N$ SPHINX collaboration	[79]	< 1.1	< 7	< 2.5

The obtained data were used to impose upper limits on the corresponding production cross sections for anomalously narrow heavy meson and baryon resonance states in the diffractive process (67). These estimations are presented in Fig. 21. Comparison with data taken from some other papers is made in Ref. [79] and in Table 10.

The diffractive reaction

$$p + N \to (pp\bar{p}\pi^0) + N\,. \tag{95}$$

was also studied in the SPHINX experiments with a sample of 195 observed events. However, the limited statistics proved to be insufficient for the statistically significant analysis of the secondary particle effective mass spectra in reaction (95).

7. Results of other experiments on the search for exotic baryons

In Sections 5 and 6 we mostly described the experiments on the search for cryptoexotic baryons with hidden strangeness; in this section we will briefly discuss results of other studies devoted to the search for exotic baryons of various types.

7.1 Search for exotic baryons in processes with baryon exchange

As was noted in Sections 3 and 4, the model for baryons with open exotic quantum numbers $I = J = 5/2$ (E_{55}-baryons) and $I = J > 5/2$ based on the superconvergent sum rules analysis of reggeon scattering on baryons was treated in Refs. [29, 30]. It was proposed to look for these exotic baryons in backward production reactions with baryon exchange, such as

$$\pi^+ + p \to (E_{55}^{+++})_f + \pi_b^- \tag{96}$$

(the indices 'f' and 'b' denote the particles which fly out in the forward and backward direction, respectively, in the laboratory frame). These exotic baryons are assumed to decay mainly according to the scheme $(I, J) \to (I-1, J-1) + \pi$, for example

$$E_{55} \to \Delta + \pi\,. \tag{97}$$

The searches for E_{55}-baryons were performed in several experiments on backward production reactions as well as on some other processes (see Refs [93]–[95] and the review in Ref. [31]). Let us consider as an example the results obtained in the measurements with the spark chamber

magnetic spectrometer TISS-3 on the ITEP accelerator. The following reactions were studied in this experiment at momentum $P_{\pi^+} = 3.94$ GeV [93]:

$$\pi^+ p \to (p\pi^+\pi^+)_f + \pi_b^- , \quad (98)$$

$$\pi^+ p \to (p\pi^+\pi^+)_f + \pi^0 + \pi_b^- . \quad (99)$$

The combined effective mass spectrum for the $p\pi^+\pi^+$-system in reactions (98) and (99) is shown in Fig. 22. The authors of Ref. [93] come to the conclusion that their data do not contradict the existence of three exotic states with an isospin $I = 5/2$ and parameters

$$M_1 = 1.39 \pm 0.01 \text{ GeV}, \quad \Gamma_1 = 40 \pm 20 \text{ MeV}; \quad (100)$$

$$M_2 = 1.48 \pm 0.01 \text{ GeV}, \quad \Gamma_2 = 60 \pm 30 \text{ MeV}; \quad (101)$$

$$M_3 = 1.62 \pm 0.01 \text{ GeV}, \quad \Gamma_3 = 80 \pm 50 \text{ MeV}. \quad (102)$$

It should be noted, however, that the statistical significances of these results very strongly depend on the background approximation and are insufficient.

The data obtained in some bubble chamber experiments (see [31], [94]) are characterised by even worse statistical reliability. The results of the different experiments are in rather poor agreement with each other. So the problem of the possible existence of the E_{55}-baryons still remains unsolved.

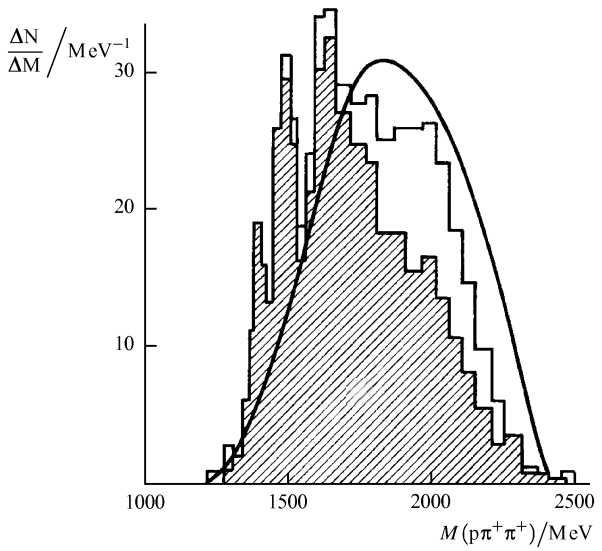

Figure 22. The combined effective mass spectrum of $p\pi^+\pi^+$-systems in the reactions (98) and (99) [93]. The hatched hystogram corresponds to the events, consistent with the $\Delta(1232)^{++}\pi^+$-system formation. The curve represents the sum of the phase space curves used for the description of spectrum $p\pi^+\pi^+$ in the reactions (98) and (99).

7.2 Study of diffractive dissociation reactions $\pi^+ + p \to \pi^+ + (\pi^+ n)_{dif.dis}$ and $\pi^+ + p \to \pi^+ + (\pi^0 p)_{dif.dis}$

In the CERN experiments with the liquid hydrogen bubble chamber, the reactions of diffractive π^+-dissociation of target protons [43] were singled out in $\pi^+ p$ interactions at primary momentum of 16 GeV

$$\pi^+ + p \to \pi^+ + (\pi^+ n)_{dif.dis} , \quad (103)$$

$$\pi^+ + p \to \pi^+ + (\pi^0 p)_{dif.dis} . \quad (104)$$

To select these diffractive dissociation processes and to distinguish them from other reactions ($\pi^+ p \to \rho^+ p$, $\pi\Delta$, etc.), a special filtration method was used (so-called PPA-analysis; see Ref. [96]).

The combined effective mass spectra of the πN-system in the diffractive reactions (103) and (104) were obtained for small transferred momenta $|t'| < 0.1$ GeV^2 (Fig. 23a) and intermediate transferred momenta $|t'| > 0.2$ GeV^2 (Fig. 23b). Three baryonic structures with main parameters listed in Table 11 appear in these spectra. Fig. 23 also shows contributions of the Deck-type threshold effects into the continuum of these mass spectra. The remaining part of this continuum is caused by the summary contribution of a number of known isobars observed earlier in the πN-formation reactions.

In Ref. [43] the analysis of other data obtained in diffractive production processes with the πN- and $\pi\pi N$-systems is also given. It is shown, in particular, that the $\pi\pi N$-system studies revealed the presence of the baryonic states with the averaged parameters

$$M = 1450 \pm 3 \text{ MeV}, \quad \Gamma = 98 \pm 7 \text{ MeV};$$

$$M = 1705 \pm 3 \text{ MeV}, \quad \Gamma = 84 \pm 4 \text{ MeV}. \quad (105)$$

Fig. 24 compares the masses of possible baryonic states with isotopic spin $I = 1/2$ obtained in the processes of diffractive dissociation and in formation reactions with the s-channel resonance production (see Section 4.2 and Table 3).

Possible differences between the baryonic states obtained in these two quite different classes of reactions have been discussed. It was concluded that at least the state X(1344) (Fig. 23a) is quite different by its properties (mass and width) from N^*-isobars observed in the formation reactions. In particular, the X(1344)-state is characterised by a comparatively small width. All attempts to expain this structure as being a result of interference between the P-wave amplitude of a Deck-type threshold nonresonant process and the known isobar $P_{11}(1470)$ production mechanism have failed. Therefore, in Ref, [43] a suggestion was made that the X(1344)-state, which is out of the framework of baryonic isobars of the ordinary qqq-type, is possibly a cryptoexotic pentaquark baryon $|qqqq\bar{q}\rangle$ consisting of u- and d-quarks.

7.3 Search for narrow s-channel resonances in the $\pi^- p$ formation reactions

The searches for narrow nonstrange baryonic resonances in the $\pi^- p$ formation reactions were performed in the two experiments at the CERN PS accelerator [97, 98]. In these experiments a high-precision scanning of the cross sections of the corresponding processes over the initial momentum of pions in the beam was undertaken. The P_{π^-} momentum measurements were done with the precision $\Delta P/P \approx 5 \times 10^{-4}$.

In the first experiment [97] the differential cross sections of elastic $\pi^- p$-scattering at c.m. angles near 90° were measured. The momentum dependence of elastic scattering cross sections was studied in the P_{π^-} momentum range from 5.75 to 13.02 GeV (3.42 GeV $< M(\pi^- p) <$ 5.03 GeV) in 22 intervals, each of which during the P_{π^-} measurements was subdivided by mini-intervals $\Delta P/P = 5 \times 10^{-4}$ (in total 1700 points by energy were obtained, with statistics at each point corresponding to a luminosity of 0.4 event nb^{-1}).

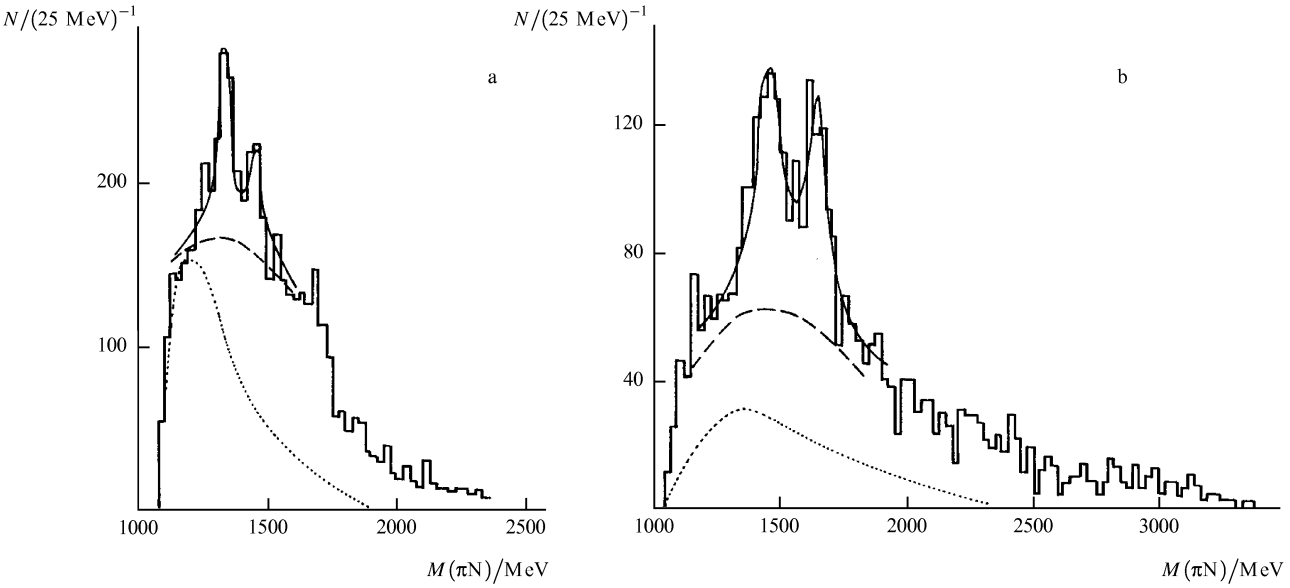

Figure 23. The combined effective mass spectra of the πN-system in the diffractive dissociation reactions (103) and (104): (a) for $|t'| < 0.1$ GeV^2 region; (b) for $|t'| > 0.2$ GeV^2 region. The solid and dashed lines show the results of the spectrum fitting by Breit–Wigner peaks (with parameters from Table 11) and by smooth background curves. The Deck-type threshold mechanism contribution is shown by the dotted lines. The narrow peak with mass 1344 ± 5 MeV and width 66 ± 14 MeV in Fig. 23a has a statistical significance exceeding five standard deviations.

Table 11. Data on the structure in the combined effective mass spectra $[(\pi^+\mathrm{n}) + (\pi^0\mathrm{p})]_{\mathrm{dif.dis}}$ for the diffractive production reactions (103) and (104) [43].

Mass/MeV	Width/MeV	Cross-section of diffractive formation/μb	Slope parameter b/GeV^{-2} (for t'-distribution $\mathrm{d}\sigma/\mathrm{d}\lvert t'\rvert = A \exp bt'$)
1344± 5	66± 14	26± 6	9.0± 0.2
1451± 7	132± 22	48± 11	3.8± 0.2
1639± 7	96± 20	29± 8	3.4± 0.2

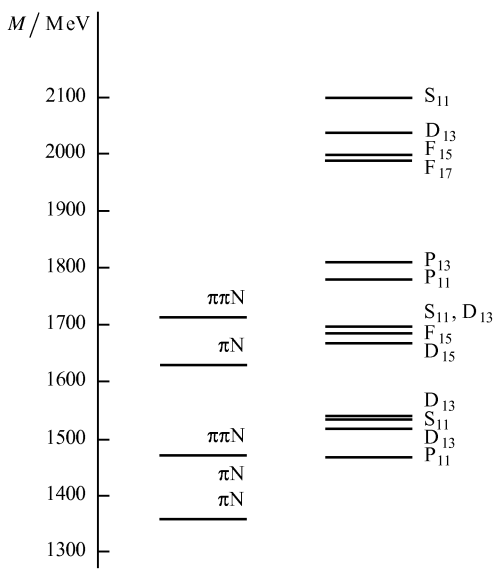

Figure 24. Masses of baryonic πN- and ππN-structures observed in the processes of diffractive production (to the left) and in the formation reactions (to the right).

The sensitivity of the measurements [97] to the baryonic s-channel resonances was determined by the product ΓX^2, where Γ is the resonance width, and X is its elasticity (that is $X = \Gamma(\pi^-\mathrm{p})/\Gamma$). The measurements [97] were able to discover nonstrange resonances with width $\Gamma > 0.1$ MeV and elasticity X exceeding several per cent. No resonance structures were found within this sensitivity. The upper bounds for ΓX^2 (at a level of six standard deviations) for different masses of possible resonances lie within the limits $\Gamma X^2 < (0.2-2) \times 10^{-4}$ MeV.

The same group made the experiment [98] to perform the energetic scanning of the total cross sections of π^-p-interactions in the primary momentum P_{π^-} range from 2 to 14 GeV (2.16 GeV $< M(\pi^-\mathrm{p}) < 5.21$ GeV). They determined the total cross sections for 4500 mini-intervals by momentum with a statistical uncertainty in each bin $\Delta\sigma/\sigma = \pm 0.3\%$. Unlike the elastic scattering experiments, the total cross section measurements have a sensitivity to baryonic resonances determined by the product ΓX (that is, the elasticity X of the baryonic resonance does not strongly influence the results). However, the nonresonance background level under possible peaks exceeds by a few orders of magnitude the background level of the elastic scattering processes. So, by measuring the total cross sections, the effect of possible nonstatistical fluctuations becomes important.

The experiments in Ref. [98] also revealed no statistically significant resonant structures. The sensitivity of the measurements at the six standard deviations level depends on the width of the resonance and its elasticity as $X\sqrt{\Gamma}(J + 1/2)/(I + 1/2) = A$ (J is the spin, I isotopic spin, Γ is measured in MeV and X in per cent). The quantity A depends on the primary momentum to vary from $A \approx 7$ at $P_{\pi^-} = 2$ GeV to $A \approx 100$ for $P_\pi = 14$ GeV. These experiments exclude existence of heavy nonstrange baryons with decay widths greater than a few MeV and elasticity greater than several per cent.

Note, however, that for cryptoexotic five-quark baryons with hidden strangeness $|qqqs\bar{s}\rangle$ the elasticity can be very small (down to 10^{-3}) because of the OZI selection rule. Therefore, the sensitivity of the experiments [97, 98] can be insufficient for the observation of such cryptoexotic states.

A detailed energetic scanning of the elastic π^-p-scattering cross sections in the momentum range P_{π^-} from 1.34 to 1.49 GeV, inside which the threshold for the reaction $\pi^- + p \to \eta' + n$ lies $[P_{\pi^-}(\eta')_{\text{thres}} = 1431.7 \pm 0.6$ MeV], were carried out in Ref. [99]. The same group performed the simultaneous cross section study of the reaction $\pi^- + p \to \eta' + n$ near the threshold [100]. During the elastic π^-p-scattering cross section scanning (in 81 points of the momentum range under study), some narrow structure with a mass $M(\pi^- p) = 1876$ MeV ($P_{\pi^-} = 1389$ MeV) and a width $\Gamma \approx 4$ MeV appears at a confidence level of five standard deviations. This structure lies below the η'-meson formation threshold. The existence of a structure with a mass of 1899 MeV and a width of 5 MeV lying somewhat above this threshold is also possible. However, its reliability is only about three standard deviations.

On the other hand, the near-threshold cross section $\sigma(\pi^- p \to \eta' n)$ dependence on momentum p^* in the c.m. frame has an unusual character: it decreases with increasing p^*. This can be explained by assuming that a narrow 'under-threshold' resonance state with a mass of 1890 MeV and a width of 2–10 MeV appears in the η'-meson production reaction. All these results require further confirmation, as their statistical significance is obviously insufficient.

7.4 Some other investigations

At the end of the seventies some other narrow baryonic structures were claimed to be observed with masses higher than 2 GeV (in the mass spectra of $\Lambda\pi\pi$, $\Lambda\pi\pi\pi$ and $\Sigma\omega$; see, for example, the data presented in Refs [34, 35]). Such states can also be considered as possible candidates for cryptoexotic baryons. These data, however, seemed to be communicated only in the conference proceedings and have not been published since. So we will not consider them here. Other results that require additional study (see, e.g., Ref. [101]) were cited as well.

The search for baryonic resonances with an exotic value of strangeness of $S = +1$ ($|qqqq\bar{s}\rangle$, so called Z-baryons) has been carried out for a long time. The results of these experiments are summarized in PDG data [11], where the corresponding references are also cited. It is noted that the Z-baryon studies, performed for more than twenty years, did not lead to somehow unique results. Their future prospects do not appear to be very encouraging.

8. Exotic states with heavy quarks

Let us now consider possible exotic states with heavy c- and b-quarks. As is shown in Refs [102–105], such states may possess rather specific properties. In particular, one may expect that among the lightest multiquark states with strangeness and charm, or with strangeness and beauty, or with beauty and charm, the hadrons with open exotic, i.e. with exotic values of electric charge and flavours (strangeness, isospin, charm, etc.) are excited.

Moreover, with high probability these heavy exotic hadrons not only can exist, but may be quasistable and may decay only by weak or electromagnetic interactions.

All these new properties of hadrons which contain quarks with four different flavours (e.g. c, s, u, d) follow from the general principle of 'maximal flavour antisymmetry', which was formulated by Lipkin [84]. In agreement with this principle (or rather hypothesis), all other conditions being equal, the quark systems characterised by the maximum possible antisymmetry of quark flavours (both for quarks and antiquarks) turn out to be most strongly bound. For instance, this means that the $u\bar{u}d\bar{s}$ system would be more strongly bound, than the $uud\bar{s}$ one, etc. This also means that for dibaryons with six light quark configurations the most strongly bound will be H = udsuds system, for which not more than 2 quarks are in the states with identical flavours.

We shall consider 4-quark mesons $qq\bar{q}\bar{q}$ as an example. If there are only u, d, s, quarks in these mesons then for the most strongly bound system one quark–antiquark pair (e.g. $u\bar{u}$ for the $u\bar{u}d\bar{s}$ systems, considered earlier) will be characterised by opposite values of one and the same flavour, i.e. it will correspond to the zero total value of this flavour. Then the quantum numbers of hadrons are determined by the remaining $q\bar{q}$ pair (in our case, $d\bar{s}$), i.e. this hadron has cryptoexotic quantum numbers.

Hence, from the flavour antisymmentry it follows that the lightest and the most strongly bound (narrow) $qq\bar{q}\bar{q}$ hadrons consisting of u, d, and s quarks are cryptoexotic. Weakly bound systems with open exotic (like $uu\bar{d}\bar{s}$) can have very large decay widths and would be practically unobservable.

However the situation changes if $qq\bar{q}\bar{q}$ mesons contain quarks with four different flavours. In this case the 'flavour antisymmetry' principle admits the existence of states with obviously exotic values for the quantum numbers, e.g. $\tilde{F}_S = cs\bar{u}\bar{d}$ mesons with 'wrong' (i.e. exotic) values of strangeness or $\tilde{F}_I = c\bar{s}(q\bar{q})_{I=1}$ with a 'wrong' isospin, among the lightest mesons of this type. The properties of such mesons are discussed in Refs [102–105].

The existence of 5-quark obviously exotic 'anticharmed' baryons (pentaquarks) of the $P^0 = \bar{c}suud$ type or analoguous 'antibeauty' baryons is also possible [106]. Refs [102–106] give arguments in favour of the quasistable character of $\tilde{F}_S$, $\tilde{F}_I$, P^0 hadrons due to the chromomagnetic interaction between quarks. The properties of a number of exotic states with heavy c- and b-quarks are presented in Table 12.

To search for hadrons with heavy quarks in the experiments with high-energy beams, a careful choice of their possible production processes is needed, which, on the one hand, must have large enough cross sections (not less than several or even tens of nanobarns), and on the other hand, must be characterised by favourable background conditions and primarily by an insignificant combinatorial background. These two requirements are often not easy to match. In particular, the cross sections for most exclusive reactions with a very low combinatorial background which were successfully used in searching for exotic states with light quarks in the intermediate energy domain, become too small at high energies. Of course, if the heavy hadron is quasistable, as one can expect for some types of particles presented in Table 12 (P-baryons, $\tilde{F}_S$-mesons etc.), and has a life time of the order 10^{-13} s (weak decays), it can be straightforwardly registered in the precision vertex detectors. This removes the combinatorial background and allows one to use inclusive reactions to search for such

Table 12. Some types of exotic hadrons with heavy quarks.

Type of exotic particles	Notation	Quark composition	Quantum numbers	Decay modes
Strange-charmed mesons with openly exotic set of quantum numbers I, S, C and cryptoexotic mesons of this type [102, 103]	$\tilde{F}_S^0$	$cs\bar{u}\bar{d}$	$(I, S, C) = (0, -1, +1)$	$\tilde{F}_S^0 \to D^+K^- \to K^-K^-\pi^+\pi^+$. If the mass of meson is below the DK, threshold, a weak decay occurs $\tilde{F}_S^0 \to K^-K^-\pi^+\pi^+$
	$\left.\begin{array}{l}\tilde{F}_I^{++}\\ \tilde{F}_I^{+}\\ \tilde{F}_I^{0}\end{array}\right\} c\bar{s}(q\bar{q})_{I=1}$	$c\bar{s}(u\bar{d})$ $c\bar{s}(u\bar{u} - d\bar{d})/\sqrt{2}$ $c\bar{s}(d\bar{u})$	$(I, S, C) = (1, 1, 1)$	$\tilde{F}_I^{++} \to D^+K^+$; $D_s^+\pi^+$ $\tilde{F}_I^{+} \to D_s^+\pi^0$; $D^+K_s^0$ $\tilde{F}_I^{0} \to D_s^+\pi^-$; $D^0K_s^0$
	F_x^+	$c\bar{s}(q\bar{q})_{I=0}$	$(I, S, C) = (0, 1, 1)$	Electromagnetic decays: $F_x^+ \to D_s^+ + 2\gamma$ transition $0^+ \to 0^+$); $D_s^+\pi^0$; $D_s^+\pi^0\gamma$, if $M(F_x) < M(D) + M(K)$
Beauty-beauty, beauty-charmed etc. mesons with two heavy quarks [104]		$QQ\bar{q}\bar{q}$ etc.	$B = 2$ or $B = 1$, $C = 1$ etc.	QCD-analysis showed that the lightest states like $bb\bar{u}\bar{d}$, $bc\bar{u}\bar{d}$ should be stable relative to strong and electromagnetic interactions
Strange-anticharmed baryons with exotic quantum numbers [106]	P^0 P^-	$\bar{c}suud$ $\bar{c}sudd$	$(I, S, C) = (1/2, -1, -1)$	$P^0 \to p\phi\pi^-$; $p\eta\pi^-$; $\Lambda K^+\pi^-$ (weak decays). With a large probability these states are stable relative to strong and electromagnetic interactions
	$P'^{-}_{I=0}$	$\bar{c}ssud$	$(I, S, C) = (0, -2, -1)$	$P'^{-} \to \Sigma^-\phi$; ΛK^-K^0 (weak decays). These states can be stable relative to strong and electromagnetic interactions.
	$P'^{0,-,--}_{I=1}$	$\bar{c}ss(qq)_{I=1}$	$(I, S, C) = 1, -2, -1$	
Analogous states with b-quarks		$\bar{b}sqqq$ $\bar{b}ssqq$		
Cryptoexotic mesons with hidden charm (four-quark mesons and hybrids)	$M_\psi^{(1)}$ M_ψ^0 $M_{\psi\phi}$ H_ψ	$c\bar{c}(q\bar{q})_{I=1}$ $\left.\begin{array}{l}c\bar{c}(q\bar{q})_{I=0}\\ c\bar{c}s\bar{s}\\ c\bar{c}g\end{array}\right\}$	$(I, S, C) = (1, 0, 0)$ $(I, S, C) = (0, 0, 0)$	$M_\psi^{(1)} \to \psi\pi$; $\psi\rho$ $M_\psi^{(0)} \to \psi\eta$; $\psi\eta'$; $\psi\omega$ $M_{\psi\phi} \to \psi\phi$; $\psi K\bar{K}$ $H_\psi \to \psi\eta$; $\psi\eta'$
Analogous states with hidden beauty	$M_\Upsilon^{(1)}$ etc.	$b\bar{b}(q\bar{q})_{I=1}$ etc.		$M_\Upsilon^{(1)} \to \Upsilon\pi$
Cryptoexotic baryons with hidden charm	B_ψ Y_ψ	$c\bar{c}qqq$ $c\bar{c}sqq$	$I = 3/2$ and $I = 1/2$ $I = 0$ and $I = 1$	$B_\psi \to \psi N$; $\Lambda_c^+\bar{D}$ $Y_\psi \to \psi Y$; $\Lambda_c^+D_s^-$
Analogous baryons with hidden beauty	B_Υ etc.	$b\bar{b}qqq$	$I = 3/2$ and $I = 1/2$ etc.	$B_\Upsilon \to \Upsilon N$

Note. Different decay channels for strange-charmed mesons, some of which are given in the Table, are determined by the mass vqlues of these particles: $M(\tilde{F}) > M(DK)$, $M(DK) > M(\tilde{F}) > M(D_s\pi)$, $M(D_s\pi) > M(\tilde{F})$. For example, for $\tilde{F}_I$-mesons with $M(\tilde{F}_I) < M(D_s\pi)$, only electromagnetic and weak decays are possible, and for $\tilde{F}_S^0$-mesons with $M(\tilde{F}_S^0) < M(DK)$, only weak decays are possible. The mesons with open exotics are designated as: $\tilde{F}_S$ particles with an 'incorrect' strangeness, $\tilde{F}_I$ particles with an 'incorrect' isospin. The Table does not pretend to be complete. Other exotic states with beauty and charmed quarks were also considered (see, for example, Ref. [107]).

particles in a wide kinematic range.

For heavier exotic hadrons with massive quarks decaying due to strong interactions, the inclusive formation processes in the fragmentation region (see Sections 4.3.3) can be used to reduce the combinatorial background.

8.1 On possible searches for pentaquark charmed baryons

In this section we will consider the prospects of the high-energy experiments (at several hundred GeV and higher) for searching for heavy exotic baryons P^0, P^- and mesons $\tilde{F}_S^0$ with charmed and strange quarks that were described

Table 13. Production cross-sections data for charmed baryons $P^0 = |\bar{c}suud\rangle$, $P^- = |\bar{c}sddu\rangle$, and $\Xi_c^+ = |csu\rangle$ in Σ^-N-interactions.

$\Xi_c^+ = \lvert csu\rangle \to \Lambda K^- \pi^+ \pi^+$ (weak decay)	$P^0 = \lvert\bar{c}suud\rangle \to \phi p \pi^-$; $\Lambda K^+ \pi^-$ $P^- = \lvert\bar{c}sddu\rangle \to \phi p \pi^- \pi^-$; $\Lambda K^+ \pi^- \pi^-$
$\Sigma^- + N \to \Xi_c^+ + X$ $\hookrightarrow \Lambda K^- \pi^+ \pi^+$	$\Sigma^- + N \to P^0 + X$ $\hookrightarrow \phi \pi^-$ $\hookrightarrow \Lambda K^+ \pi^-$ $\Sigma^- + N \to P^- + X\ \pi^- \pi^-$ $\hookrightarrow \Lambda K^+ \pi^- \pi^-$ $\hookrightarrow \phi P p$
$P_{\Sigma^-} = 135$ GeV, $\sigma_{x_F > 0.6} \times \mathrm{BR} \approx 0.5$ μb/nucleon Extrapolation for whole region $x_F > 0$ for $\frac{d\sigma}{dx_F} \sim (1 - x_F)^3$ gives $\sigma_{x_F > 0} \times \mathrm{BR} = 10 - 20$ μb/nucleon. If $\mathrm{BR}(\Xi_c^+ \to \Lambda K^- \pi^+ \pi^+) \approx 0.1$, $\sigma_{x_F > 0.6} \approx 5$ μb/nucleon, $\sigma_{x_F > 0} \approx 100 - 200$ μb/nucleon, which is a very large cross section, possibly due to the incorrect extrapolation or the BR errors. Transition from $P_\Sigma = 135$ GeV to $P_\Sigma \approx 600$ GeV must increase the cross section by about a factor of 5; we, however, will ignore this correction factor	Instead of the three-quark system Ξ_c, a five-quark system is formed in pentaquark baryons, i.e. an additional ud-pair must be fused. The estimation of the reduction factor R, in the cross sections of P-baryon production in comparison with Ξ_c-baryon production, yields $R > 10^{-2}$ from the antideuteron formation data: $\left.\begin{matrix}\sigma(P^0)\\ \sigma(P^-)\end{matrix}\right\} \approx R \times \sigma(\Xi_c) > 10^{-2}\sigma(\Xi_c)$ or $\sigma(P)_{x_F > 0.6} > 50$ nb/nucleon, $\sigma(P)_{x_F > 0} > 1 - 2$ μb/nucleon
Note. To estimate the reduction factor $R \gtrsim 10^{-2}$ for exotic baryon production cross sections (with the fusing of additional ud pair), one can use (as was proposed in Ref. [108]) the data on antideuteron yield $\bar{d}/\bar{p} \sim 10^{-3}$ (fusing with three additional quarks). This reduction factor $R \sim 10^{-2}$ seems to be underestimated, as the antideuteron $\bar{d}$ is a weakly bound system, which additionally reduces the antidentron yields. Additionally, in the reaction of the P^0 production the transition of two quarks from the primary Σ-hyperon (sd) into P^0 take place, and during formation of P^- even three quarks sdd are transmitted. It is well known that for such 'quark-sharing' reactions the corresponding cross sections are considerably increased.	

above. First attempts to look for the P^0-baryons took place in experiment E791 (Fermilab) in π^-N-interactions at $E_\pi \approx 500$ GeV [108].

However, the quark composition of heavy exotic hadrons implies that the most promising are searches for these states in intensive particle beams with strange quarks and above all in the beams of negative charged particles with large longitudinal momenta ($x_F > 0.75 - 0.8$), which are enriched by hyperons by kinematical and dynamical production conditions (Σ^--hyperons constitute more than 50% of the particles in such a beam).

The following reactions can occur in the hyperon beams at high energies [109–110]:

$$\Sigma^- + N \to |\bar{c}suud\rangle^0 + X \quad (106)$$
$$\hookrightarrow p\phi\pi^-,\ \Lambda K^+ \pi^-$$

for P^0-baryons,

$$\Sigma^- + N \to |\bar{c}sudd\rangle^- + X \quad (107)$$
$$\hookrightarrow \Lambda K^+ \pi^- \pi^-$$

for P^--baryons,

$$\Sigma^- + N \to |cs\bar{u}\bar{d}\rangle^0 + X \quad (108)$$
$$\hookrightarrow K^- K^- \pi^+ \pi^+$$

for $\tilde{F}_S$-mesons.

It is assumed that the P^0, P^-, and $\tilde{F}_S^0$ are quasistable particles. Their weak decays can be registered in vertex detectors, in analogy with other charmed particle decays. The background conditions for such experiments must be good enough, as the registration of the weak decay of a particle in a vertex detector will remove the combinatorial background.

If the hypothesis about the quasistable character of the particles P^0, P^-, and $\tilde{F}_S$ is not justified (that is, their mass is too large) and strong decays of these hadrons occur, then the background situation will be significantly harder. In this case inclusive reactions (106)–(108) in the fragmentation region, that is with $x_F > 0.6$ (see Section 4.3.3), can be used for exotic hadron searches.

To illustrate this, Table 13 contains estimates of the cross sections of pentaquark P-baryon production under the conditions of the E781 experiment on the hyperon beam of the Tevatron accelerator at Fermilab (this experiment is now under preparation). The estimates are based on the experimental production cross-section data for strange–charmed baryons in Σ^-N-interactions [111].

Thus, it seems that there is a good chance of seeing exotic pentaquark P baryons in the Fermibab hyperon beam experiment, if these objects exist as quasistable particles or as resonances with not very large decay width ($\Gamma \lesssim 100$–150 MeV). This conclusion seems to be correct even if the production cross sections in Table 13 are overstimated by an order of magnitude (see Refs [49, 112] for further details).

8.2 Cryptoexotic baryons with hidden charm

Consider briefly cryptoexotic baryons with hidden charm, which we will denote by $B_\psi = |qqqc\bar{c}\rangle$. If the mass of such baryons satisfies the conditions

$$M(B_\psi) < \left\{ \begin{array}{l} M(P) + M(J/\psi) \\ M(P) + M(\eta_c) \end{array} \right\} \approx 3.9-4 \text{ GeV}, \qquad (109)$$

the B_ψ-decays can occur only through the OZI suppressed channels, and the corresponding baryon state must have a very small decay width. Such baryons to some extent look like mesons with hidden charm (J/ψ- and ψ'-particles).

Depending on the quantum numbers of $c\bar{c}$-system in B_ψ-baryons, the following decay channels for these particles are possible:

1. Decay via virtual orto-charmonium states:

$$B_\psi \to p + (J/\psi)_{\text{virt}} \to p + (l^+l^-). \qquad (110)$$

As $BR(J/\psi \to l^+l^-) \approx 0.12$, decay (110) with lepton pair production can be expected to occur with a relative probability $BR[B_\psi \to p + (l^+l^-)] \approx 0.1$. In the mass spectrum of the dilepton system in (110), one should expect the dominance of higher effective masses. The decay channel (110) seems to be sufficiently convenient and perspective to the search for the B_ψ-baryons.

2. Decay via virtual para-charmonium states:

$$B_\psi \to p + (\eta_c)_{\text{virt}} \to p + (K^+K^-\pi^+\pi^-; 2\pi^+2\pi^-; K\bar{K}\pi; \eta\pi\pi). \qquad (111)$$

By considering only fully reconstructed decay modes one can expect from the η_c-meson data that the summed branching ratio for the easily detected decays of type (111) has the value

$$BR[B_\psi \to p + (\eta_c)_{\text{virt}} \to p + (K^+K^-\pi^+\pi^- \text{ etc.}) \approx 0.05. \qquad (112)$$

If the mass of the B_ψ-baryon exceeds 4.2 GeV, the OZI allowed decays of this state will occur

$$B_\psi^+ \to \left\{ \begin{array}{l} p + J/\psi, \\ p + \eta_c, \\ \Lambda_c^+ + D^0 \end{array} \right. , \qquad (113)$$

etc. Although for $M(B_\psi) > 4.2$ GeV one cannot predict with full confidence the existence of narrow baryon resonances with hidden charm, it is still possible to expect relatively small widths of several exotic states of this type due to their complicated inner colour structure and the influence of the colour rearrangement decay mechanisms. Thus, the searches for these states by analysing decay mode (113) seems to be completely justified.

Let us consider now possible directions in the search for the B_ψ-baryons in high-energy experiments. As the cross sections for charmed quark–antiquark pair production continue to increase significantly in the region up to 1 TeV, it is desirable to carry out these experiments at energies exceeding 400–600 GeV. In this energy domain one should consider at first processes of diffractive formation of cryptoexotic baryons (see Section 4.3.1)

$$p + N \to |qqqc\bar{c}\rangle + N. \qquad (114)$$

As was shown in Ref. [113] with the aid of data on diffractive production of baryons with hidden strangeness, one can expect the cross-section of B_ψ-baryon formation in reaction (114) to be 5–25 nb/nucleon. Such baryons have a chance of being discovered by specially prepared high-sensitivity experiments [113].

9. Conclusion

The search for exotic baryons has only just passed through the initial stage in which, however, some interesting results have been obtained and require further intensive studies. New data on candidates for cryptoexotic baryons with hidden strangeness which were discussed in Sections 5 and 6, must be obtained in further experiments on the diffractive production of the YK-states processes in proton beams, in nonperipherical processes in the region of large transverse momenta $P_T^2 \gtrsim 0.3-0.5$ GeV^2, as well as possibly in the experiments with precision energy scanning of cross sections for some formation reactions.

Photoproduction reactions on high-current electronic accelerators (Bonn, CEBAF) can be of great interest. One should also perform some searches for hyperon states with additional hidden strangeness in the experiments with hyperon beams. In future we expect to look for charmed exotic pentaquark P^0-baryons and baryons with hidden charm in hyperon experiments and in reactions in high-energy proton beams.

References

1. *Proceedings of the Second International Conference on Hadron Spectroscopy (KEK, Tsukuba, Japan*, April 16–18, 1987), KEK Report 87-7 (1987)
2. Chung S-U (Ed.) *Glueballs, Hybrids and Exotic Hadrons: Workshop* (Upton, N.Y., August 29–September 1, 1988) (New York: 1989)
3. Binon F et al. (Eds), Hadron-89 *Proceedings of the Third International Conference on Hadron Spectroscopy* (Aiaccio, Corsica, September 23-27, 1989) (Paris: 1989)
4. *Proceedings of the First Biennial Conference on Low Energy Antiproton Physics* (Stockholm, July 2–6, 1990)
5. Gill D R (Ed.) *Proceedings of the Workshop on Science at the Kaon Factory, TRIUMF* (July 23–28, 1990)
6. Klempt E, Peters K (Eds) *Proceedings of the Rheinfels Workshop on the Hadron Mass Spectrum* (St. Goar, Germany, September 3–6, 1990); *Nucl. Phys. B (Proc. Suppl.)* **211** (1991)
7. Pancheri G (Ed.) *Proceedings of the Workshop on Phys. and Detectors for DANNE, INFN* (Frascati, April 9–12, 1991)
8. Kalashnikova Yu S et al. (Eds), NAN-91 *Proceedings of the Workshop on Nucleon-Antinucleon Interactions, Institute of Theoretical and Experimental Physics, Moscow, July 8–11, 1991*; *Yad. Fiz.* **55** No 5, 6 (1992)
9. Peaslee D (Ed.), Hadron-91 *Proceedings of the Fourth International Conference on Hadron Spectroscopy* (College Park, August 12–16, 1991)
10. Guaraldo C, et al. (Eds), LEAP-92 *Proceedings of the Second Biennial Conference on Low Energy Antiproton, Phys. Courmayeur* (Aosta Valley, Italy, September 14–19, 1992)
11. Hikasa K et al. (PDG) *Phys. Rev. D* **45** 51 (1992)
12. Landsberg LG *Usp. Fiz. Nauk* **160** (3) 1 (1990) [*Sov. Phys. Usp.* **33** 169 (1990)]
13. Landsberg L G *Surv. in High Energy Phys.* **6** 257 (1992)
14. Landsberg L G *Yad. Fiz* **57** 47 (1994) [*Phys. At. Nucl.* **57** 47 (1994)]
15. Close F E Preprint RAL-87-072 (Chilton, 1987)
16. Chung S-U Preprint BNL 40599 (Upton, 1987); Chung S-U *Nucl. Phys. A* **473** 511 (1988); Chung S-U *Z. Phys. C* **46** 111 (1990)
17. Kopke L, Wermes N *Phys. Rep.* **174** 67 (1989)
18. Palano A *Invited Talk on the XXII Rencontres de Moriond* (March 1987); Preprint CERN EP/87-92 (Geneva, 1987)
19. Peters K, See [10] p.93

20. Dalitz R, in *Proc. of Conf. 'Baryon Resonances-73'* (Purdue University, 1973) p.393
21. Hey A J G, Kelly R L *Phys. Rep.* **95** 71 (1983)
22. Close F E *An Introduction to Quarks and Partons* (New York: Academic Press, 1979)
23. Isgur N, Karl G *Phys. Lett. B* **72** 109 (1977); **74** 353 (1978); *Phys. Rev. D* **18** 4187 (1978); **19** 2653 (1979); **20** 1191 (1979); **21** 3175 (1980)
24. Burkert V D, see Ref. [6] p.232
25. Ishida S et al., Preprint Nihon University NUP-A-93-21 (Tokyo, 1993)
26. Ferrer A et al. *Z. Phys. C* **56** 215 (1992)
27. Jaffe R L *Phys. Rev. D* **15** 267, 281 (1977); **17** 1444 (1978)
28. Jaffe R L, Low F E *Phys. Rev. D* **19** 2105 (1979)
29. Grigoryan A A, Kaidanov A B *Pis'ma Zh. Eksp. Teor. Fiz.* **28** 318 (1978) [*JETP Lett.* **28** 293 (1978)]
30. Grigoryan A A, Kaidanov A B *Nucl. Phys.* **32** 540 (1980)
31. Smolyankin V T et al. Preprint 89-189 (Moscow: Institute of Theoretical and Experimental Physics, 1989)
32. Chan Hong-Mo, Hogaasen H *Phys. Lett. B* **72** 121 (1977); Chan Hong-Mo et al. *Phys. Lett. B* **76** 634 (1978)
33. Fukugita M *Invited Talk at the 1979 INS Symposium on Particle Physics in GeV Region* (Tokyo, November 21–23, 1979); Preprint KEK-TH 9 (Tokyo, 1980)
34. Hogaasen H, Sorba P *Nucl. Phys. B* **145** 119 (1978); *Invited Talk on Conference on Hadron Interactions at High Energy* (Marseille, June 1978)
35. De Crombrugghe M et al. *Nucl. Phys. B* **156** 347 (1979)
36. Fukugita M et al. *Phys. Lett. B* **74** 261 (1978)
37. Pietrzyk B *Talk, given at the Fifth European Symposium on Nucleon Interactions* (Bressanone, June 23–28, 1980); Preprint CERN-EP/80-116 (Geneva, 1980)
38. Gershtein S S et al. *Z. Phys. C* **24** 305 (1984)
39. Barnes T *Invited Talk on 1984 Bonn ELSA Meeting* (Bad Honnef, October 29–31, 1984); Preprint RAL-85-005 (Chilton, 1985); Barnes T, Close F E, Preprint RAL-82-110 (Chilton, 1982)
40. Golowich E et al. *Phys. Rev. D* **28** 160 (1983); Barnes T, Close F E *Phys. Lett. B* **123** 89 (1983)
41. Landsberg L G *Yad. Fiz.* **53** 1048 (1991) [*Sov. J. Nucl. Phys.* **53** 650 (1991)]
42. Flamino V et al., Preprint CERN-HERA 83-01 (Geneva, 1983)
43. Hirose T et al. *Nuovo Cimento A* **50** 120 (1979); Fukunaga C et al. *Nuovo Cimento A* **58** 199 (1980)
44. Aleev A N et al. *Z. Phys. C* **25** 205 (1984)
45. Bityukov S I et al. *Phys. Lett. B* **72** 269 (1977)
46. Vavilov D V et al. *Yad. Fiz.* **57** (8) 129 (1994) [*Phys. At. Nucl.* **57** 1376 (1994)]
47. Bellini G et al. *Nuovo Cimento A* **79** 282 (1984)
48. Moinester M A et al. *Phys. Rev. C* **46** 1082 (1992)
49. Landsberg L G et al., Preprint No. 94-19 (Protvino: Institute of High-Energy Physics, 1994)
50. Baksay L et al. *Phys. Lett. B* **55** 491 (1975)
51. Alde D et al. *Pis'ma Zh. Eksp. Teor. Fiz.* **44** 441 (1986) [*JETP Lett.* **44** 567 (1986)];
Alde D et al. *Phys. Lett. B* **182** 105 (1986);
Alde D et al. *Yad. Fiz.* **54** 745 (1991) [*Sov. J. Nucl. Phys.* **54** 451 (1991)]
52. Alde D et al. *Phys. Lett. B* **216** 447 (1989);
Alde D et al. *Yad. Fiz.* **54** 751 (1991) [*Sov. J. Nucl. Phys.* **54** 455 (1991)]
53. Gershtein S S, see Ref. [3] p. 175
54. Fisyak Yu V *Characteristics of inclusive formation process of hadrons in π^--interactions at 360 GeV/s and in pp-interactions at 400 GeV/s.* Dr. Sci. Thesis (Moscow, NPRI MSU, 1991)
55. Balitskii Ya Ya et al. *Nucl. Phys.* **35** 130 (1982)
56. Rosner J *Phys. Rev. Lett.* **21** 950; 1468(E) (1968)
57. Jacob M, Weyers J *Nuovo Cimento B* **69** 521 (1970)
58. Landsberg L G *Yad. Fiz.* **52** 192 (1990) [*Sov. J. Nucl. Phys.* **52** 121 (1990)]
59. Balats M Ya et al. Preprint No. 85-92 (Moscow: Institute of Theoretical and Experimental Physics, 1992)
60. Burkert V D, see [6] p.287
61. Li Z et al. *Phys. Rev. D* **46** 70 (1992)
62. Barnes T, Close F E *Phys. Lett. B* **128** 277 (1983)
63. Koncuk R, Isgur N *Phys. Rev. D* **21** 1868 (1980)
64. Burkert V D *Invited Talk on Baryon-92* (June 1–5, 1992); Preprint CEBAF-PR-92-021 (New Haven, 1992)
65. Dytman S A, see [9] p. 155
66. Papanicolas C N, See [9] p. 145
67. Borquin M et al. *Phys. Lett. B* **172** 113 (1986)
68. Aleev A N et al. *Z. Phys. C* **47** 533 (1990)
69. Tatishvili G T, see Ref. [8] p.1512; [9] p. 733
70. Amirzadeh J et al. *Phys. Lett. B* **89** 205 (1979)
71. Aston D et al. *Phys. Rev. D* **32** 2270 (1985)
72. Karnakov V M et al. *Phys. Lett. B* **281** 148 (1992)
73. Bushnin Yu B et al. *Phys. Lett. B* **72** 269 (1977)
74. Vavilov D V et al. *Yad. Fiz.* **57** 253 (1994) [*Phys. At. Nucl.* **57** 238 (1994)]
75. Balatz M Ya et al. *Z. Phys. C* **61** 399 (1994)
76. Vavilov D V et al. *Yad. Fiz.* **57** 1449 (1994) [*Phys. At. Nucl.* **57** 1376 (1994)]
77. Landsberg L G *Nuovo Cimento A* **107** 2441 (1994)
78. Kurshetsov V F, Landsberg L G *Yad. Fiz.* **57** 2030 (1994) [*Phys. At. Nucl.* **57** 1954 (1994)]
79. Vavilov DV et al. *Yad. Fiz.* **57** 2046 (1994) [*Phys. At. Nucl.* **57** 1970 (1994)]
80. Arenton M W et al. *Phys. Rev. D* **25** 2241 (1982)
81. Montanet L et al. *Phys. Rep.* **63** 149 (1980)
82. Shapiro I S *Phys. Rep.* **35** 129 (1978)
83. Carrol A S et al. *Phys. Rev. Lett.* **32** 247 (1974)
84. Chaloupkat V et al. *Phys. Lett. B* **61** 487 (1976)
85. Brukner W et al. *Phys. Lett. B* **67** 222 (1977)
86. Benkheiri P et al. *Phys. Lett. B* **68** 483 (1977)
87. Gibbard B G et al. *Phys. Rev.* **42** 1593 (1979)
88. Ferrer A et al., See Ref. [10] p. 191
89. Barber D P et al. *Phys. Lett. B* **90** 470 (1980)
90. Kooijman S et al. *Phys. Rev. Lett.* **45** 316 (1980)
91. Armstrong T A et al., Preprint CERN/EP 87-32 (Geneva, 1987)
92. Busenitz J et al. *Phys. Rev. D* **40** 1 (1989)
93. Arefiev A V et al. *Nucl. Phys.* **51** 414 (1990)
94. Brovkin L Yu et al. *Nucl. Phys.* **55** 986 (1992)
95. Abramov B M et al. *Yad. Fiz.* **53** 179 (1991) [*Sov. J. Nucl. Phys.* **53** 114 (1991)]
96. Deutschmann M et al. *Nucl. Phys. B* **86** 227 (1975)
97. Baillon P et al. *Phys. Lett. B* **94** 533 (1980)
98. Barrelet E et al. *Phys. Lett. B* **94** 541 (1980)
99. Moyssides P G et al. *Nuovo Cimento* **75** 122 (1983)
100. Moyssides P G et al. *Nuovo Cimento* **75** 162 (1983)
101. Shahbazian B A et al. *Z. Phys. C* **39** 151 (1988)
102. Lipkin H J *Phys. Lett. B* **70** 113 (1977)
103. Isgur N, Lipkin H J *Phys. Lett. B* **99** 151 (1981)
104. Cignoux C et al. *Phys. Lett. B* **193** 323 (1987)
105. Richard J et al., see Ref. [6] p. 2 54
106. Lipkin H J *Phys. Lett. B* **195** 484 (1987);
Lipkin H J, see Ref. [6] p. 258
107. Vysotskii MI et al. in *Proceedings of the Workshop on the Experimental Programme UNK* (Protvino: Institute of High-Energy Physics, Protvino, December 14 – 17 1983) (Serpukhov 1983), p. 94
108. Lichtenstadt J, see [6] p.264; Ashery D *Invited Talk* (Lake Lonise Winter Institute, 1991)
109. Landsberg L G, see [6] p.306; Garkusha V I et al., Preprint No. 90-81 (Protvino: Institute of High-Energy Physics, 1990)
110. Sibert H W, see Ref. [6] p. 270
111. Biagi S F et al. *Phys. Lett. B* **122** 455 (1983); **150** 230 (1985)
112. Moinester M A et al. *Invited Talk on the Charm 2000 Workshop* (Fermilab, June 1994)
113. Landsberg L G *Yad. Fiz.* **57** 2210 (1994) [*Phys. At. Nucl.* **57** 2127 (1994)]